MINISTRY OF AVIATION

AERONAUTICAL RESEARCH COUNCIL
REPORTS AND MEMORANDA

Oscillatory Aerodynamic Forces in Linearised Supersonic Flow for Arbitrary Frequencies, Planforms and Mach Numbers

By D. J. ALLEN and D. S SADLER

Oscillatory Aerodynamic Forces in Linearised Supersonic Flow for Arbitrary Frequencies, Planforms and Mach Numbers

By D. J. ALLEN and D. S. SADLER

---

*Reports and Memoranda No. 3415**
January, 1963

Summary.

A method is described of performing a numerical integration to solve the integral equation connecting downwash and velocity potential in linearised unsteady supersonic flow. Supersonic and subsonic leading edges and wakes are dealt with, and some practical results are given. By using this approach, a sufficiently general computer programme could deal accurately with kinked and curved edges.

LIST OF CONTENTS

---

1. *Introduction.*

Due to the complexity of the integral equations relating downwash and potential, it is clear that for arbitrary Mach numbers, planforms and frequency parameters no analytical solution will be possible. Because of this a numerical approach to the problem had to be made. The three possibilities

2

considered are listed below. In making a choice of method, it was borne in mind that, for some of the planforms for which results were required by the National Physical Laboratory, Mach numbers as low as 1·01 combined with frequency parameters of order unity would be involved.

(i) *Richardson's Collocation Method (Ref. 1).*

This method uses the equation which gives the downwash at any given point as an integral involving the loading taken over the fore-cone of the point concerned. If one assumes a certain family of loadings then the downwash at a certain set of control points due to each member of the family can be determined. By inverting the matrix relating the basic loadings to the downwash it is possible to obtain, once and for all, a matrix which will give the loading corresponding to any given downwash distribution at the control points.

Although this method has the desirable quality of only requiring one matrix inversion to deal with any number of downwash vectors, there are other factors which militate against it. In the first place the loading is normally discontinuous across the shocks which emanate from kinks in the leading edge. This is not allowed for by Richardson in his formulation. Secondly for transonic Mach numbers and high frequency parameters the chordwise variation in the potential will probably be rather oscillatory and is not likely to be represented very well by the interpolation functions envisaged by Richardson.

(ii) *The Integrated Downwash Method.*

This method uses the equation which gives the potential at any point as an integral involving the downwash taken over the fore-cone of the point concerned. Since initially one only knows the downwash on the wing planform it is necessary in general to compute the downwash over certain regions forward of the leading edge and in the wake to obtain the potential all over the planform.

For a wing with a sharply swept leading edge at transonic Mach numbers the region forward of the leading edge over which values of the downwash have to be calculated and stored can become very extensive. From the digital computer point of view it is clear that such cases will take a long time to compute and will require a large storage space.

(iii) *The Integrated Potential Method.*

This is the method described in this report. It uses the equation which gives the downwash at any given point as an integral involving the potential taken over the fore-cone of the point concerned. Since the potential is zero forward of the planform leading edge the integrations involve only values of the potential on the planform (except for the wake region) which makes it superior to method (ii) both as regards speed and the storage required.

A characteristic mesh is constructed and the potential is determined first for the most upstream rhombus. Successive potentials can be determined working down each row of characteristics. Each potential determined depends on those potentials upstream in its fore-cone. Thus if any given potential is slightly in error this produces further errors downstream. It will be clear that to keep this 'propagation error' small, each potential should be determined as accurately as possible.

2. *The Basic Integral Equation.*

Let the vertex of the wing be the origin of co-ordinates and let the x-axis coincide with the direction of the free-stream velocity which is assumed to be horizontal. The z-axis is taken vertically upwards and the y-axis as positive to starboard. The wing is regarded as infinitely thin and as lying effectively in the plane $z = 0$, the camber and twist therefore are understood to be small.

3

The basic integral equation as obtained by W. P. Jones (Ref. 2) is

$$w(x, y) = -\frac{1}{\pi} \operatorname{Lt}_{z \to 0} \frac{\partial^2}{\partial z^2} \iint_{S'} \phi(\xi, \eta) \exp\left\{-\frac{iM^2\omega(x-\xi)}{\beta^2 U}\right\} \cos\left(\frac{M\omega R}{\beta^2 U}\right) \frac{1}{R} d\xi \, d\eta \tag{1}$$
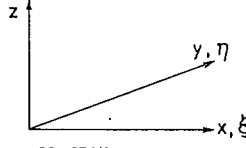
where

$$R = [(x-\xi)^2 - \beta^2(y-\eta)^2 - \beta^2 z^2]^{1/2}$$

S' is that part of the plane $z = 0$ cut off by the cone $R = 0$ for which $\xi < x$

$$w = \frac{\partial \phi}{\partial z} = \text{upwash}$$

M = free-stream Mach number

ω = circular frequency of harmonic oscillation

ϕ = velocity potential

$\beta = (M^2 - 1)^{1/2}$

U = free-stream velocity.

Putting $\lambda = x - \xi$ and $\mu = y - \eta$ and $\overline{\omega} = \omega/U\beta^2$, we get

$$w(x, y) = \frac{\beta^2}{\pi} \iint_{S'} \phi(\lambda, \mu) \exp\{-iM^2\overline{\omega}\lambda\} \times$$
$$\times \left[\frac{\cos\{M\overline{\omega}(\lambda^2 - \beta^2\mu^2)^{1/2}\}}{(\lambda^2 - \beta^2\mu^2)^{3/2}} + \frac{M\overline{\omega}\sin\{M\overline{\omega}(\lambda^2 - \beta^2\mu^2)^{1/2}\}}{\lambda^2 - \beta^2\mu^2}\right] d\lambda \, d\mu. \tag{2}$$

Let the equation of the oscillating lifting surface be

$$z = g(x, y)e^{i\omega t}, \tag{3}$$

then the linearised tangential flow condition is

$$\left(U\frac{\partial}{\partial x} + w\frac{\partial}{\partial z}\right)\{z - g(x, y)e^{i\omega t}\} = \frac{\partial}{\partial t}\{g(x, y)e^{i\omega t}\}$$

and hence

$$w(x, y) = U\frac{\partial g}{\partial x} + i\omega g. \tag{4}$$

Substituting (4) into (2) and expanding out into real and imaginary parts, using

$$\phi(\xi, \eta) = \phi_R + i\phi_I, \tag{5}$$

we obtain

$$U\frac{\partial g}{\partial x} = \frac{\beta^2}{\pi} \iint_{S'} (\phi_R \cos M^2\overline{\omega}\lambda + \phi_I \sin M^2\overline{\omega}\lambda) \times$$
$$\times \left[\frac{\cos\{M\overline{\omega}(\lambda^2 - \beta^2\mu^2)^{1/2}\}}{(\lambda^2 - \beta^2\mu^2)^{3/2}} + \frac{M\overline{\omega}\sin\{M\overline{\omega}(\lambda^2 - \beta^2\mu^2)^{1/2}\}}{\lambda^2 - \beta^2\mu^2}\right] d\lambda \, d\mu \tag{6a}$$

$$\omega g = \frac{\beta^2}{\pi} \iint_{S'} (\phi_I \cos M^2\overline{\omega}\lambda - \phi_R \sin M^2\overline{\omega}\lambda) \times$$
$$\times \left[\frac{\cos\{M\overline{\omega}(\lambda^2 - \beta^2\mu^2)^{1/2}\}}{(\lambda^2 - \beta^2\mu^2)^{3/2}} + \frac{M\overline{\omega}\sin\{M\overline{\omega}(\lambda^2 - \beta^2\mu^2)^{1/2}\}}{\lambda^2 - \beta^2\mu^2}\right] d\lambda \, d\mu. \tag{6b}$$

4

We now introduce characteristic co-ordinates ρ and σ having an origin at the pivotal point (x, y), as shown below.
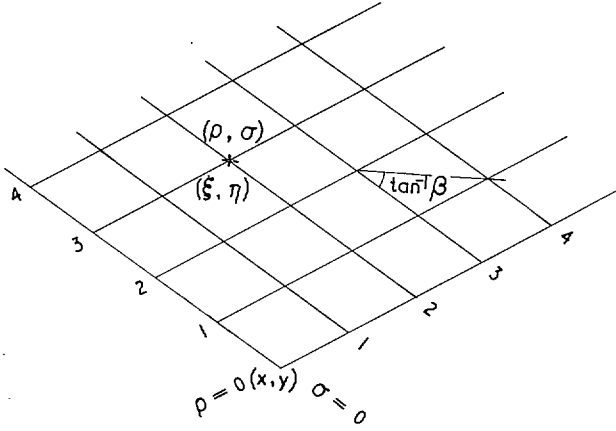
If l is the side of a basic rhombus in the characteristic mesh, we have

$$\xi = x - \frac{\rho l \beta}{M} - \frac{\sigma l \beta}{M} \qquad (7a)$$

$$\eta = y - \frac{\rho l}{M} + \frac{\sigma l}{M}. \qquad (7b)$$

Hence

$$\lambda = (\rho + \sigma)\frac{l\beta}{M}, \qquad \mu = (\rho - \sigma)\frac{l}{M}$$

and

$$\frac{\partial(\lambda, \mu)}{\partial(\rho, \sigma)} = 2\frac{l^2\beta}{M^2}.$$

We now introduce

$$\phi' = \frac{\phi}{UL} \qquad (8)$$

where L is an arbitrary reference length
and

$$\nu' = \frac{l\omega}{\beta U} \qquad (9)$$

so that equations (6a) and (6b) become

$$\frac{\alpha \pi l}{ML} = \int\int [\phi_R{'} \cos\{M\nu'(\rho + \sigma)\} + \phi_I{'} \sin\{M\nu'(\rho + \sigma)\}] \times$$

$$\times \left[\frac{1}{4}\frac{\cos 2\nu'(\rho\sigma)^{1/2}}{(\rho\sigma)^{3/2}} + \nu'^2\frac{\dfrac{\sin 2\nu'(\rho\sigma)^{1/2}}{2\nu'(\rho\sigma)^{1/2}}}{(\rho\sigma)^{1/2}}\right] d\rho\, d\sigma \qquad (10a)$$

$$-\frac{\pi l\omega g}{MLU} = \int\int [\phi_I{'} \cos\{M\nu'(\rho + \sigma)\} - \phi_R{'} \sin\{M\nu'(\rho + \sigma)\}] \times$$

$$\times \left[\frac{1}{4}\frac{\cos 2\nu'(\rho\sigma)^{1/2}}{(\rho\sigma)^{3/2}} + \nu'^2\frac{\dfrac{\sin 2\nu'(\rho\sigma)^{1/2}}{2\nu'(\rho\sigma)^{1/2}}}{(\rho\sigma)^{1/2}}\right] d\rho\, d\sigma \qquad (10b)$$

where

$$\alpha(x, y) = -\frac{\partial g}{\partial x}.$$

5

In a more compact form these equations can be written

$$\frac{\alpha \pi l}{ML} = \int\int \left[\frac{\phi_R' K_1}{4(\rho\sigma)^{3/2}} + \frac{\phi_I' K_2}{4(\rho\sigma)^{3/2}} + \frac{\phi_R' L_1}{(\rho\sigma)^{1/2}} + \frac{\phi_I' L_2}{(\rho\sigma)^{1/2}} \right] d\rho\, d\sigma \tag{11a}$$

$$-\frac{\pi l \omega g}{MLU} = \int\int \left[\frac{\phi_I' K_1}{4(\rho\sigma)^{3/2}} - \frac{\phi_R' K_2}{4(\rho\sigma)^{3/2}} + \frac{\phi_I' L_1}{(\rho\sigma)^{1/2}} - \frac{\phi_R' L_2}{(\rho\sigma)^{1/2}} \right] d\rho\, d\sigma \tag{11b}$$

where

$$K_1 = \cos\{M\nu'(\rho+\sigma)\} \cos 2\nu'(\rho\sigma)^{1/2} \tag{12a}$$

$$K_2 = \sin\{M\nu'(\rho+\sigma)\} \cos 2\nu'(\rho\sigma)^{1/2} \tag{12b}$$

$$L_1 = \cos\{M\nu'(\rho+\sigma)\} \nu'^2 \frac{\sin 2\nu'(\rho\sigma)^{1/2}}{2\nu'(\rho\sigma)^{1/2}} \tag{13a}$$

$$L_2 = \sin\{M\nu'(\rho+\sigma)\} \nu'^2 \frac{\sin 2\nu'(\rho\sigma)^{1/2}}{2\nu'(\rho\sigma)^{1/2}} . \tag{13b}$$

It will be noted that the right-hand side of (11b) can be obtained from that of (11a) by replacing ϕ_R' by ϕ_I' and ϕ_I' by $-\phi_R'$.
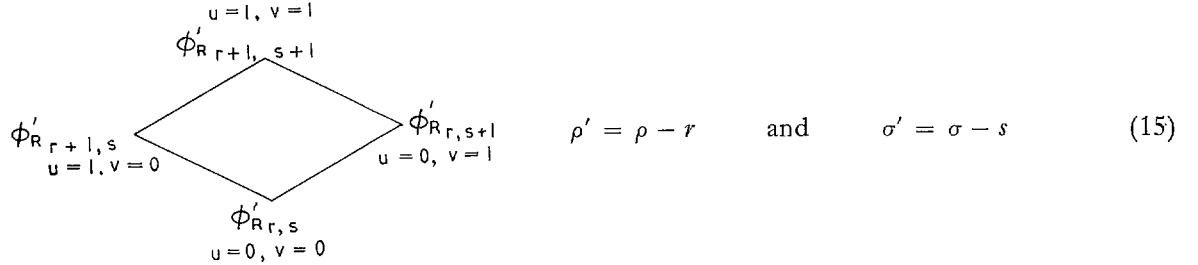
3. Solution of Integral Equation Using a Characteristic Mesh.

3.1. Conversion of the Double Integrals into Weighted Sums of the Potentials.

Let us consider how the double integration for the first term on the right-hand side of (11a) can be carried out. If we assume initially that only full rhombuses occur in the fore-cone of the pivotal point concerned, then we can write

$$\int\int \frac{\phi_R'(\rho,\sigma)K_1(\rho,\sigma)}{4(\rho\sigma)^{3/2}} d\rho\, d\sigma = \sum_{r=0}\sum_{s=0}\int_r^{r+1}\int_s^{s+1} \frac{\phi_R'(\rho,\sigma)K_1(\rho,\sigma)}{4(\rho\sigma)^{3/2}} d\rho\, d\sigma. \tag{14}$$

Consider now the contribution to the integral of the rhombus with base-point r, s. To make the integration possible some assumption has to be made about the variation of $\phi_R'(\rho,\sigma)$ over the rhombus. If we introduce variables

$$\rho' = \rho - r \quad \text{and} \quad \sigma' = \sigma - s \tag{15}$$

it will be seen that we can represent $\phi_R'(\rho,\sigma)$ as

$$\phi_R'(\rho,\sigma) = \lambda_{00}(\rho',\sigma')\phi_R'{}_{r,s} + \lambda_{10}(\rho',\sigma')\phi_R'{}_{r+1,s} + \lambda_{01}(\rho',\sigma')\phi_R'{}_{r,s+1} + \lambda_{11}(\rho',\sigma')\phi_R'{}_{r+1,s+1}. \tag{16}$$

where $\lambda_{uv}(\rho',\sigma')$ is an interpolation function such that $\lambda_{uv}(\rho',\sigma') = 1$ at the vertex $\rho' = u, \sigma' = v$ and equals zero at the other vertices of the rhombus. Thus the contribution of rhombus r, s can be written,

$$\int_0^1\int_0^1 \frac{\left[\sum_{u=0}^1\sum_{v=0}^1 \lambda_{uv}(\rho',\sigma')\phi_R'{}_{r+u,s+v}\right] K_1}{4(\rho'+r)^{3/2}(\sigma'+s)^{3/2}} d\rho'\, d\sigma'.$$

6

However, even with the simplest choice of the $\lambda_{uv}(\rho', \sigma')$ functions, the complexity of K_1 precludes an integration in closed form and because of this a somewhat different approach is made.

The alternative approach is to assume that along lines $\sigma' = $ constant or $\rho' = $ constant, the product $\phi_R' K_1$ varies parabolically with the other variable, fitting exactly at the 9 points: $\rho' = 0, \frac{1}{2}, 1; \sigma' = 0, \frac{1}{2}, 1$.

We introduce therefore a system of parabolic interpolation functions $g_i(\rho')$, $i = 0, \frac{1}{2}, 1$ having the properties

$$g_i(\rho') = 1, \quad \text{if} \quad \rho' = i; \qquad g_i(\rho') = 0, \quad \text{if} \quad \rho' \neq i.$$

Thus

$$\left.\begin{aligned} g_0(\rho') &= 2(\rho' - \tfrac{1}{2})(\rho' - 1) \\ g_{1/2}(\rho') &= -4\rho'(\rho' - 1) \\ g_1(\rho') &= 2\rho'(\rho' - \tfrac{1}{2}). \end{aligned}\right\} \tag{17}$$

$\phi_R' K_1$ can now be written as

$$\phi_R' K_1 = \sum_{i=0, 1/2, 1} \sum_{j=0, 1/2, 1} \phi_R'(r+i, s+j) K_1(r+i, s+j) g_i(\rho') g_j(\sigma'),$$

giving the correct values at the 9 points shown below.
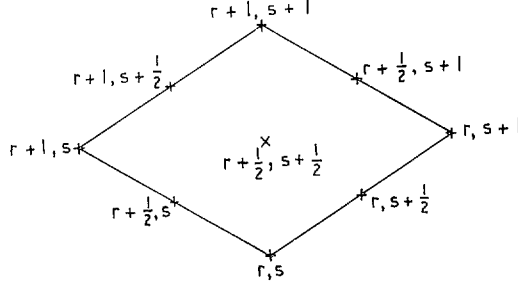
We now introduce the representation for ϕ_R' introduced earlier, and obtain finally

$$\phi_R' K_1 = \sum_{i=0, 1/2, 1} \sum_{j=0, 1/2, 1} \left[\sum_{u=0}^{1} \sum_{v=0}^{1} \lambda_{uv}(i, j) \phi_R'(r+u, s+v) \right] K_1(r+i, s+j) g_i(\rho') g_j(\sigma').$$

If we now write the contribution of rhombus r, s as

$$\int_0^1 \int_0^1 \frac{\phi_R'(\rho', \sigma') K_1(\rho', \sigma')}{4(\rho'+r)^{3/2}(\sigma'+s)^{3/2}} d\rho' d\sigma' = \sum_{u=0}^{1} \sum_{v=0}^{1} C_{r+u, s+v} \phi_R'(r+u, s+v)$$

$$= C_{r,s} \phi_{R'r,s} + C_{r+1,s} \phi_{R'r+1,s} + C_{r,s+1} \phi_{R'r,s+1} + C_{r+1,s+1} \phi_{R'r+1,s+1} \tag{18}$$

we see that

$$C_{r+u, s+v} = \sum_{i=0, 1/2, 1} \sum_{j=0, 1/2, 1} \lambda_{uv}(i, j) K_1(r+i, s+j) \int_0^1 \frac{g_i(\rho')}{2(\rho'+r)^{3/2}} d\rho' \int_0^1 \frac{g_j(\sigma')}{2(\sigma'+s)^{3/2}} d\sigma'. \tag{19}$$

Thus, if we write

$$\int_0^1 \frac{g_i(\rho')}{2(\rho'+r)^{3/2}} d\rho' = G_i(r), \tag{20}$$

we have

$$C_{r+u, s+v} = \sum_{i=0, 1/2, 1} \sum_{j=0, 1/2, 1} \lambda_{uv}(i, j) K_1(r+i, s+j) G_i(r) G_j(s). \tag{21}$$

7

Although there appear to be 9 terms in this sum, there are in fact only 6, due to the properties of $\lambda_{uv}(i,j)$ which for a given u, v (i.e. given vertex of the rhombus) must vanish at the other 3 vertices. If, furthermore, we take the simplest possible variation for ϕ_R', i.e. a linear variation in ρ, times a linear variation in σ, the number of terms reduces to 4. The non-zero terms for $u = 0$, $v = 0$ are illustrated below.
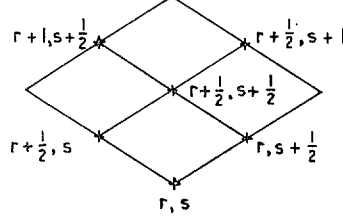
General variation for ϕ_R': $u = 0$, $v = 0$.
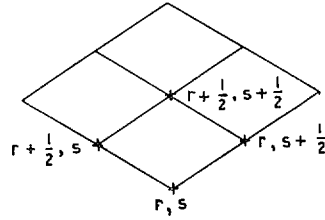
Double linear variation for ϕ_R': $u = 0$, $v = 0$.

At this stage we have obtained the contribution to the integral from rhombus r, s. Our next task is to obtain the net coefficient of $\phi_{R\,r,s}'$ by considering the contributions from all those rhombuses which involve $\phi_{R\,r,s}'$.

In general only 4 rhombuses at most can contribute to the net coefficient of $\phi_{R\,r,s}'$. These are the rhombuses having base points:

$$r, s; \qquad r-1, s; \qquad r, s-1; \qquad r-1, s-1.$$
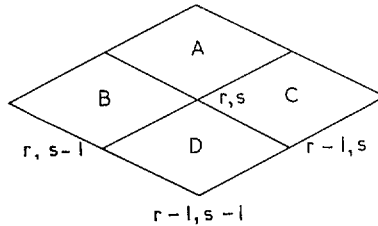
The contribution to the net coefficient of $\phi_{R\,r,s}'$ will be

$$C_{r+u,\,s+v} \text{ for } u = 0, v = 0 \text{ from rhombus A}$$

$$C_{r+u,\,s-1+v} \text{ for } u = 0, v = 1 \text{ from rhombus B}$$

$$C_{r-1+u,\,s+v} \text{ for } u = 1, v = 0 \text{ from rhombus C}$$

$$C_{r-1+u,\,s-1+v} \text{ for } u = 1, v = 1 \text{ from rhombus D}.$$

Thus the net coefficient of $\phi_{R\,r,s}'$ will be

$$\sum_{u=0}^{1} \sum_{v=0}^{1} \left[\sum_{i=0,\,1/2,\,1} \sum_{j=0,\,1/2,\,1} \lambda_{uv}(i,j) K_1(r+i-u,\, s+j-v) G_i(r-u) G_j(s-v) \right], \qquad (22)$$

where the contributions from rhombuses A, B, C, D can be obtained by considering the combinations of u and v indicated above.

If we now return to the other terms on the right-hand side of (11a), we see that ultimately the equation can be written as a weighted sum of the potentials in the form

$$\frac{\alpha \pi l}{ML} = \sum_{r=0} \sum_{s=0} [W_{rs}\phi'_{R\,r,s} + \overline{W}_{rs}\phi'_{I\,r,s}] \tag{23}$$

where

$$W_{rs} = \sum_{u=0}^{1} \sum_{v=0}^{1} \left[\sum_{i=0,1/2,1} \sum_{j=0,1/2,1} \lambda_{uv}(i,j)\{K_1(r+i-u,\,s+j-v)G_i(r-u)G_j(s-v) + \right.$$
$$\left. + L_1(r+i-u,\,s+j-v)G_i^*(r-u)G_j^*(s-v)\} \right] \tag{24}$$

$$\overline{W}_{rs} = \sum_{u=0}^{1} \sum_{v=0}^{1} \left[\sum_{i=0,1/2,1} \sum_{j=0,1/2,1} \lambda_{uv}(i,j)\{K_2(r+i-u,\,s+j-v)G_i(r-u)G_j(s-v) + \right.$$
$$\left. + L_2(r+i-u,\,s+j-v)G_i^*(r-u)G_j^*(s-v)\} \right] \tag{25}$$

and

$$G_i^*(r) = \int_0^1 \frac{g_i(\rho')}{(\rho'+r)^{1/2}}\,d\rho'. \tag{26}$$

When $r = 0$, the C and D rhombuses lie outside the pivotal fore-cone and the contributions from these rhombuses do not occur. Similarly when $s = 0$ there are no contributions from the B and D rhombuses. These effects are allowed for by taking the functions G and G^* as zero if the argument is negative. Explicit forms for $\lambda_{uv}(i,j)$ and $G_i(r)$, $G_i^*(r)$ will be given later.

Similarly equation (11b) becomes

$$-\frac{\pi l\omega g}{MLU} = \sum_{r=0} \sum_{s=0} [W_{rs}\phi'_{I\,r,s} - \overline{W}_{rs}\phi'_{R\,r,s}]. \tag{27}$$

Since K_1, K_2, L_1, L_2 are symmetric functions of r and s, in the sense that $K_1(r,s) = K_1(s,r)$, etc., it will be seen from (24) and (25) that the regular weights are also symmetric, i.e. $W_{rs} = W_{sr}$, $\overline{W}_{rs} = \overline{W}_{sr}$. Thus it is sufficient to hold only the right-hand half of the weight array for which $s \geqslant r$.

It is not difficult to see that, even when irregular rhombuses are present, equations (23) and (27) are still of the same form, except that the expressions for W_{rs} and $\overline{W}_{rs}$ will be somewhat modified. Before going on to discuss the treatment of irregular rhombuses, we first indicate the technique for solving equations (23) and (27).

3.2. *Solution of the Basic Integral Equations for the Pivotal ϕ_R' and ϕ_I'.*

As an example of the method of solution let us consider the simple planform shown, which is symmetric about an axis in the free-stream direction. We assume that ϕ_R' and ϕ_I' are either symmetric or anti-symmetric functions of y, so that the potentials need only be computed on the starboard side of the wing.

We first find that row of rhombuses on the starboard side of the planform which has the greatest σ co-ordinate. In this row we start with that rhombus on the starboard side of the wing (including the centre-line) which has the greatest ρ co-ordinate. After computing the first ϕ_R' and ϕ_I' we work down this row $\sigma = $ const. decreasing ρ each time. At each stage, if the current rhombus is on the planform, we compute ϕ_R' and ϕ_I'. If it is not on the planform, i.e. if it is forward of the leading edge, we jump down the row until a rhombus is encountered which is on the planform. This

9

procedure is continued until the row is finished. It will be noted that, as shown in the diagram, when the row is finished the symmetric row on the port side of the wing can be filled in. The same
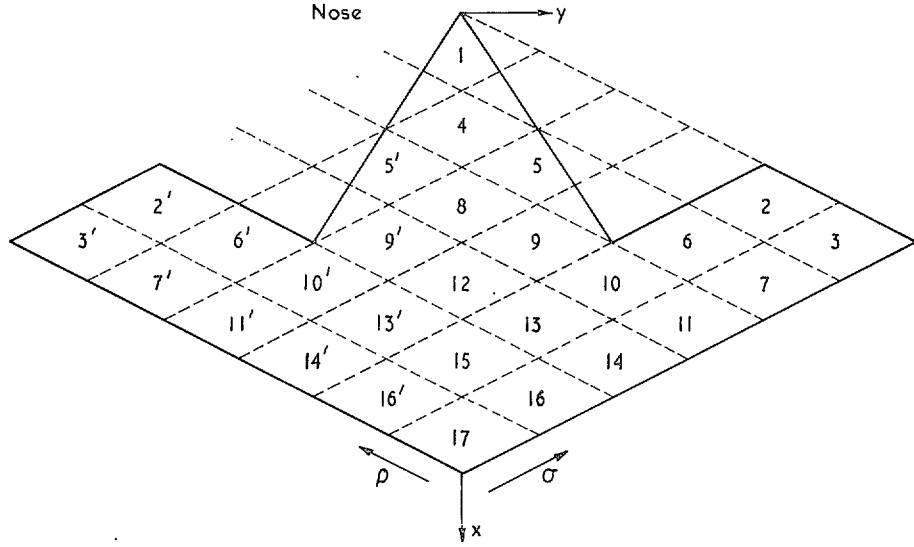
procedure is now followed for the next downstream row $\sigma = $ const. and it will be seen that the rhombuses will be dealt with in the order shown on the diagram. Proceeding in this way it can be seen that, at any given stage, all the upstream potentials in the fore-cone are known and it remains each time to determine the pivotal ϕ_R' and ϕ_I'.

Equations (23) and (27) can be written

$$W_{0,0}\phi_{R\,0,0}' + \overline{W}_{00}\phi_{I\,0,0}' = \frac{\alpha\pi l}{ML} - \Sigma\,\Sigma'\,[W_{rs}\phi_{R\,r,s}' + \overline{W}_{rs}\phi_{I\,r,s}']$$

$$-\overline{W}_{00}\phi_{R\,0,0}' + W_{00}\phi_{I\,0,0}' = -\frac{\pi l\omega g}{MLU} - \Sigma\,\Sigma'\,[W_{rs}\phi_{I\,r,s}' - \overline{W}_{rs}\phi_{R\,r,s}']$$

and hence

$$\phi_{R\,0,0}' = k_1 A - k_2 B \tag{28a}$$

$$\phi_{I\,0,0}' = k_2 A + k_1 B, \tag{28b}$$

where

$$k_1 = \frac{W_{00}}{W_{00}{}^2 + \overline{W}_{00}{}^2} \tag{29a}$$

$$k_2 = \frac{\overline{W}_{00}}{W_{00}{}^2 + \overline{W}_{00}{}^2} \tag{29b}$$

$$A = \frac{\alpha\pi l}{ML} - \Sigma\,\Sigma'\,[W_{rs}\phi_{R\,r,s}' + \overline{W}_{rs}\phi_{I\,r,s}'] \tag{30a}$$

$$B = -\frac{\pi l\omega g}{MLU} - \Sigma\,\Sigma'\,[W_{rs}\phi_{I\,r,s}' - \overline{W}_{rs}\phi_{R\,r,s}']. \tag{30b}$$

The dash on the double summation indicates that the pivotal rhombus is not to be included in the summation.

This procedure applies generally, even if irregular rhombuses are present, provided the appropriate W_{rs} and $\overline{W}_{rs}$ are taken.

10

3.3. *Determination of the Potential in the Wake.*

For wings with subsonic trailing edges, to determine the potential over certain regions of the planform, it will be necessary to know the potential over parts of the wake region.
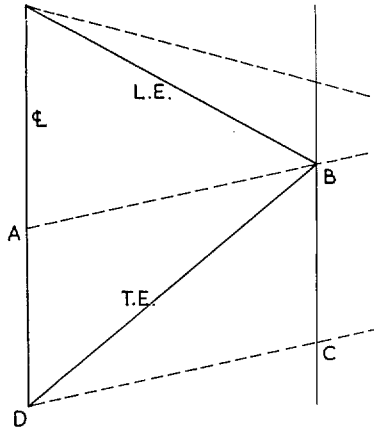
This is illustrated in the diagram shown, where it is clear that for any point on the planform in the region ABD the fore-cone always contains part of the wake region BCD. By making use of the fact that no pressure difference can be sustained between the upper and lower surfaces of the wake, which is assumed to lie in the plane $z = 0$, the potential at any point in the wake can be related to the value of the potential directly upstream at the trailing edge.

The Euler equations of motion are:

$$- \frac{1}{\rho} \operatorname{grad} p = \frac{D\mathbf{V}}{Dt}.$$

Thus taking the x component of this equation and the linearised form of D/Dt, we get

$$- \frac{1}{\rho} \frac{\partial p}{\partial x} = \left(U \frac{\partial}{\partial x} + \frac{\partial}{\partial t} \right) \frac{\partial \phi}{\partial x}.$$

Integrating with respect to x, we obtain

$$p - p_\infty = - \rho_\infty \left(U \frac{\partial \phi}{\partial x} + i\omega\phi \right).$$

Since ϕ is an anti-symmetric function of z and no pressure difference can be sustained between the upper and lower surfaces of the wake, we have

$$U \frac{\partial \phi}{\partial x} = - i\omega\phi$$

and hence

$$\phi = \phi_{\text{T.E.}} \exp \left\{ - i\omega(x - x_{\text{T.E.}})/U \right\}.$$

If we now write $\phi = \phi_R + i\phi_I$ and put $\omega(x - x_{\text{T.E.}})/U = \alpha'$ we get

$$\phi_R + i\phi_I = (\phi_{\text{T.E.}R} + i\phi_{\text{T.E.}I}) (\cos \alpha' - i \sin \alpha')$$

and hence

$$\phi_R = \phi_{\text{T.E.}R} \cos \alpha' + \phi_{\text{T.E.}I} \sin \alpha' \tag{31a}$$

$$\phi_I = - \phi_{\text{T.E.}R} \sin \alpha' + \phi_{\text{T.E.}I} \cos \alpha'. \tag{31b}$$

11

Thus, if at any stage ϕ_R and ϕ_I are required for a rhombus in the wake, they can always be computed from the trailing-edge values directly upstream, which will have been computed at some earlier stage.

It is assumed that the actual trailing edge will be replaced by an indented version which approximates to it but fits exactly on the characteristic mesh. In this case, if $\phi_{\text{T.E.}}$ is in row $n_{\text{T.E.}}$ and ϕ_{wake} is in row n, where $n > n_{\text{T.E.}}$, we have

$$\alpha' = \frac{\omega(x - x_{\text{T.E.}})}{U} = \frac{2l\beta\omega}{MU}(n - n_{\text{T.E.}}) \tag{32}$$

since $2l\beta/M$ is the length of the streamwise diagonal of a basic rhombus.
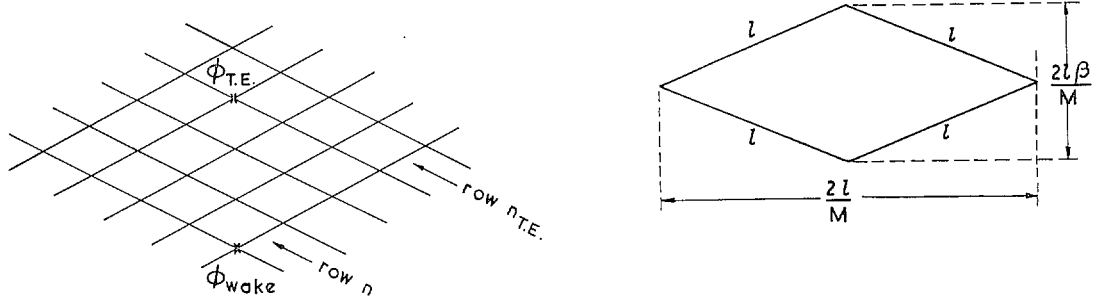
4. *Regular Pivotal Weights.*

4.1. *Parabolic Interpolation Weights.*

From equations (20) and (17), we have

$$
\left.
\begin{aligned}
G_0(r) &= \int_0^1 \frac{(\rho' - \tfrac{1}{2})(\rho' - 1)}{(\rho' + r)^{3/2}}\, d\rho' \\[2mm]
G_{1/2}(r) &= -\int_0^1 \frac{2\rho'(\rho' - 1)}{(\rho' + r)^{3/2}}\, d\rho' \\[2mm]
G_1(r) &= \int_0^1 \frac{\rho'(\rho' - \tfrac{1}{2})}{(\rho' + r)^{3/2}}\, d\rho'
\end{aligned}
\right\} \tag{33}
$$

Performing the integrations, we get answers in which initially each term appearing is of order $r^{3/2}$, although the final answer is of order $r^{-3/2}$. To avoid heavy cancellation with consequent loss of accuracy for the larger values of r, the answers were manipulated into the better conditioned forms shown below, in which each term is of order $r^{1/2}$.

$$G_0(r) = \frac{2(r+1)(r+\tfrac{1}{2})}{r^{1/2}(r+1)^{1/2}\{(r+1)^{1/2} + r^{1/2}\}} - \frac{4r+3}{r^{1/2} + (r+1)^{1/2}} + \frac{2r^2 + 2r + \tfrac{2}{3}}{(r+1)^{3/2} + r^{3/2}} \qquad r \geqslant 1$$

$$G_0(0) = -\frac{10}{3}$$

$$G_{1/2}(r) = 2\left[\frac{-2r(r+1)}{r^{1/2}(r+1)^{1/2}\{(r+1)^{1/2} + r^{1/2}\}} + \frac{2(2r+1)}{r^{1/2} + (r+1)^{1/2}} - \frac{2r^2 + 2r + \tfrac{2}{3}}{(r+1)^{3/2} + r^{3/2}}\right] \qquad r \geqslant 1$$

$$G_{1/2}(0) = \frac{8}{3}$$

$$G_1(r) = \frac{r(2r+1)}{r^{1/2}(r+1)^{1/2}\{(r+1)^{1/2} + r^{1/2}\}} - \frac{4r+1}{r^{1/2} + (r+1)^{1/2}} + \frac{2r^2 + 2r + \tfrac{2}{3}}{(r+1)^{3/2} + r^{3/2}} \qquad r \geqslant 1$$

$$G_1(0) = -\frac{1}{3}. \tag{34}$$

12

For the case $r = 0$ the integrated forms are singular at the lower limit and, in accordance with the usual rules for manipulating integrals of this type in supersonic aerodynamics, the singular parts are ignored.

In a similar manner from equations (26) and (17), we have

$$G_0(r)^* = \int_0^1 \frac{2(\rho' - \frac{1}{2})(\rho' - 1)}{(\rho' + r)^{1/2}}\, d\rho'$$

$$G_{1/2}(r)^* = -\int_0^1 \frac{4\rho'(\rho' - 1)}{(\rho' + r)^{1/2}}\, d\rho'$$

$$G_1(r)^* = \int_0^1 \frac{2\rho'(\rho' - \frac{1}{2})}{(\rho' + r)^{1/2}}\, d\rho'. \tag{35}$$

Performing the integrations, we get answers in which initially each term appearing is of order $r^{5/2}$, although the final answer is of order $r^{-1/2}$. As before the answers were manipulated into the better conditioned forms shown below, in which each term is of order $r^{1/2}$.

$$G_0(r)^* = \frac{4r(72r + 121)}{15\{(8r + 11)(r + 1)^{1/2} + (8r + 15)r^{1/2}\}} + \frac{4}{5}(r + 1)^{1/2} - 2r^{1/2} \qquad r \geqslant 0$$

$$G_0(0)^* = \frac{4}{5}$$

$$G_{1/2}(r)^* = \frac{16}{15}\left[(r + 1)^{1/2} - \frac{r(8r + 9)}{(4r + 3)(r + 1)^{1/2} + (4r + 5)r^{1/2}}\right] \qquad r \geqslant 0$$

$$G_{1/2}(0)^* = \frac{16}{15}$$

$$G_1(r)^* = \frac{2}{15}\left[(r + 1)^{1/2} + \frac{2r(1 - 8r)}{(8r + 1)(r + 1)^{1/2} + (8r + 5)r^{1/2}}\right] \qquad r \geqslant 0$$

$$G_1(0)^* = \frac{2}{15}. \tag{36}$$

These integrated forms are regular at the lower limit for $r = 0$.

4.2. The Regular Parabolic Interpolation Weights for a Linear Variation of Potential.

We assume that along lines $\sigma = \text{const.}$ or $\rho = \text{const.}$, ϕ varies linearly in the other variable. Thus in (16) we must take

$$\lambda_{uv}(\rho', \sigma') = f_u(\rho')f_v(\sigma')$$

where

$$f_u(\rho'), \qquad u = 0 \quad \text{or} \quad 1,$$

is such that

$$f_u(\rho') = 1, \qquad \text{for} \qquad \rho' = u$$
$$= 0, \qquad \text{for} \qquad \rho' \neq u.$$

Thus

$$f_0(\rho') = 1 - \rho'$$
$$f_1(\rho') = \rho'$$

Hence

$$\lambda_{00}(\rho', \sigma') = (1 - \rho')(1 - \sigma')$$
$$\lambda_{10}(\rho', \sigma') = \rho'(1 - \sigma')$$
$$\lambda_{01}(\rho', \sigma') = (1 - \rho')\sigma'$$
$$\lambda_{11}(\rho', \sigma') = \rho'\sigma'. \tag{37}$$

13

We can now obtain the requisite values for $i = \rho' = 0, \frac{1}{2}, 1$; $j = \sigma' = 0, \frac{1}{2}, 1$.

	λ_{00}			λ_{10}			λ_{01}			λ_{11}		
i \ j	0	$\frac{1}{2}$	1	0	$\frac{1}{2}$	1	0	$\frac{1}{2}$	1	0	$\frac{1}{2}$	1
0	1	$\frac{1}{2}$	0	0	0	0	0	$\frac{1}{2}$	1	0	0	0
$\frac{1}{2}$	$\frac{1}{2}$	$\frac{1}{4}$	0	$\frac{1}{2}$	$\frac{1}{4}$	0	0	$\frac{1}{4}$	$\frac{1}{2}$	0	$\frac{1}{4}$	$\frac{1}{2}$
1	0	0	0	1	$\frac{1}{2}$	0	0	0	0	0	$\frac{1}{2}$	1

Let us consider first the $K_1 G_i G_j$ terms in (24), taking the A, B, C, D contributions in turn, then

$$\delta W_{rs} = K_1(r, s)G_0(r)G_0(s) + \tfrac{1}{2}K_1(r+\tfrac{1}{2}, s)G_{1/2}(r)G_0(s) + \tfrac{1}{2}K_1(r, s+\tfrac{1}{2})G_0(r)G_{1/2}(s) +$$
$$+ \tfrac{1}{4}K_1(r+\tfrac{1}{2}, s+\tfrac{1}{2})G_{1/2}(r)G_{1/2}(s) + K_1(r, s)G_0(r)G_1(s-1) + \tfrac{1}{2}K_1(r, s-\tfrac{1}{2})G_0(r)G_{1/2}(s-1) +$$
$$+ \tfrac{1}{2}K_1(r+\tfrac{1}{2}, s)G_{1/2}(r)G_1(s-1) + \tfrac{1}{4}K_1(r+\tfrac{1}{2}, s-\tfrac{1}{2})G_{1/2}(r)G_{1/2}(s-1) +$$
$$+ K_1(r, s)G_1(r-1)G_0(s) + \tfrac{1}{2}K_1(r-\tfrac{1}{2}, s)G_{1/2}(r-1)G_0(s) + \tfrac{1}{2}K_1(r, s+\tfrac{1}{2})G_1(r-1)G_{1/2}(s) +$$
$$+ \tfrac{1}{4}K_1(r-\tfrac{1}{2}, s+\tfrac{1}{2})G_{1/2}(r-1)G_{1/2}(s) + K_1(r, s)G_1(r-1)G_1(s-1) +$$
$$+ \tfrac{1}{2}K_1(r, s-\tfrac{1}{2})G_1(r-1)G_{1/2}(s-1) + \tfrac{1}{2}K_1(r-\tfrac{1}{2}, s)G_{1/2}(r-1)G_1(s-1) +$$
$$+ \tfrac{1}{4}K_1(r-\tfrac{1}{2}, s-\tfrac{1}{2})G_{1/2}(r-1)G_{1/2}(s-1). \tag{38}$$

Collecting up terms we get

$$\delta W_{rs} = K_1(r, s)\left[G_0(r)G_0(s) + G_0(r)G_1(s-1) + G_1(r-1)G_0(s) + G_1(r-1)G_1(s-1)\right] +$$
$$+ \tfrac{1}{2}K_1(r+\tfrac{1}{2}, s)\left[G_{1/2}(r)G_0(s) + G_{1/2}(r)G_1(s-1)\right] +$$
$$+ \tfrac{1}{2}K_1(r, s+\tfrac{1}{2})\left[G_0(r)G_{1/2}(s) + G_1(r-1)G_{1/2}(s)\right] +$$
$$+ \tfrac{1}{2}K_1(r-\tfrac{1}{2}, s)\left[G_{1/2}(r-1)G_0(s) + G_{1/2}(r-1)G_1(s-1)\right] +$$
$$+ \tfrac{1}{2}K_1(r, s-\tfrac{1}{2})\left[G_0(r)G_{1/2}(s-1) + G_1(r-1)G_{1/2}(s-1)\right] +$$
$$+ \tfrac{1}{4}K_1(r+\tfrac{1}{2}, s+\tfrac{1}{2})G_{1/2}(r)G_{1/2}(s) + \tfrac{1}{4}K_1(r+\tfrac{1}{2}, s-\tfrac{1}{2})G_{1/2}(r)G_{1/2}(s-1) +$$
$$+ \tfrac{1}{4}K_1(r-\tfrac{1}{2}, s+\tfrac{1}{2})G_{1/2}(r-1)G_{1/2}(s) + \tfrac{1}{4}K_1(r-\tfrac{1}{2}, s-\tfrac{1}{2})G_{1/2}(r-1)G_{1/2}(s-1). \tag{39}$$

If we now introduce

$$I(r) = G_0(r) + G_1(r-1), \tag{40}$$

we get

$$\delta W_{rs} = K_1(r, s)I(r)I(s) + \tfrac{1}{2}K_1(r+\tfrac{1}{2}, s)I(s)G_{1/2}(r) +$$
$$+ \tfrac{1}{2}K_1(r, s+\tfrac{1}{2})I(r)G_{1/2}(s) + \tfrac{1}{2}K_1(r-\tfrac{1}{2}, s)I(s)G_{1/2}(r-1) +$$
$$+ \tfrac{1}{2}K_1(r, s-\tfrac{1}{2})I(r)G_{1/2}(s-1) +$$
$$+ \tfrac{1}{4}K_1(r+\tfrac{1}{2}, s+\tfrac{1}{2})G_{1/2}(r)G_{1/2}(s) + \tfrac{1}{4}K_1(r+\tfrac{1}{2}, s-\tfrac{1}{2})G_{1/2}(r)G_{1/2}(s-1) +$$
$$+ \tfrac{1}{4}K_1(r-\tfrac{1}{2}, s+\tfrac{1}{2})G_{1/2}(r-1)G_{1/2}(s) + \tfrac{1}{4}K_1(r-\tfrac{1}{2}, s-\tfrac{1}{2})G_{1/2}(r-1)G_{1/2}(s-1). \tag{41}$$

14

The final expression for W_{rs} is

$$W_{rs} = \delta W_{rs} + \text{ a similar expression with } L_1 \text{ replacing } K_1 \text{ and } G^* \text{ replacing } G. \quad (42)$$

From (25) and (12a), (12b), (13a), (13b) it will be seen that $\overline{W}_{rs}$ can be obtained from the expression for W_{rs} by replacing $\cos\{M\nu'(\rho+\sigma)\}$ terms by $\sin\{M\nu'(\rho+\sigma)\}$ throughout.

A computer programme has been written for use with the Ferranti Pegasus to evaluate the array of weights according to the formulae given above. Apart from the choice of the array geometry, the only other parameters entering are M and ν'.

By substituting in the values $r = 0$, $s = 0$ in the expressions given above, it can be shown that

$$W_{00} = \frac{1}{9}\left[100 - 80\cos\left(\tfrac{1}{2}M\nu'\right) + 16\cos(M\nu')\cos\nu'\right] +$$

$$+ \frac{\nu'^2}{225}\left[144 + 192\cos\left(\tfrac{1}{2}M\nu'\right) + 64\cos(M\nu')\frac{\sin\nu'}{\nu'}\right] \quad (43)$$

$$\overline{W}_{00} = \frac{1}{9}\left[16\cos\nu'\sin(M\nu') - 80\sin\left(\tfrac{1}{2}M\nu'\right)\right] +$$

$$+ \frac{\nu'^2}{225}\left[192\sin\left(\tfrac{1}{2}M\nu'\right) + 64\sin(M\nu')\frac{\sin\nu'}{\nu'}\right]. \quad (44)$$

These quantities are needed to evaluate k_1 and k_2, see (29a), (29b), when the pivotal rhombus is regular. Also W_{00} is normally used to non-dimensionalise and scale the weight array.

4.3. The Regular Parabolic Interpolation Weights for a Variation of Potential $\phi = a + by + cy^2 + dx$.

This variation of potential was introduced in dealing with delta wings of low aspect ratio, where it seems desirable to allow the potential to have some curvature in the spanwise direction.

We introduce an x, y system which has a different origin and scale from the usual one. The x, y co-ordinates and their relation to the points $i = 0, \tfrac{1}{2}, 1; j = 0, \tfrac{1}{2}, 1$ are illustrated in the diagram below.

15
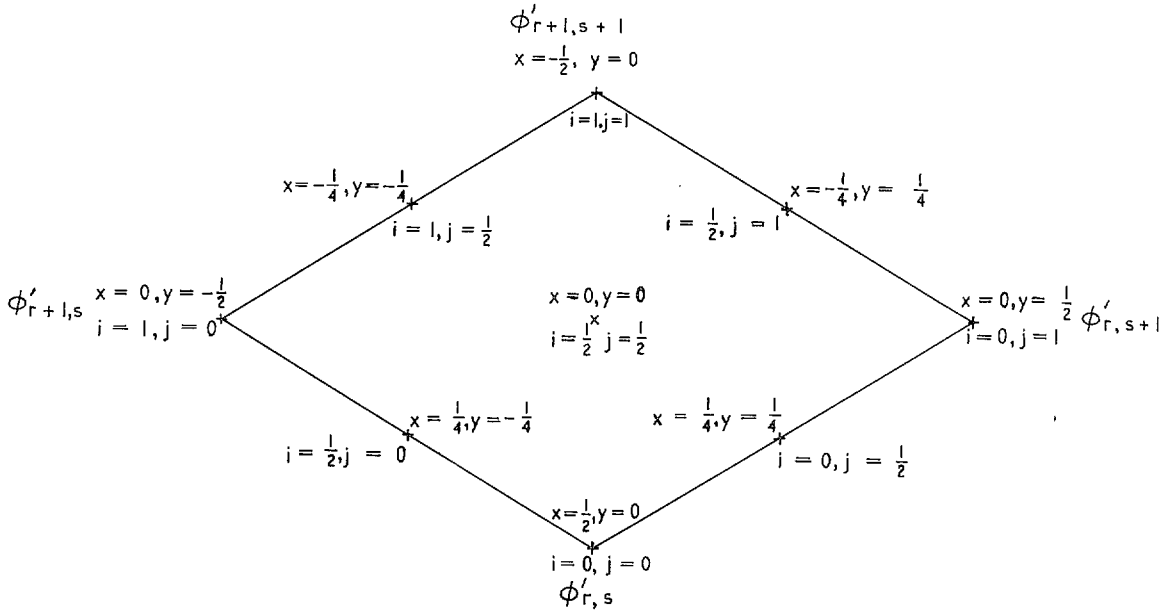
A suitable representation for ϕ' is

$$\phi' = 2\phi'_{r+1,s}y(y-\tfrac{1}{2}) - 4(\tfrac{1}{2}\phi'_{r+1,s+1}+\tfrac{1}{2}\phi'_{r,s})(y-\tfrac{1}{2})(y+\tfrac{1}{2}) +$$
$$+ 2\phi'_{r,s+1}y(y+\tfrac{1}{2}) + x(\phi'_{r,s} - \phi'_{r+1,s+1}). \tag{45}$$

Hence

$$\left.\begin{aligned}
\lambda_{00}(x,y) &= -2(y-\tfrac{1}{2})(y+\tfrac{1}{2}) + x \\
\lambda_{10}(x,y) &= 2y(y-\tfrac{1}{2}) \\
\lambda_{01}(x,y) &= 2y(y+\tfrac{1}{2}) \\
\lambda_{11}(x,y) &= -2(y-\tfrac{1}{2})(y+\tfrac{1}{2}) - x.
\end{aligned}\right\} \tag{46}$$

We can now obtain the requisite values for $i = 0, \tfrac{1}{2}, 1; j = 0, \tfrac{1}{2}, 1$.

	λ_{00}			λ_{10}			λ_{01}			λ_{11}		
$i \backslash j$	0	$\tfrac{1}{2}$	1	0	$\tfrac{1}{2}$	1	0	$\tfrac{1}{2}$	1	0	$\tfrac{1}{2}$	1
0	1	$\tfrac{5}{8}$	0	0	$-\tfrac{1}{8}$	0	0	$\tfrac{3}{8}$	1	0	$\tfrac{1}{8}$	0
$\tfrac{1}{2}$	$\tfrac{5}{8}$	$\tfrac{1}{2}$	$\tfrac{1}{8}$	$\tfrac{3}{8}$	0	$-\tfrac{1}{8}$	$-\tfrac{1}{8}$	0	$\tfrac{3}{8}$	$\tfrac{1}{8}$	$\tfrac{1}{2}$	$\tfrac{5}{8}$
1	0	$\tfrac{1}{8}$	0	1	$\tfrac{3}{8}$	0	0	$-\tfrac{1}{8}$	0	0	$\tfrac{5}{8}$	1

Let us consider first the $K_1 G_i G_j$ terms in (24), taking the A, B, C, D contributions in turn, then

$$\delta W_{rs} = K_1(r,s)G_0(r)G_0(s) + \tfrac{5}{8}K_1(r+\tfrac{1}{2},s)G_{1/2}(r)G_0(s) + \tfrac{1}{8}K_1(r+\tfrac{1}{2},s+1)G_{1/2}(r)G_1(s) +$$

$$+ \tfrac{5}{8}K_1(r,s+\tfrac{1}{2})G_0(r)G_{1/2}(s) + \tfrac{1}{2}K_1(r+\tfrac{1}{2},s+\tfrac{1}{2})G_{1/2}(r)G_{1/2}(s) +$$

$$+ \tfrac{1}{8}K_1(r+1,s+\tfrac{1}{2})G_1(r)G_{1/2}(s) - \tfrac{1}{8}K_1(r+\tfrac{1}{2},s-1)G_{1/2}(r)G_0(s-1) +$$

$$+ \tfrac{3}{8}K_1(r,s-\tfrac{1}{2})G_0(r)G_{1/2}(s-1) - \tfrac{1}{8}K_1(r+1,s-\tfrac{1}{2})G_1(r)G_{1/2}(s-1) +$$

$$+ K_1(r,s)G_0(r)G_1(s-1) + \tfrac{3}{8}K_1(r+\tfrac{1}{2},s)G_{1/2}(r)G_1(s-1) +$$

$$+ \tfrac{3}{8}K_1(r-\tfrac{1}{2},s)G_{1/2}(r-1)G_0(s) + K_1(r,s)G_1(r-1)G_0(s) -$$

$$- \tfrac{1}{8}K_1(r-1,s+\tfrac{1}{2})G_0(r-1)G_{1/2}(s) + \tfrac{3}{8}K_1(r,s+\tfrac{1}{2})G_1(r-1)G_{1/2}(s) -$$

$$- \tfrac{1}{8}K_1(r-\tfrac{1}{2},s+1)G_{1/2}(r-1)G_1(s) + \tfrac{1}{8}K_1(r-\tfrac{1}{2},s-1)G_{1/2}(r-1)G_0(s-1) +$$

$$+ \tfrac{1}{8}K_1(r-1,s-\tfrac{1}{2})G_0(r-1)G_{1/2}(s-1) + \tfrac{1}{2}K_1(r-\tfrac{1}{2},s-\tfrac{1}{2})G_{1/2}(r-1)G_{1/2}(s-1) +$$

$$+ \tfrac{5}{8}K_1(r,s-\tfrac{1}{2})G_1(r-1)G_{1/2}(s-1) + \tfrac{5}{8}K_1(r-\tfrac{1}{2},s)G_{1/2}(r-1)G_1(s-1) +$$

$$+ K_1(r,s)G_1(r-1)G_1(s-1). \tag{47}$$

16

Collecting up terms, the coefficients of $K_1(\rho, \sigma)$ can best be displayed in tabular form, as given below.

$\frac{\sigma}{\rho}$	$s-1$	$s-\frac{1}{2}$	s	$s+\frac{1}{2}$	$s+1$
$r+1$	0	$-\frac{1}{8}G_1(r)G_{1/2}(s-1)$	0	$\frac{1}{8}G_1(r)G_{1/2}(s)$	0
$r+\frac{1}{2}$	$-\frac{1}{8}G_{1/2}(r)G_0(s-1)$	0	$\frac{5}{8}G_{1/2}(r)G_0(s) + \frac{3}{8}G_{1/2}(r)G_1(s-1)$	$\frac{1}{2}G_{1/2}(r)G_{1/2}(s)$	$\frac{1}{8}G_{1/2}(r)G_1(s)$
r	0	$\frac{3}{8}G_0(r)G_{1/2}(s-1) + \frac{5}{8}G_1(r-1)G_{1/2}(s-1)$	$[G_0(r)+G_1(r-1)]$ $[G_0(s)+G_1(s-1)]$	$\frac{5}{8}G_0(r)G_{1/2}(s) + \frac{3}{8}G_1(r-1)G_{1/2}(s)$	0
$r-\frac{1}{2}$	$\frac{1}{8}G_{1/2}(r-1)G_0(s-1)$	$\frac{1}{2}G_{1/2}(r-1)G_{1/2}(s-1)$	$\frac{3}{8}G_{1/2}(r-1)G_0(s) + \frac{5}{8}G_{1/2}(r-1)G_1(s-1)$	0	$-\frac{1}{8}G_{1/2}(r-1)G_1(s)$
$r-1$	0	$\frac{1}{8}G_0(r-1)G_{1/2}(s-1)$	0	$-\frac{1}{8}G_0(r-1)G_{1/2}(s)$	0

The final expression for W_{rs} is

$$W_{rs} = \delta W_{rs} + \text{a similar expression with } L_1 \text{ replacing } K_1 \text{ and } G^* \text{ replacing } G. \tag{48}$$

$\overline{W}_{rs}$ can be obtained from the expression for W_{rs} by replacing $\cos\{Mv'(\rho+\sigma)\}$ by $\sin\{Mv'(\rho+\sigma)\}$ throughout.

By substituting in the values $r = 0$, $s = 0$ in the expressions given above, it can be shown that

$$W_{00} = \frac{2}{9}\left[50 - 50\cos\left(\frac{1}{2}Mv'\right) + 16\cos v' \cos(Mv') - \cos(\sqrt{2}\,v')\cos\left(\frac{3}{2}Mv'\right)\right] +$$

$$+ \frac{8}{225}v'^2\left[18 + 30\cos\left(\frac{1}{2}Mv'\right) + 16\frac{\sin v'}{v'}\cos(Mv') + \frac{\sin(\sqrt{2}\,v')}{\sqrt{2}\,v'}\cos\left(\frac{3}{2}Mv'\right)\right] \tag{49}$$

$$\overline{W}_{00} = \frac{2}{9}\left[-50\sin\left(\frac{1}{2}Mv'\right) + 16\cos v' \sin(Mv') - \cos(\sqrt{2}\,v')\sin\left(\frac{3}{2}Mv'\right)\right] +$$

$$+ \frac{8}{225}v'^2\left[30\sin\left(\frac{1}{2}Mv'\right) + 16\frac{\sin v'}{v'}\sin(Mv') + \frac{\sin(\sqrt{2}\,v')}{\sqrt{2}\,v'}\sin\left(\frac{3}{2}Mv'\right)\right] \tag{50}$$

4.4. Regular Linear Interpolation Weights.

As we have previously shown, the starting point in deriving the regular weights is equation (14). We have already discussed certain cases where $\phi_R'(\rho, \sigma)\,K_1(\rho, \sigma)$ is allowed to vary parabolically along lines $\rho = \text{constant}$ or $\sigma = \text{constant}$, this variation being necessary when v' is large enough for the trigonometrical terms appearing in K_1 to have an appreciable curvature over a basic rhombus. However, when v' is small it may be sufficiently accurate to allow only a linear variation of the product $\phi_R'(\rho, \sigma)\,K_1(\rho, \sigma)$. As we shall now show, this simplifies the formulae for the weights considerably.

17

We make use of the functions

$$f_0(\rho') = 1 - \rho', f_1(\rho') = \rho'. \tag{51}$$

A suitable representation of $\phi_R'(\rho, \sigma)K_1(\rho, \sigma)$, over the rhombus whose base point is r, s, is now seen to be

$$\phi_R'K_1 = \sum_{u=0}^{1} \sum_{v=0}^{1} f_u(\rho')f_v(\sigma') [\phi_R'K_1]_{r+u, s+v}. \tag{52}$$

The contribution of rhombus r, s can now be written

$$\int_0^1 \int_0^1 \frac{\sum_{u=0}^{1} \sum_{v=0}^{1} f_u(\rho')f_v(\sigma') [\phi_R'K_1]_{r+u, s+v}}{4(\rho'+r)^{3/2}(\sigma'+s)^{3/2}} \, d\rho' \, d\sigma'$$

$$= \sum_{u=0}^{1} \sum_{v=0}^{1} C_{r+u, s+v}\phi_R'(r+u, s+v). \tag{53}$$

We deduce that

$$C_{r+u, s+v} = K_1(r+u, s+v) \int_0^1 \int_0^1 \frac{f_u(\rho')f_v(\sigma')}{4(\rho'+r)^{3/2}(\sigma'+s)^{3/2}} \, d\rho' \, d\sigma'$$

$$= K_1(r+u, s+v)F_u(r)F_v(s), \tag{54}$$

where

$$F_u(r) = \int_0^1 \frac{f_u(\rho')}{2(\rho'+r)^{3/2}} \, d\rho', \qquad u = 0 \quad \text{or } 1. \tag{55}$$

The contributions to the net coefficient of $\phi_R'_{r,s}$ will be

$$C_{r+u, s+v} \text{ for } u = 0, \ v = 0 \text{ from rhombus A} = K_1(r, s)F_0(r)F_0(s)$$

$$C_{r+u, s-1+v} \text{ for } u = 0, \ v = 1 \text{ from rhombus B} = K_1(r, s)F_0(r)F_1(s-1)$$

$$C_{r-1+u, s+v} \text{ for } u = 1, \ v = 0 \text{ from rhombus C} = K_1(r, s)F_1(r-1)F_0(s)$$

$$C_{r-1+u, s-1+v} \text{ for } u = 1, \ v = 1 \text{ from rhombus D} = K_1(r, s)F_1(r-1)F_1(s-1).$$

Thus the net coefficient of $\phi_R'_{r,s}$ will be

$$K_1(r, s) [F_0(r)F_0(s) + F_0(r)F_1(s-1) + F_1(r-1)F_0(s) + F_1(r-1)F_1(s-1)] \tag{56}$$

$$= K_1(r, s)E(r)E(s),$$

where

$$E(r) = F_0(r) + F_1(r-1). \tag{57}$$

If we now return to the other terms on the right-hand side of (11a), we see that ultimately the equation can again be written in the form (23), where

$$W_{r, s} = K_1(r, s)E(r)E(s) + L_1(r, s)E^*(r)E^*(s) \tag{58}$$

$$\overline{W}_{r, s} = K_2(r, s)E(r)E(s) + L_2(r, s)E^*(r)E^*(s) \tag{59}$$

and

$$E^*(r) = F_0^*(r) + F_1^*(r-1) \tag{60}$$

with

$$F_u^*(r) = \int_0^1 \frac{f_u(\rho')}{(\rho'+r)^{1/2}} \, d\rho', \qquad u = 0 \quad \text{or } 1. \tag{61}$$

18

Making use of equations (12) and (13), we obtain finally

$$W_{rs} = \cos\{Mv'(r+s)\}\,H(v', r, s) \tag{62}$$

$$\overline{W}_{rs} = \sin\{Mv'(r+s)\}\,H(v', r, s), \tag{63}$$

where

$$H(v', r, s) = \cos\{2v'(rs)^{1/2}\}\,E(r)E(s) + v'^2\,\frac{\sin\{2v'(rs)^{1/2}\}}{2v'(rs)^{1/2}}\,E^*(r)E^*(s). \tag{64}$$

As before we have the rule that, for $r = 0$ or $s = 0$, the F_0, F_1 and F_0^*, F_1^* functions are taken zero for negative arguments.

We now derive explicit forms for $E(r)$ and $E^*(r)$. From (55) and (51), we have

$$F_0(r) = \int_0^1 \frac{1 - \rho'}{2(\rho' + r)^{3/2}}\,d\rho' = \int_r^{r+1} \frac{1 + r - \rho}{2\rho^{3/2}}\,d\rho = -(1+r)\left[\frac{1}{(r+1)^{1/2}} - \frac{1}{r^{1/2}}\right] - [(r+1)^{1/2} - r^{1/2}] \tag{65}$$

$$F_1(r) = \int_0^1 \frac{\rho'}{2(\rho' + r)^{3/2}}\,d\rho' = \int_r^{r+1} \frac{\rho - r}{2\rho^{3/2}}\,d\rho = [(r+1)^{1/2} - r^{1/2}] + r\left[\frac{1}{(r+1)^{1/2}} - \frac{1}{r^{1/2}}\right] \tag{66}$$

Hence

$$E(r) = [r^{1/2} - (r-1)^{1/2}] + (r-1)\left[\frac{1}{r^{1/2}} - \frac{1}{(r-1)^{1/2}}\right] - (r+1)\left[\frac{1}{(r+1)^{1/2}} - \frac{1}{r^{1/2}}\right] - [(r+1)^{1/2} - r^{1/2}] \tag{67}$$

$$E(0) = -2, \qquad E(1) = 4 - 2\sqrt{2}. \tag{68}$$

In evaluating $E(r)$, for $r = 0$ or 1, the rule is that any singular terms must be omitted. For $r = 0$, the terms stemming from F_1 must also be omitted.

In a similar manner

$$F_0^*(r) = \int_0^1 \frac{1 - \rho'}{(\rho' + r)^{1/2}}\,d\rho' = \int_r^{r+1} \frac{1 + r - \rho}{\rho^{1/2}}\,d\rho = 2(1+r)[(r+1)^{1/2} - r^{1/2}] - \tfrac{2}{3}[(r+1)^{3/2} - r^{3/2}] \tag{69}$$

$$F_1^*(r) = \int_0^1 \frac{\rho'}{(\rho' + r)^{1/2}}\,d\rho' = \int_r^{r+1} \frac{\rho - r}{\rho^{1/2}}\,d\rho = \frac{2}{3}[(r+1)^{3/2} - r^{3/2}] - 2r[(r+1)^{1/2} - r^{1/2}] \tag{70}$$

Hence

$$E^*(r) = 2(1+r)[(r+1)^{1/2} - r^{1/2}] - \frac{2}{3}[(r+1)^{3/2} - r^{3/2}] + \frac{2}{3}[r^{3/2} - (r-1)^{3/2}] -$$

$$- 2(r-1)[r^{1/2} - (r-1)^{1/2}] \tag{71}$$

$$E^*(0) = 4/3 \text{ omitting } F_1^* \text{ terms.} \tag{72}$$

By substituting $r = 0$, $s = 0$ in equations (62), (63), (64), we obtain

$$W_{00} = 4 + \frac{16}{9}\,v'^2 \tag{73}$$

$$\overline{W}_{00} = 0. \tag{74}$$

It will be noted that, when using weights of this type, since $\overline{W}_{00} = 0$, the equations for the pivotal potentials (28), simplify to

$$\phi_{R\,0,0}' = \frac{1}{W_{00}}\left[\frac{\alpha\pi l}{ML} - \Sigma\,\Sigma'\,(W_{rs}\phi_{R\,r,s}' + \overline{W}_{rs}\phi_{I\,r,s}')\right] \tag{75}$$

$$\phi_{I\,0,0}' = \frac{1}{W_{00}}\left[-\frac{\pi l\omega g}{MLU} - \Sigma\,\Sigma'\,(W_{rs}\phi_{I\,r,s}' - \overline{W}_{r,s}\phi_{R\,r,s}')\right]. \tag{76}$$

19

5. Irregular Rhombus Weights.

5.1. Formation of Irregular Weights when One or More of the A, B, C or D Rhombuses is Irregular.

In general, unless the planform edges are transonic, near the edges of the planform irregular rhombuses will occur in the integration mesh. These irregular rhombuses will be bounded, in general, by three characteristics and the planform edge. Two typical cases, where three vertices lie inside the planform edge, are illustrated below for a subsonic and supersonic leading edge.
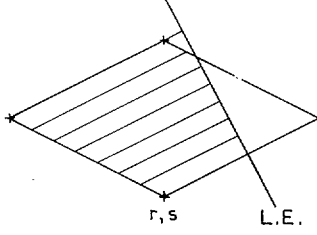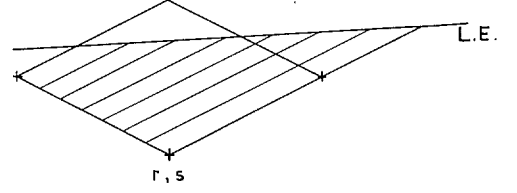
Subsonic L.E.   Supersonic L.E

If we return to equation (14) it will be seen that the contribution of an irregular rhombus, whose leading edge has the equation $\sigma = \sigma_{\text{L.E.}}(\rho)$, will be

$$\int_r^{r+1} \int_s^{\sigma_{\text{L.E.}}(\rho)} \frac{\phi_R{}'(\rho,\,\sigma)K_1(\rho,\,\sigma)}{4(\rho\sigma)^{3/2}}\,d\rho\,d\sigma. \tag{77}$$

As previously we introduce ρ', σ' via equation (15). Assuming that there may be four vertices inside the leading edge, we can write equation (16) as

$$\phi_R{}'(\rho,\,\sigma) = \sum_{u=0}^{1}\sum_{v=0}^{1}\lambda_{uv}(\rho',\,\sigma')\phi_R{}'_{r+u,\,s+v}. \tag{78}$$

It will be noted that interpolation functions $\lambda_{uv}(\rho',\,\sigma')$ must be chosen which have the appropriate behaviour near the leading edge, i.e. λ_{uv} must vary like $(\sigma_{\text{L.E.}} - \sigma)^{1/2}$ near a subsonic edge but like $\sigma_{\text{L.E.}} - \sigma$ near a supersonic edge.

Substituting (78) in (77) and performing the requisite integrations, the contribution of the irregular rhombus whose base point is r, s can be written

$$\tau_{00}(r,\,s)\phi_R{}'_{r,s} + \tau_{10}(r,\,s)\phi_R{}'_{r+1,\,s} + \tau_{01}(r,\,s)\phi_R{}'_{r,\,s+1} + \tau_{11}(r,\,s)\phi_R{}'_{r+1,\,s+1} \tag{79}$$

where

$$\tau_{uv}(r,\,s) = \int_r^{r+1}\int_s^{\sigma_{\text{L.E.}}(\rho)} \frac{\lambda_{uv}(\rho',\,\sigma')K_1(\rho,\,\sigma)}{4(\rho\sigma)^{3/2}}\,d\rho\,d\sigma. \tag{80}$$

Considering the other terms on the right-hand side of equation (11a), we get as the total contribution of the irregular rhombus with base point r, s

$$\sum_{u=0}^{1}\sum_{v=0}^{1}[\tau_{uv}(r,\,s) + \delta_{uv}(r,\,s)]\phi_R{}'_{r+u,\,s+v} + \sum_{u=0}^{1}\sum_{v=0}^{1}[\bar{\tau}_{uv}(r,\,s) + \bar{\delta}_{uv}(r,\,s)]\phi_I{}'_{r+u,\,s+v} \tag{81}$$

where

$$\bar{\tau}_{uv}(r,\,s) = \int_r^{r+1}\int_s^{\sigma_{\text{L.E.}}(\rho)} \frac{\lambda_{uv}(\rho',\,\sigma')K_2(\rho,\,\sigma)}{4(\rho\sigma)^{3/2}}\,d\rho\,d\sigma \tag{82}$$

$$\delta_{uv}(r,\,s) = \int_r^{r+1}\int_s^{\sigma_{\text{L.E.}}(\rho)} \frac{\lambda_{uv}(\rho',\,\sigma')L_1(\rho,\,\sigma)}{(\rho\sigma)^{1/2}}\,d\rho\,d\sigma \tag{83}$$

$$\bar{\delta}_{uv}(r,\,s) = \int_r^{r+1}\int_s^{\sigma_{\text{L.E.}}(\rho)} \frac{\lambda_{uv}(\rho',\,\sigma')L_2(\rho,\,\sigma)}{(\rho\sigma)^{1/2}}\,d\rho\,d\sigma. \tag{84}$$

20

In the summation (81), if any given vertex of the irregular rhombus is missing, the appropriate combination of u, v is deleted from the expression.

If we now consider the way in which the regular weight is formed up from the A, B, C, D contributions, we arrive at the following formula for the weight at the point r, s, assuming any one or more of A, B, C, D to be irregular.

Let

$$W_{rs\,\mathrm{reg}} = W_{rs}(\mathrm{A}) + W_{rs}(\mathrm{B}) + W_{rs}(\mathrm{C}) + W_{rs}(\mathrm{D}),\qquad(85)$$

then

$$W_{rs\,\mathrm{irreg}} = W_{rs\,\mathrm{reg}} -$$

$$- W_{rs}(\mathrm{A}) + \tau_{00}(r, s) + \delta_{00}(r, s),\ \text{if A irregular}$$

$$- W_{rs}(\mathrm{B}) + \tau_{01}(r, s-1) + \delta_{01}(r, s-1),\ \text{if B irregular}$$

$$- W_{rs}(\mathrm{C}) + \tau_{10}(r-1, s) + \delta_{10}(r-1, s),\ \text{if C irregular}$$

$$- W_{rs}(\mathrm{D}) + \tau_{11}(r-1, s-1) + \delta_{11}(r-1, s-1),\ \text{if D irregular}\qquad(86)$$

A similar equation holds for $\overline{W}_{rs\,\mathrm{irreg}}$, by replacing W, τ, δ by $\overline{W}$, $\bar{\tau}$, $\bar{\delta}$ in equation (86).

5.2. The Pivotal Weights W_{00} and $\overline{W}_{00}$ for an Irregular Rhombus adjacent to a Subsonic Leading Edge.

From equation (86), putting $r = 0$, $s = 0$, we have

$$W_{00} = \tau_{00}(0, 0) + \delta_{00}(0, 0)$$

$$= C_1(0, 0) + \nu'^2 D_1(0, 0),\ \text{using (A.19), (A.35), (12a), (13a)}.$$

From (A.20) and (A.9) to (A.15)

$$C_1(0, 0) = \pi/\sqrt{8},$$

where any singular terms occurring are discarded.

Similarly from (A.36), (A.33), (A.34)

$$D_1(0, 0) = \frac{2}{3}\frac{\pi}{g^{1/2}}\left[g + \frac{1}{5}K\right].$$

Hence

$$W_{00} = \frac{\pi}{g^{1/2}}\left[1 + \frac{2}{3}\nu'^2\left(g + \frac{1}{5}K\right)\right].\qquad(87)$$

In a similar manner

$$\overline{W}_{00} = \bar{\tau}_{00}(0, 0) + \bar{\delta}_{00}(0, 0)\qquad(88)$$

$$= 0,$$

in virtue of (A.21), (A.37), (12b), (13b). These results are valid for the 2 or 3 vertex cases.

It is not difficult to see that, had the more rigorous equations (80), (82), (83), (84) for τ_{uv}, $\bar{\tau}_{uv}$, δ_{uv}, $\bar{\delta}_{uv}$ been used, leaving the explicit variation of K_2 and L_2 in the integrals rather than applying interpolation to ϕK_2, ϕL_2, then $\overline{W}_{00}$ would not be zero, but would be of order ν'.

Returning to equation (11a) and discarding terms of order ν'^2 on the right-hand side the contribution of the pivotal rhombus is seen to be

$$\int_{r=0}^{1}\int_{s=0}^{\sigma\mathrm{L.E.}(\rho)}\left[\frac{\phi_R'}{4(\rho\sigma)^{3/2}} + \frac{\phi_I' M\nu'(\rho+\sigma)}{4(\rho\sigma)^{3/2}}\right]d\rho\,d\sigma.\qquad(88a)$$

21

The first term in this expression can be handled by the same technique as given earlier, using a variation $(a\sigma+b\rho+c)\,(\sigma_{\text{L.E.}}-\sigma)^{1/2}$ for $\phi_R{}'$. Hence its contribution is

$$C_1(0,0)\phi_R{}'_{0,0} + C_2(0,0)\phi_R{}'_{1,0} + C_3(0,0)\phi_R{}'_{1,1}$$

for the 3 vertex case

or

$$C_1{}'(0,0)\phi_R{}''_{0,0} + C_2{}'(0,0)\phi_R{}'_{1,0}$$

for the 2 vertex case.

Consider now the second integral and assume a variation $(a\sigma+b\rho+c)\,(\sigma_{\text{L.E.}}-\sigma)^{1/2}$ for $\phi_I{}'$, then

$$\int_{r=0}^{1}\int_{s=0}^{\sigma_{\text{L.E.}(\rho)}} \frac{\phi_I{}'M\nu'(\rho+\sigma)}{4(\rho\sigma)^{3/2}}\,d\rho\,d\sigma$$

$$= \frac{\pi M\nu'}{4}\left[a\left(\frac{1}{12}K^2+\frac{1}{2}Kg-\frac{1}{4}g^2+\frac{1}{3}K+g\right)+b\left(\frac{1}{3}K+g-\frac{2}{3}\right)+c(K-g-2)\right]. \quad (89)$$

Using formulae similar to (A.16), (A.17), (A.18), for a, b, c in the 3 vertex case, we obtain the contribution as

$$\epsilon_{00}\phi_I{}'(0,0) + \epsilon_{1,0}\phi_I{}'(1,0) + \epsilon_{1,1}\phi_I{}'(1,1) \quad (90)$$

where

$$\epsilon_{00} = \frac{\pi M\nu'}{4g^{1/2}}\left[\frac{2}{3}K-2g-\frac{4}{3}\right] \quad (91)$$

$$\epsilon_{10} = \frac{\pi M\nu'}{4(g+K)^{1/2}}\left[\frac{2}{3}+\frac{1}{12}K^2+\frac{1}{2}Kg-\frac{1}{4}g^2\right] \quad (92)$$

$$\epsilon_{11} = \frac{\pi M\nu'}{4(g+K-1)^{1/2}}\left[\frac{1}{12}K^2+\frac{1}{2}Kg-\frac{1}{4}g^2+\frac{1}{3}K+g\right]. \quad (93)$$

Using formulae similar to (A.23), (A.24), (A.25) for the 2 vertex case, we obtain the contribution as

$$\epsilon_{00}{}'\phi_I{}'(0,0) + \epsilon_{0,1}{}'\phi_I{}'(1,0) \quad (94)$$

where

$$\epsilon_{00}{}' = \epsilon_{00} \quad (95)$$

$$\epsilon_{10}{}' = \frac{\pi M\nu'}{4(g+K)^{1/2}}\left(\frac{1}{3}K+g-\frac{2}{3}\right). \quad (96)$$

Thus neglecting terms of order ν'^2, we get, in either the 2 or 3 vertex cases,

$$W_{00} = C_1(0,0) = \frac{\pi}{g^{1/2}} \quad (97)$$

$$\overline{W}_{00} = \epsilon_{00} = \frac{\pi M\nu'}{4g^{1/2}}\left[\frac{2}{3}K-2g-\frac{4}{3}\right] \quad (98)$$

5.3. The Pivotal Weights W_{00} and $\overline{W}_{00}$ for an Irregular Rhombus adjacent to a Supersonic Leading Edge.

From equation (86) putting $r=0$, $s=0$ we have

$$W_{00} = \tau_{00}(0,0) + \delta_{00}(0,0),$$

i.e.

$$\begin{aligned}
W_{00} &= C_1(0,0) + \nu'^2 D_1(0,0), &\text{for 3 vertex case} \\
&= C_1{}'(0,0) + \nu'^2 D_1{}'(0,0), &\text{for 2 vertex case} \\
&= C_1{}''(0,0) + \nu'^2 D_1{}''(0,0), &\text{for 1 vertex case}
\end{aligned} \quad (99)$$

From (B.10), (B.16), (B.20), (B.29), (B.31), (B.34), respectively, we have

$$C_1(0, 0) = \frac{1}{g}\left[-L(0, 0) - M(0, 0) + N(0, 0)\right],$$

$$D_1(0, 0) = \frac{1}{g}\left[-\bar{L}(0, 0) - \bar{M}(0, 0) + \bar{N}(0, 0)\right] \quad \text{3 vertex}$$

$$C_1{}'(0, 0) = \frac{1}{g}\left[-M(0, 0) + N(0, 0)\right], \quad D_1{}'(0, 0) = \frac{1}{g}\left[-\bar{M}(0, 0) + \bar{N}(0, 0)\right] \quad \text{2 vertex}$$

$$C_1{}''(0, 0) = \frac{N(0, 0)}{g}, \qquad D_1{}''(0, 0) = \frac{\bar{N}(0, 0)}{g}. \qquad \text{1 vertex}$$

From (B.2), (B.3), (B.4): (B.23), (B.24), (B.25), we have

$$L(0, 0) = -\frac{1}{3}\left[2g(g+K)^{1/2} + 3g(-K)^{1/2}\left\{\frac{\pi}{2} - \sin^{-1}\left(\frac{g+K}{g}\right)^{1/2}\right\} - K(g+K)^{1/2}\right]$$

$$M(0, 0) = -\left[\frac{g}{(-K)^{1/2}}\sin^{-1}\left(\frac{-K}{g}\right)^{1/2} + (g+K)^{1/2}\right]$$

$$N(0, 0) = 2\left[(-K)^{1/2}\sin^{-1}\left(\frac{-K}{g}\right)^{1/2} + (g+K)^{1/2}\right]$$

$$\bar{L}(0, 0) = \frac{8}{15}(g+K)^{5/2} - \frac{4}{3}Kj_1(0)$$

$$\bar{M}(0, 0) = \frac{4}{3}j_1(0)$$

$$\bar{N}(0, 0) = \frac{4}{3}j_2(0),$$

where

$$j_1(0) = \frac{g^3}{8(-K)^{3/2}}\sin^{-1}\left(\frac{-K}{g}\right)^{1/2} + (g+K)^{1/2}\left(\frac{g^2}{8K} + \frac{7}{12}g + \frac{1}{3}K\right)$$

$$j_2(0) = \frac{3g^2}{4(-K)^{1/2}}\sin^{-1}\left(\frac{-K}{g}\right)^{1/2} + (g+K)^{1/2}\left(\frac{5}{4}g + \frac{1}{2}K\right).$$

Hence

$$W_{00} = \frac{1}{g}\left[(g+K)^{1/2}\left(\frac{2}{3}g - \frac{1}{3}K + 3\right) + \left\{\frac{g}{(-K)^{1/2}} + 2(-K)^{1/2}\right\}\sin\left(\frac{-K}{g}\right)^{1/2} + \right.$$

$$\left. + g(-K)^{1/2}\left\{\frac{\pi}{2} - \sin^{-1}\left(\frac{g+K}{g}\right)\right\}\right] +$$

$$+ \frac{\nu'^2}{g}\left[-\frac{8}{15}(g+K)^{5/2} + \frac{4}{3}(K-1)j_1(0) + \frac{4}{3}j_2(0)\right], \qquad \text{3 vertex case} \quad (100)$$

$$W_{00} = \frac{1}{g}\left[(-K)^{1/2}\sin^{-1}\left(\frac{-K}{g}\right)^{1/2} + (g+K)^{1/2}\right] + \frac{\nu'^2}{g}\frac{4}{3}\left[j_2(0) - j_1(0)\right], \quad \text{2 vertex case} \quad (101)$$

$$W_{00} = \frac{2}{g}\left[(-K)^{1/2}\sin^{-1}\left(\frac{-K}{g}\right)^{1/2} + (g+K)^{1/2}\right] + \frac{\nu'^2}{g}\frac{4}{3}j_2(0), \qquad \text{1 vertex case}. \quad (102)$$

23

Due to (12b), (13b)

$$\overline{W}_{00} = 0 \text{, in all cases.} \tag{103}$$

As in the subsonic leading-edge case, we can develop an expression correct to first power in ν' in which $\overline{W}_{00}$ is not zero. As shown earlier, the contribution of the pivotal rhombus is the expression given in (88a). It is not difficult to see that the first term in this expression will lead to expressions for W_{00} as given in (100), (101), (102), but with the ν'^2 term omitted.

Consider now the second integral in (88a) and assume a variation $(a\sigma + b\rho + c)(\sigma_{\text{L.E.}} - \sigma)$ for ϕ_I', then

$$\int_{r=0}^{1} \int_{s=0}^{\sigma_{\text{L.E.}}(\rho)} \frac{\phi_I' M\nu'(\rho + \sigma)}{4(\rho\sigma)^{3/2}} d\rho\, d\sigma$$

$$= M\nu'[aP + bQ + cR], \tag{104}$$

where

$$P = -\frac{2}{15}(g+K)^{5/2} + \frac{g^2}{4}\left\{\frac{1}{(-K)^{1/2}} - (-K)^{1/2}\right\}\sin^{-1}\left(\frac{-K}{g}\right)^{1/2} +$$

$$+ \frac{1}{12}(1+K)(g+K)^{1/2}(5g+2K) \tag{105}$$

$$Q = \frac{g^2}{4}\left[\frac{1}{(-K)^{1/2}} - \frac{1}{(-K)^{3/2}}\right]\sin^{-1}\left(\frac{-K}{g}\right)^{1/2} + \frac{1}{12}(g+K)^{1/2}(5g+2K) -$$

$$- \frac{1}{4K}(g+2K)(g+K)^{1/2} \tag{106}$$

$$R = -(g+K)^{1/2}\left[1 + \frac{2}{3}g - \frac{1}{3}K\right] - \frac{g}{(-K)^{1/2}}\sin^{-1}\left(\frac{-K}{g}\right)^{1/2} -$$

$$- g(-K)^{1/2}\left[\frac{\pi}{2} - \sin^{-1}\left(\frac{g+K}{g}\right)^{1/2}\right]. \tag{107}$$

Using the appropriate formulae for the 3, 2, and 1 vertex cases the contribution becomes

$$\epsilon_{00}\phi_I'(0,0) + \epsilon_{10}\phi_I'(1,0) + \epsilon_{01}\phi_I'(0,1), \quad \text{3 vertex} \tag{108}$$

$$\epsilon_{00}'\phi_I'(0,0) + \epsilon_{10}'\phi_I'(1,0), \quad \text{2 vertex} \tag{109}$$

$$\epsilon_{00}''\phi_I'(0,0), \quad \text{1 vertex} \tag{110}$$

where

$$\epsilon_{00} = \frac{M\nu'}{g}[-P - Q + R], \qquad \epsilon_{10} = \frac{M\nu'Q}{g+K}, \qquad \epsilon_{01} = \frac{M\nu'P}{g-1} \tag{111}$$

$$\epsilon_{00}' = \frac{M\nu'}{g}[-Q + R], \qquad \epsilon_{10}' = \frac{M\nu'Q}{g+K} \tag{112}$$

$$\epsilon_{00}'' = \frac{M\nu'R}{g}. \tag{113}$$

$\overline{W}_{00}$ is given by ϵ_{00}, ϵ_{00}' or ϵ_{00}'' as appropriate.

24

5.4. *Further Remarks for the Supersonic Leading Edge: One Vertex Case.*

The results given earlier for the 1 vertex case, are only valid for the case $g = -K$. This is because in equation (81) the limits for the ρ integration were assumed to be r to $r + 1$. As we see from the diagram below, in the 1 vertex case, these limits are more generally r to $r - g/K$.
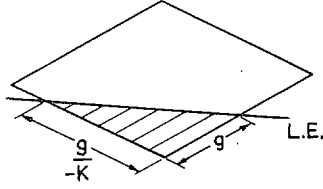
$$\sigma_{\text{L.E.}} = (\rho - r)K + s + g.$$

In this case equation (B.20) still holds, i.e. $C_1'' = N/g$, except that N is now given by

$$N = 2 \left[(-K)^{1/2} \sin^{-1} \left(\frac{-K\rho}{E} \right)^{1/2} + \left(\frac{E + K\rho}{\rho} \right)^{1/2} \right]_r^{r-g/K} - \left[s^{1/2} + \frac{E}{s^{1/2}} \right] \left[\frac{1}{\left(r - \frac{g}{K} \right)^{1/2}} - \frac{1}{r^{1/2}} \right] +$$

$$+ \frac{K}{s^{1/2}} \left[\left(r - \frac{g}{K} \right)^{1/2} - r^{1/2} \right].$$

Similarly in equation (B.34), $D_1'' = \bar{N}/g$, $\bar{N}$ is now given by

$$\bar{N} = \frac{4}{3} \left[\frac{3E^2}{4(-K)^{1/2}} \sin^{-1} \left(\frac{-K\rho}{E} \right)^{1/2} + \frac{1}{4} \{ \rho(E + K\rho) \}^{1/2} (5E + 2K\rho) \right]_r^{r-g/K} +$$

$$+ \left[\frac{4}{3} s^{3/2} - 4Es^{1/2} \right] \left[\left(r - \frac{g}{K} \right)^{1/2} - r^{1/2} \right] - \frac{4}{3} s^{1/2} K \left[\left(r - \frac{g}{K} \right)^{3/2} - r^{3/2} \right],$$

where

$$E = s + g - rK.$$

Putting $r = 0$, $s = 0$ we obtain

$$W_{00} = C_1''(0, 0) + v'^2 D_1''(0, 0) = \frac{\pi(-K)^{1/2}}{g} + v'^2 \frac{\pi g}{2(-K)^{1/2}}. \tag{112a}$$

Using the same principles as earlier, we obtain for $\bar{W}_{00}$

$$\bar{W}_{00} = \frac{Mv'}{4g} \int_{\rho=0}^{\rho=-g/K} \frac{1}{\rho^{3/2}} \left[\int_{\sigma=0}^{\rho K+g} \frac{(\rho K + g - \sigma)(\rho + \sigma)}{\sigma^{3/2}} d\sigma \right] d\rho \tag{113a}$$

$$= -\frac{\pi}{2} \frac{Mv'}{(-K)^{1/2}} [1 - K].$$

5.5. *Some Comments on the Treatment of Irregular Rhombuses.*

The main problem in computing the irregular A, B, C or D contributions, is the computation of the C_1, C_2, C_3; D_1, D_2, D_3 coefficients, etc. Inspection of the equations giving these, shows that they are complicated functions of four variables r, s, g, K. Because of the complexity of the functions their computation is time-consuming and hence a once and for all tabulation would be desirable. However, the dependence on four variables obviously precludes this.

In order to keep the computation down to practicable proportions the approach shown below was made.

(i) In the main programme, which computes ϕ_R', ϕ_I' from the basic integral equation, the correct irregular weights are only formed when $r + s \leqslant 5$. If $r + s \geqslant 6$, the corresponding regular weight

is taken. This can be justified because the weights fall off rapidly as one moves away from the pivotal point. Beyond $r + s \geqslant 6$, the use of regular weights instead of irregular ones will produce only very small errors in the potentials.

(ii) For each given value of K (i.e. for a given Mach number and for each kinked portion of the leading edge), the functions C_1, C_2, C_3; D_1, D_2, D_3 (or C_1', C_2'; D_1', D_2', or C_1'', D_1'' as appropriate) are tabulated against g for each combination of r, s such that $r + s \leqslant 5$. The range of g is taken large enough to cover all the irregular rhombuses of that particular type. The condition $g > rK - s$ helps to reduce the number of combinations of r, s required. If g_{crit} is greater than the largest g occurring, this case need not be computed. A parabola is now fitted over the appropriate range of g by the least squares method and we obtain, for instance, for the given K

$$C_1(r, s, g) = C_1^2(r, s)g^2 + C_1^1(r, s)g + C_1^0(r, s).$$

In the main programme a table of $C_1^p(r, s)$, ($p = 0, 1, 2$), is provided for $r + s \leqslant 5$ for each value of K occurring. Thus, when any given rhombus of this type is encountered, once g is known, the appropriate C and D coefficients for any combination of r, s can be determined very rapidly.

This method has the merit that it does not slow down the main programme with lengthy calculations of the C's and D's from the original formulae. However, it does imply that a considerable amount of computation has to be done in forming the tables of $C_1^p(r, s)$, $C_2^p(r, s)$, etc., prior to the main programme. Furthermore, in fitting a parabola to the values originally computed, some accuracy will be lost, in general.

(iii) In effect, tables are provided as data for K_1, K_2, L_1, L_2 for $r + s \leqslant 5$, for the given M and v'. This again saves time in the programme by avoiding the repeated computation of the trigonometrical functions involved.

It may be remarked that, although in principle the formulae for τ, $\bar{\tau}$, δ, $\bar{\delta}$ are more correctly given by equations (80), (82), (83), (84), in practice, the formulae derived later, of the type

$$\tau = K_1(r, s, M, v')C(r, s, g, K), \text{ etc.},$$

have a distinct advantage in that the C's and D's do not depend on v'. Thus, if the same planform at a given Mach number is to be done for several frequencies, step (ii) above need only be done once. The preparation of the tables in step (iii) for given M and v' is a comparatively simple task.

(iv) In the formulae for the total irregular weight, it will be seen that, if we start with the regular weight, not only must we add to it the appropriate irregular A, B, C or D contribution, but we must also subtract from it the appropriate regular A, B, C, D contribution.
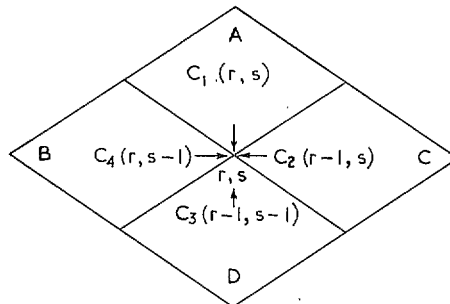
With a view to again making the treatment frequency decoupled as far as possible, the subtractions are normally performed using the A, B, C or D contributions as derived for the regular linear interpolation weights, for which the appropriate equations are given following equation (55).

It will be seen that, in effect, the appropriate subtractions can be carried out by replacing:

$C_1^0(r, s)$ by $C_1^0(r, s) - F_0(r)F_0(s)$, if A is irregular

$C_2^0(r-1, s)$ by $C_2^0(r-1, s) - F_1(r-1)F_0(s)$, if C is irregular

$C_3^0(r-1, s-1)$ by $C_3^0(r-1, s-1) - F_1(r-1)F_1(s-1)$, if D is irregular

$C_4^0(r, s-1)$ by $C_4^0(r, s-1) - F_0(r)F_1(s-1)$, if B is irregular

Similar combinations are used with the D's with F replaced by F^*.

In practice making use of symmetry, we need only consider irregular rhombuses on the starboard wing, and hence the case where B is irregular never occurs on swept-back wings. Furthermore, when the D rhombus is irregular, it can be assumed that the irregular C rhombus part is included already as part of the irregular D contribution.
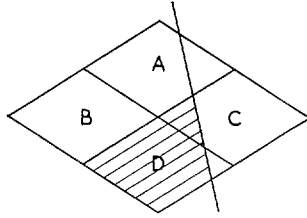
Hence when D is irregular replace

$$C_3^0(r-1, s-1) \text{ by } C_3^0(r-1, s-1) - F_1(r-1)F_0(s) - F_1(r-1)F_1(s-1).$$

The approach described above is strictly only consistent when used with regular linear interpolation weights. When used with regular parabolic interpolation weights, the parts subtracted out are not strictly equal to the regular A, B, C or D contributions and therefore small errors occur. It has been found that, at least on certain types of wings (e.g. the rectangular wing), this procedure produces only small errors in the potentials. The smaller ν' the more accurate it is likely to be.

6. Choice of Mesh Size.

6.1. Limitations on ν'.

A rigorous discussion of the accuracy to be expected in determining ϕ_R' and ϕ_I' in any given case, is not possible. The treatment given here is intended to be a guide to the choice of a suitable value of ν'. It is assumed that the variation in ϕ_R' and ϕ_I' is small over the pivotal rhombus and that conditions in the pivotal rhombus will be the most critical.

Let us consider the right-hand side of (11a), assuming that ϕ_R' and ϕ_I' take some constant mean value over the pivotal rhombus. The contribution of this rhombus becomes

$$\phi_R' \int_0^1 \int_0^1 \left[\frac{K_1}{4(\rho\sigma)^{3/2}} + \frac{L_1}{(\rho\sigma)^{1/2}} \right] d\rho \, d\sigma + \phi_I' \int_0^1 \int_0^1 \left[\frac{K_2}{4(\rho\sigma)^{3/2}} + \frac{L_2}{(\rho\sigma)^{1/2}} \right] d\rho \, d\sigma. \tag{114}$$

Using equations (12a), (12b), (13a), (13b) and expanding out in powers of ν', it can be shown that

$$\int_0^1 \int_0^1 \frac{K_1}{4(\rho\sigma)^{3/2}}\, d\rho\, d\sigma = 1 - \frac{2}{3} M^2\nu'^2 - 2\nu'^2 + \frac{104}{105}\frac{1}{12} M^4\nu'^4 + \frac{2}{27}\nu'^4 + \frac{28}{45} M^2\nu'^4 + O(\nu'^6) \quad (115)$$

$$\int_0^1 \int_0^1 \frac{L_1}{(\rho\sigma)^{1/2}}\, d\rho\, d\sigma = 4\nu'^2 \left[1 - \frac{14}{45} M^2\nu'^2 - \frac{2}{27}\nu'^2 \right] + O(\nu'^6) \quad (116)$$

$$\int_0^1 \int_0^1 \frac{K_2}{4(\rho\sigma)^{3/2}}\, d\rho\, d\sigma = -2M\nu' - \frac{4}{15} M^3\nu'^3 - \frac{4}{3} M\nu'^3 + O(\nu'^5). \quad (117)$$

$$\int_0^1 \int_0^1 \frac{L_2}{(\rho\sigma)^{1/2}}\, d\rho\, d\sigma = \frac{8}{3} M\nu'^3 + O(\nu'^5). \quad (118)$$

These results can be used to estimate the accuracy of the various integration techniques. Using parabolic interpolation, we obtain for the same integrals

$$\int_0^1 \int_0^1 \frac{K_1}{4(\rho\sigma)^{3/2}}\, d\rho\, d\sigma = \sum_{i=0, 1/2, 1} \sum_{j=0, 1/2, 1} K_1(i,j) G_i(0) G_j(0) \quad (119)$$

$$\int_0^1 \int_0^1 \frac{L_1}{(\rho\sigma)^{1/2}}\, d\rho\, d\sigma = \sum_{i=0, 1/2, 1} \sum_{j=0, 1/2, 1} L_1(i,j) G_i^*(0) G_j^*(0), \quad (120)$$

with similar equations for the K_2 and L_2 integrals. If now equations (12a), (12b), (13a), (13b), (34), (36) are used and the results are expanded in powers of ν', we obtain

$$\int_0^1 \int_0^1 \frac{K_1}{4(\rho\sigma)^{3/2}}\, d\rho\, d\sigma = 1 - \frac{2}{3} M^2\nu'^2 - 2\nu'^2 + \frac{1}{24} M^4\nu'^4 + \frac{2}{27}\nu'^4 + \frac{2}{9} M^2\nu'^4 + O(\nu'^6) \quad (121)$$

$$\int_0^1 \int_0^1 \frac{L_1}{(\rho\sigma)^{1/2}}\, d\rho\, d\sigma = 4\nu'^2 \left[1 - \frac{14}{45} M^2\nu'^2 - \frac{2}{27}\nu'^2 \right] + O(\nu'^6) \quad (122)$$

$$\int_0^1 \int_0^1 \frac{K_2}{4(\rho\sigma)^{3/2}}\, d\rho\, d\sigma = -2M\nu' - \frac{1}{3} M^3\nu'^3 - \frac{4}{3} M\nu'^3 + O(\nu'^5) \quad (123)$$

$$\int_0^1 \int_0^1 \frac{L_2}{(\rho\sigma)^{1/2}}\, d\rho\, d\sigma = \frac{8}{3} M\nu'^3 + O(\nu'^5). \quad (124)$$

Comparing the exact expanded answer with the expanded form of the parabolic interpolation answer, we see that the error in the coefficient of ϕ_R' is

$$- M^2\nu'^4 \left[\frac{2}{5} + \frac{1}{24} M^2 \right] + O(\nu'^6), \quad (125)$$

replacing (104)/(105) in (115) by unity. The error in the coefficient of ϕ_I' is

$$- \frac{1}{15} M^3\nu'^3 + O(\nu'^5). \quad (126)$$

28

Thus to make the error in these coefficients less than 1%, we must have

$$\nu' < \sqrt[4]{\left/ \left\{ \frac{0\cdot01}{M^2 \left(\frac{2}{5} + \frac{1}{24} M^2 \right)} \right\} \right.} = \nu_1' \tag{127}$$

$$\nu' < \frac{1}{M} \sqrt{(0\cdot01 \times 30)} = \nu_2'. \tag{128}$$

M	1	$1\cdot5$	2
ν_1'	$0\cdot39$	$0\cdot31$	$0\cdot26$
ν_2'	$0\cdot55$	$0\cdot37$	$0\cdot27$

From the table displayed it will be seen that between $M = 1$ and $M = 2$ it is (127) which is the more critical condition.

Using linear interpolation, we obtain

$$\int_0^1 \int_0^1 \frac{K_1}{4(\rho\sigma)^{3/2}} \, d\rho \, d\sigma = \sum_{u=0}^1 \sum_{v=0}^1 K_1(u, v) F_u(0) F_v(0) \tag{129}$$

$$\int_0^1 \int_0^1 \frac{L_1}{(\rho\sigma)^{1/2}} \, d\rho \, d\sigma = \sum_{u=0}^1 \sum_{v=0}^1 L_1(u, v) F_u^*(0) F_v^*(0), \tag{130}$$

with similar equations for the K_2 and L_2 integrals. If now equations (12a), (12b), (13a), (13b), (65), (66), (69), (70) are used and the results are expanded in powers of ν', we obtain

$$\int_0^1 \int_0^1 \frac{K_1}{4(\rho\sigma)^{3/2}} \, d\rho \, d\sigma = 1 - 2\nu'^2 + O(\nu'^4) \tag{131}$$

$$\int_0^1 \int_0^1 \frac{L_1}{(\rho\sigma)^{1/2}} \, d\rho \, d\sigma = 4\nu'^2 + O(\nu'^4) \tag{132}$$

$$\int_0^1 \int_0^1 \frac{K_2}{4(\rho\sigma)^{3/2}} \, d\rho \, d\sigma = -2M\nu' - \frac{2}{3} M^3\nu'^3 - 4M\nu'^3 + O(\nu'^5) \tag{133}$$

$$\int_0^1 \int_0^1 \frac{L_2}{(\rho\sigma)^{1/2}} \, d\rho \, d\sigma = \frac{8}{3} M\nu'^3 + O(\nu'^5). \tag{134}$$

Comparing the exact expanded answer with the expanded form of the linear interpolation answer, we see that the error in the coefficient of ϕ_R' is

$$\frac{2}{3} M^2\nu'^2 + O(\nu'^4). \tag{135}$$

The error in the coefficient of ϕ_I' is

$$-\frac{2}{5} M^3\nu'^3 - \frac{8}{3} M\nu'^3 + O(\nu'^5). \tag{136}$$

29

Thus to make the error in these coefficients less than 1% of the ϕ_R' coefficient, we must have

$$\nu' < \frac{1}{M}\sqrt{\left(0\cdot01 \times \frac{3}{2}\right)} = \nu_1' \qquad (137)$$

$$\nu' < \sqrt[3]{\frac{0\cdot01}{\left(\frac{2}{5}M^2 + \frac{8}{3}\right)M}} = \nu_2'. \qquad (138)$$

M	1	1·5	2
ν_1'	0·122	0·081	0·061
ν_2'	0·148	0·123	0·105

Between $M = 1$ and $M = 2$ we see that (137) is the more critical condition.

It will be noted that by satisfying the inequalities given above, the error in certain coefficients can be kept less than 1%. This does not necessarily imply that the pivotal potentials will be determined to the same accuracy. The errors to be expected in the final potentials can only be found from experience in applying the method to actual examples and comparing the results with exact analytical answers, where known, or alternative methods of computation.

It should not be forgotten that the inequalities on ν' derived above have only been obtained by considering the contribution of the pivotal rhombus. The contributions from the other rhombuses will be smaller and hence larger percentage errors in their weights can be tolerated. However, care should be taken to see that even in the more remote rhombuses the weights are not too seriously in error. Consider, for instance, the trigonometrical functions which appear in the integrand with argument $2\nu'(\rho\sigma)^{1/2}$. This argument exhibits its greatest variation over a rhombus in the pivotal bands $\rho = 0$ or $\sigma = 0$. The change in argument from $\sigma = 0$ to $\sigma = 1$, will be $2\nu'\rho^{1/2}$, i.e. in the rhombus $\rho = 25$, $\sigma = 0$ the change in argument will be $10\nu'$. Thus for the critical ν' at $M = 1$ using parabolic interpolation weights, the change in argument would be $3\cdot9 = 1\cdot2\,\pi$, which could be represented with rough but adequate accuracy using parabolic interpolation. Similarly for the critical ν' at $M = 1$ using linear interpolation weights, the change in argument would be $1\cdot22 = 0\cdot39\,\pi$, which could be represented with rough but adequate accuracy using linear interpolation. It will be seen that in the band $\sigma = 0$ the weights will become increasingly inaccurate beyond $\rho = 25$. However, these weights are very small anyway and experience indicates that these inaccuracies produce only a small error in determining the pivotal ϕ_R' and ϕ_I'.

6.2. *Some Considerations Concerning Choice of Mesh Size and Type of Weights.*

There are three main considerations in determining mesh size.

(i) *Adequate coverage of the planform area.*—The mesh must always be taken small enough so that ϕ_R' and ϕ_I' are obtained at enough points chordwise and spanwise to define the variation of the potentials with reasonable accuracy, bearing in mind that ϕ' is assumed to vary linearly with ρ and σ in deriving the weights. If the choice of mesh size were based on the critical ν' condition alone, one would be led to $l = \nu_{int} \times \beta U/\omega$ which for small frequencies could lead to ridiculously large mesh sizes.

(ii) *Critical conditions on ν' for required accuracy.*—The inequality (127) for parabolic interpolation weights, or (137) for linear interpolation weights, must be satisfied by taking l sufficiently small.

30

If more accuracy is required than that given by the 1% conditions, then even smaller values of l will be necessary. It must be remembered that, as explained below, the time taken by the main programme to compute the potentials increases rapidly with the number of rhombuses on the planform. Thus very high accuracies may require a prohibitive computation time.

(iii) *Time taken by the programme for computing the potentials.*—It is intended here to give some broad outline of the way in which the computation time increases as the number of rhombuses on the planform increases. To do this let us consider the effect of halving the mesh size. It will be clear that there are now four times as many rhombuses on the planform and that each of these rhombuses has four times as many rhombuses in its fore-cone as before. Thus, when we halve the mesh size we might expect the computation time to increase by a factor of sixteen. In practice due to the way the programme is organised the time does not increase quite as rapidly as this. However, the simple argument given does show how computation times increase very rapidly with the number of rhombuses on the planform.

As regards whether linear or parabolic interpolation weights are used there are two main considerations.

(i) *Time taken to compute weight array.*—Since the formulae for the linear interpolation weights are simpler than those for the parabolic interpolation weights the time taken to compute a given array is shorter for linear weights than for the parabolic weights.

However, in comparing times for computing weight arrays it must be remembered that with parabolic weights, since a larger value of v' is permitted (i.e. a larger mesh size), the weight array will have smaller dimensions.

(ii) *Time taken by main programme.*—As regards computation time, one will normally prefer parabolic interpolation weights because these allow the use of larger values of v' (i.e. larger mesh size) than the linear weights, for the same accuracy.

From the considerations given above it will be seen that in most cases parabolic interpolation weights will be used. The exceptional cases would be those low-frequency cases where l is determined solely by the desire to obtain an adequate coverage of the planform. Even for these cases better accuracy would be obtained if the parabolic weights for the same v' were used.

6.3. *Integration Errors and their Propagation.*

Consider a steady one-dimensional case. If we solve for the potential at the most upstream rhombus, we obtain an answer which, due to errors in the integration technique, we can express as $\phi_0'{}_{ex} + \delta\phi_0'$, where $\phi_0'{}_{ex}$ is the exact answer and $\delta\phi_0'$ is the integration error.
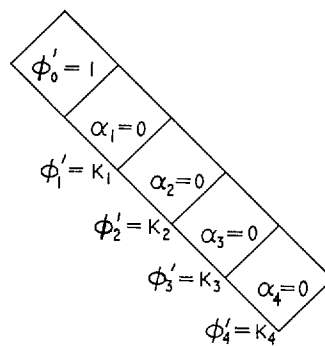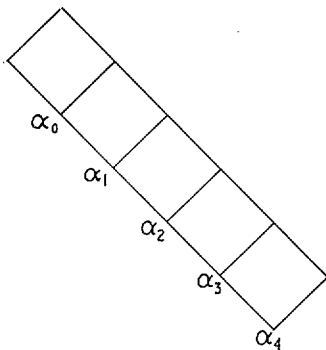
Let us consider now how the $\delta\phi_0'$ error propagates downstream. If we take $\phi_0' = 1$, $\alpha_1 = \alpha_2 = \alpha_3 = \alpha_4 = 0$ and solve for the downstream ϕ', we obtain $\phi_1' = K_1$, $\phi_2' = K_2 \ldots \phi_4' = K_4$, say. Thus in the original problem we see that $\delta\phi_0'$ contributes $K_r\delta\phi_0'$ to ϕ_r' downstream. Since we have already obtained the contribution of $\delta\phi_0'$ to ϕ_1' as $K_1\delta\phi_0'$, to obtain the remaining part of ϕ_1' we must compute ϕ_1' using $\phi_{0\,\mathrm{ex}}'$ upstream, we then obtain $\phi_1' = \phi_{1\,\mathrm{ex}}' + \delta\phi_1'$. The total ϕ_1' is thus $\phi_{1\,\mathrm{ex}}' + \delta\phi_1' + K_1\delta\phi_0'$. Similarly for ϕ_2' we obtain $\phi_{2\,\mathrm{ex}}' + \delta\phi_2' + K_1\delta\phi_1' + K_2\delta\phi_0'$, and so on.

It is easy to see that the general result is

$$\phi_r' = \phi_{r\,\mathrm{ex}}' + \delta\phi_r' + \sum_{n=1}^{r} K_n\phi_{r-n}', \tag{139}$$

where $\phi_{r\,\mathrm{ex}}' + \delta\phi_r'$ is the answer obtained using the exact values of ϕ' upstream in the fore-cone, so that $\delta\phi_r'$ is the pivotal integration error and the summation is the propagation error due to the pivotal integration errors upstream.

The corresponding two-dimensional theory for the unsteady case is now fairly obvious. If we start with rhombus $r = 0$, $s = 0$ for which $\phi_R' = 0$, $\phi_I' = 1$ and take $\alpha(x, y)$ and $g(x, y)$ zero everywhere downstream, a two-dimensional array $R_{rs} + iK_{rs}$ can be computed to give the ϕ' downst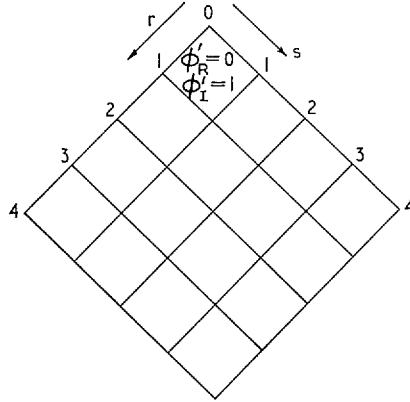ream. Similarly for $\phi_R' = 1$, $\phi_I' = 0$ we obtain an array $K_{rs} - i\overline{K}_{rs}$. These arrays are symmetric with respect to r and s, of course.

Reverting to the usual r and s measured positive upstream from the current pivotal point, it will be seen that the propagation error due to upstream pivotal integration errors is

$$\Sigma \Sigma' (K_{rs} - i\overline{K}_{rs})\delta\phi_R'(r, s) + \Sigma \Sigma' (\overline{K}_{rs} + iK_{rs})\delta\phi_I'(r, s). \tag{140}$$

Thus the pivotal ϕ_R' and ϕ_I' can be written

$$\phi_R'(0, 0) = \phi_R'(0, 0)_{\mathrm{ex}} + \delta\phi_R'(0, 0) + \Sigma \Sigma' [K_{rs}\delta\phi_R'(r, s) + \overline{K}_{rs}\delta\phi_I'(r, s)] \tag{141}$$

$$\phi_I'(0, 0) = \phi_I'(0, 0)_{\mathrm{ex}} + \delta\phi_I'(0, 0) + \Sigma \Sigma' [- \overline{K}_{rs}\delta\phi_R'(r, s) + K_{rs}\delta\phi_I'(r, s)]. \tag{142}$$

It is difficult to make any generalisations from these equations. The only case examined in any detail was the rectangular wing of aspect ratio 2 for $M = \sqrt{2}$ and $\nu = \omega c/U = 0\cdot 6$, for the mode $g = -x$. For this planform and Mach number the analytical solution is known all over the planform and hence it is possible to obtain $\delta\phi_R'$ and $\delta\phi_I'$. Attention was confined to the region in which the flow is two-dimensional and it was found that in this region the $\delta\phi_R'$ were negative while the $\delta\phi_I'$

32

were positive. Since the K_{rs} and $\overline{K}_{rs}$ arrays were both positive this meant that the errors tended to cancel in the equation for $\phi_R{}'$ and to reinforce in the equation for $\phi_I{}'$. This explained why the accuracy obtained for $\phi_R{}'$ was much better than that obtained for $\phi_I{}'$.

The only general deduction seems to be that it will pay to keep integration errors as small as possible. This indicates that for a given mesh size parabolic interpolation weights will be preferable to linear interpolation weights. For irregular rhombuses it was found that accuracy was improved when the non-zero $\overline{W}_{00}$ was included.

6.4. *The Use of Parabolic Interpolation to Reduce the Number of Points at Which the Potential Must be Computed.*

As stated earlier, whenever the mesh size is reduced by a half, the number of rhombuses at which $\phi_R{}'$, $\phi_I{}'$ have to be computed becomes four times as great. To reduce computation times a method was evolved in which the potentials do not have to be computed at all points of the mesh. Investigation of the potentials obtained using the normal method suggested that, in the regions where no discontinuities in slope occur, e.g. due to shocks, a locally parabolic representation for ϕ' should be quite accurate, except possibly near the tips.

The basic idea is that $\phi_R{}'$, $\phi_I{}'$ are only computed for alternate rows and that in these rows they are only computed for alternate rhombuses. The values at the other mesh points are filled in using parabolic interpolation. As an illustration of the method consider the example shown below.

←Planform centre-line
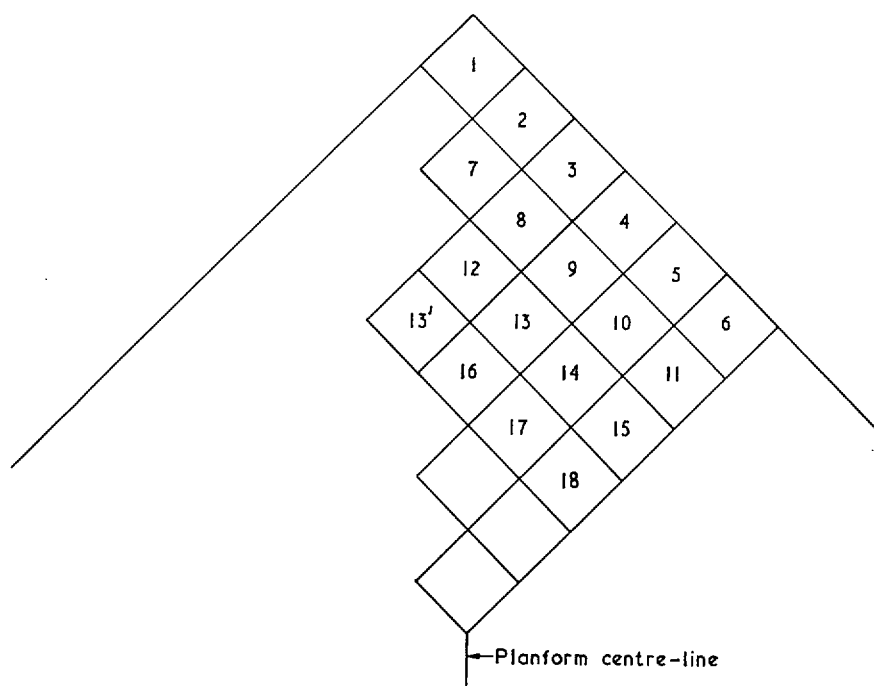
At any given stage we can assume that at least two upstream rows are known i.e. 1 to 6, 7 to 11. The rhombuses in the next row i.e. 12 to 15 are now hopped over and computation begins at rhombus 16 in the following row. $\phi_R{}'$, $\phi_I{}'$ are now computed for rhombus 16 using the equations given below, which do not involve the potentials for the three rhombuses adjacent to the pivotal one. Once $\phi_R{}'$, $\phi_I{}'$ are known at 16 the values at 12 can be interpolated using 1, 7, 16 and the values at 13 can be interpolated using 4, 9, 16. Rhombus 17 is now hopped over and $\phi_R{}'$, $\phi_I{}'$ are computed

33

for rhombus 18 using the equations given below. The values at 17, 14, 15 are now obtained by interpolating on 13', 16, 18; 3, 9, 18; 6, 11, 18, respectively. It is clear that this procedure can be continued down the row and that when finished two successive rows will be known. Thus the downstream rows can be dealt with similarly.

We now discuss the solution for the pivotal ϕ_R', ϕ_I' assuming that the values at 1, 0; 1, 1; 0, 1 are obtained using parabolic interpolation.
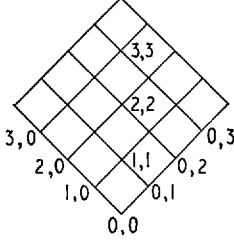
Along the line $\sigma = 0$ the variation of ϕ' can be written, using Lagrangian interpolation,

$$\phi' = \frac{(\rho-2)\rho}{1 \times 3} \phi'(3, 0) + \frac{(\rho-3)\rho}{-1 \times 2} \phi'(2, 0) + \frac{(\rho-3)(\rho-2)}{-3 \times -2} \phi'(0, 0). \quad (143)$$

Thus putting $\rho = 1$, we obtain

$$\phi'(1, 0) = -\tfrac{1}{3} \phi'(3, 0) + \phi'(2, 0) + \tfrac{1}{3} \phi'(0, 0). \quad (144)$$

$$\phi'(0, 1) = -\tfrac{1}{3} \phi'(0, 3) + \phi'(0, 2) + \tfrac{1}{3} \phi'(0, 0). \quad (145)$$

Similarly

$$\phi'(1, 1) = -\tfrac{1}{3} \phi'(3, 3) + \phi'(2, 2) + \tfrac{1}{3} \phi'(0, 0). \quad (146)$$

The first term on the right-hand side of equation (23) can be written

$$\left[\sum_{r, s = 1, 0; 1, 1; 0, 1} \sum + \sum_{r, s \neq 1, 0; 1, 1; 0, 1} \sum \right] \left[W_{rs} \phi_R'(r, s) \right].$$

Using the three equations (144) to (146) this becomes

$$W_{10}[-\tfrac{1}{3} \phi_R'(3, 0) + \phi_R'(2, 0) + \tfrac{1}{3} \phi_R'(0, 0)] + W_{11}[-\tfrac{1}{3} \phi_R'(3, 3) + \phi_R'(2, 2) + \tfrac{1}{3} \phi_R'(0, 0)] +$$

$$+ W_{01}[-\tfrac{1}{3} \phi_R'(0, 3) + \phi_R'(0, 2) + \tfrac{1}{3} \phi_R'(0, 0)] + \sum_{r, s \neq 1, 0; 1, 1; 0, 1} \sum W_{rs} \phi_R'(r, s)$$

$$= \sum_{r=0} \sum_{s=0} W_{rs}^* \phi_R'(r, s), \qquad \text{say} \quad (147)$$

where

$$W_{00}^* = W_{00} + \tfrac{2}{3} W_{01} + \tfrac{1}{3} W_{11}, \qquad W_{01}^* = W_{10}^* = 0$$

$$W_{02}^* = W_{20}^* = W_{02} + W_{01}, \qquad W_{03}^* = W_{30}^* = W_{03} - \tfrac{1}{3} W_{01}$$

$$W_{11}^* = 0, \qquad\qquad\qquad W_{22}^* = W_{22} + W_{11} \qquad (148)$$

$$W_{33}^* = W_{33} - \tfrac{1}{3} W_{11}, \qquad W_{rs}^* = W_{rs} \text{ for all other } r, s.$$

By considering the second term on the right-hand side of (23) we obtain similar equations relating $\overline{W}_{rs}^*$ and $\overline{W}_{rs}$. Thus equation (23) becomes finally

$$\frac{\alpha \pi l}{ML} = \sum_{r=0} \sum_{s=0} [W_{rs}^* \phi_R'(r, s) + \overline{W}_{rs}^* \phi_I'(r, s)]. \quad (149)$$

Since this equation is formally the same as (23), and (27) produces a similar counterpart, the procedure for solution remains exactly as before, except that seven of the W_{rs}, $\overline{W}_{rs}$ adjacent to the pivotal point must be modified. When $\phi_R'(0, 0)$ and $\phi_I'(0, 0)$ have been computed, the values at 1, 0; 1, 1; 0, 1 can be determined using equations (144) to (146).

34

This procedure seems so simple that one might well ask why it cannot be used exclusively. There are two main reasons. The first reason is that on wings with kinked leading edges (including the wing vertex and streamwise tips) shocks usually emanate from the points where the sweep is discontinuous. These will imply discontinuities in the ϕ' derivatives so that parabolic interpolation is no longer accurate. The second reason is that near the edges of the planform not all of the potentials required adjacent to the pivotal point may exist, e.g. there may not be a 0, 3 rhombus. In this case the method fails.

It is not difficult to see that a programme which uses the parabolic interpolation method where possible and reverts to the normal method elsewhere should be generally feasible. As yet no computer programme of general validity using this method has been written.

A special programme using the method described above was written for the case of a rectangular wing.
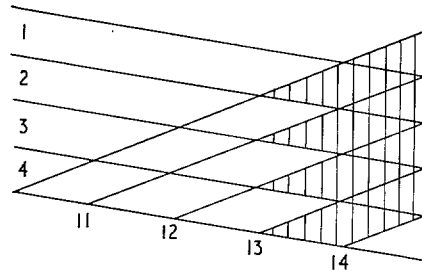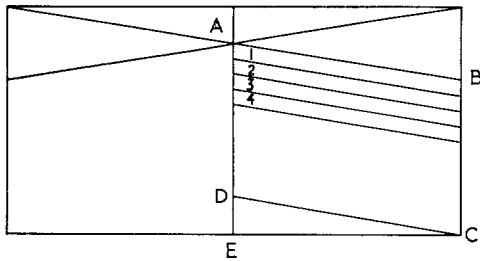
The method can only be applied to the region aft of both tip shocks, and to start two rows of ϕ_R', ϕ_I' are needed. Thus down to the end of row 2 of the diagram the computation proceeds normally. Beyond this point the new technique is used. Thus row 3 is hopped over and computation starts with alternate rhombuses in row 4, i.e. numbering rhombuses from the centre-line, 1, 3, 5, 7, 9, 11. Since for this particular case there were 14 rhombuses in each row in the region ABCD, it is clear that in row 4, rhombuses 12, 13, 14 cannot be done by parabolic interpolation because some of the relevant upstream potentials do not exist. Hence we now revert to the normal method and do rhombuses 3, 13; 3, 14; 4, 12; 4, 13; 4, 14 in the order shown. This completes rows 3 and 4. Rows 5 and 6 are now treated in the same way as 3 and 4, and so on.

Although this procedure could have been applied to the whole of region ABCE, it was only applied over the region ABCD, where each row had a constant number of rhombuses in it. This was to ease certain programming difficulties. The region CDE was completed by the normal method. For the particular case considered the method described above was about twice as fast as the normal one.

7. *The Evaluation of the Lift and Pitching-Moment Coefficients Due to a Given Mode of Oscillation for an Arbitrary Wing Planform.*

From Bernouilli's equation we have

$$p - p_\infty = - \rho_\infty \left(U \frac{\partial}{\partial x} + i\omega \right) (\phi_R + i\phi_I),$$

and hence

$$\frac{p - p_\infty}{\rho U^2} = - \left[\frac{1}{U} \frac{\partial \phi_R}{\partial x} - \frac{\omega \phi_I}{U^2} \right] - i \left[\frac{\omega \phi_R}{U^2} + \frac{1}{U} \frac{\partial \phi_I}{\partial x} \right]. \qquad (150)$$

35

Since ϕ is an anti-symmetric function of z we have the lift per unit area as

$$l(x, y) = -2(p - p_\infty), \qquad \text{positive up.} \tag{151}$$

From (150) we see that C_{LI} and C_{mI} can be obtained from the formulae for C_{LR} and C_{mR} by replacing ϕ_R by ϕ_I and ϕ_I by $-\phi_R$.

Now

$$C_{LR} = \frac{\mathscr{L}_R}{\frac{1}{2}\rho U^2 S} = \frac{1}{\frac{1}{2}\rho U^2 S} \iint_S l_R(x, y) dx \, dy, \tag{152}$$

where S is the planform area. Using equations (150), (151) and (8) and integration by parts, we obtain

$$
\begin{aligned}
C_{LR} &= \frac{4L}{S} \iint_S \left[\frac{\partial \phi_R{}'}{\partial x} - \frac{\omega}{U} \phi_I \right] dx \, dy \\
&= \frac{4L}{S} \int_{-\sigma}^{+\sigma} \phi_{\text{T.E.}\,R}{}' \, dy - \frac{4L}{S} \frac{\omega}{U} \iint_S \phi_I{}' dx \, dy, \tag{153}
\end{aligned}
$$

where σ is the semi-span and using the fact that ϕ' is zero along the leading edge.

We now introduce co-ordinates

$$\xi = \frac{x}{c_0}, \qquad \eta = \frac{y}{\sigma}, \tag{154}$$

where c_0 is the root chord, and the frequency parameter is

$$\nu = \frac{\omega c_0}{U}. \tag{155}$$

Equation (153) becomes finally

$$C_{LR} = \frac{8\sigma L}{S} \int_0^1 \phi_{\text{T.E.}\,R}{}' \, d\eta - \frac{8\sigma L}{S} \nu \int_0^1 \left[\int_{\xi_{\text{L.E.}}}^{\xi_{\text{T.E.}}} \phi_I{}' d\xi \right] d\eta. \tag{156}$$

Similarly

$$C_{LI} = \frac{8\sigma L}{S} \int_0^1 \phi_{\text{T.E.}\,I}{}' \, d\eta + \frac{8\sigma L}{S} \nu \int_0^1 \left[\int_{\xi_{\text{L.E.}}}^{\xi_{\text{T.E.}}} \phi_R{}' d\xi \right] d\eta. \tag{157}$$

The pitching-moment coefficient, positive nose up, about an axis through the wing vertex is

$$C_{mR} = -\frac{1}{\frac{1}{2}\rho U^2 S \bar{c}} \iint_S x l_R(x, y) dx \, dy, \tag{158}$$

where $\bar{c}$ is the mean chord. Using equations (150), (151), (8), (154), (155) and integration by parts, we obtain

$$C_{mR} = \frac{8\sigma L c_0}{S \bar{c}} \int_0^1 \left[\int_{\text{L.E.}}^{\text{T.E.}} \phi_R{}' d\xi - \xi_{\text{T.E.}} \phi_{\text{T.E.}\,R}{}' \right] d\eta + \frac{8\sigma L c_0}{S \bar{c}} \nu \int_0^1 \left[\int_{\text{L.E.}}^{\text{T.E.}} \xi \phi_I{}' d\xi \right] d\eta. \tag{159}$$

Similarly

$$C_{mI} = \frac{8\sigma L c_0}{S \bar{c}} \int_0^1 \left[\int_{\text{L.E.}}^{\text{T.E.}} \phi_I{}' d\xi - \xi_{\text{T.E.}} \phi_{\text{T.E.}\,I}{}' \right] d\eta - \frac{8\sigma L c_0}{S \bar{c}} \nu \int_0^1 \left[\int_{\text{L.E.}}^{\text{T.E.}} \xi \phi_R{}' d\xi \right] d\eta. \tag{160}$$

It will be seen that all of the spanwise integrations which occur, are of the same type, i.e. $\int_0^1 \chi(\eta) d\eta$. We begin by discussing a method for evaluating this type of integral. It is assumed initially that the same mesh used in obtaining the potentials is also used in obtaining the relevant integrals.

36
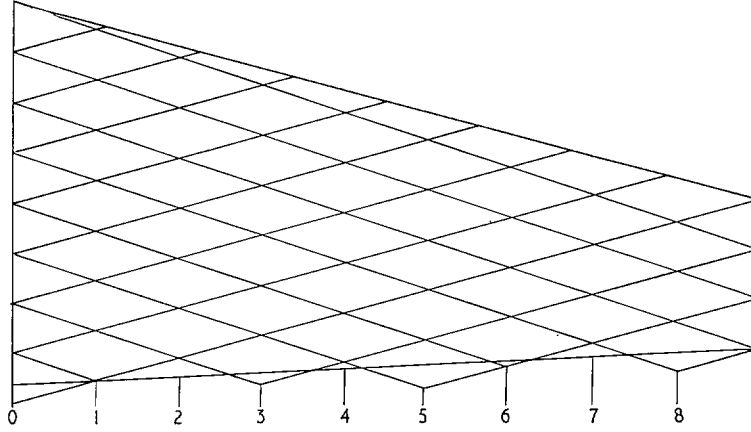
The diagram shows that the characteristic mesh can be used to define a set of equally spaced spanwise stations. Beginning at the planform centre-line these can be labelled $0, 1, 2, \ldots n$, where n is the last station inboard of the tip and can be odd or even. In evaluating the spanwise integral $\int_0^1 \chi(\eta)d\eta$, Simpson's rule is used over the range $\eta = 0$ to $\eta = \eta_n$ and an elliptic fall off to zero is assumed between $\eta = \eta_n$ and $\eta = 1$. We obtain

$$\int_0^1 \chi(\eta)d\eta = \tfrac{1}{3}\Delta\eta\,[2\chi_0 + 2\chi_1 + 4\chi_2 + 2\chi_3 + \ldots + 4\chi_{n-1} + \chi_n] + a_n\chi_n, \qquad n \text{ odd} \qquad (161)$$

$$= \tfrac{1}{3}\Delta\eta\,[\chi_0 + 4\chi_1 + 2\chi_2 + 4\chi_3 + \ldots 4\chi_{n-1} + \chi_n] + a_n\chi_n, \qquad n \text{ even} \qquad (162)$$

where

$$a_n = \tfrac{1}{2}\left[\frac{\tfrac{\pi}{2} - \sin^{-1}\eta_n}{(1-\eta_n{}^2)^{1/2}} - \eta_n\right] \qquad (163)$$

and $\Delta\eta$ is the interval between the regularly spaced stations.

If we use values of the potential halved on the centre-line the equations above can be written in the more homogeneous form

$$\frac{\int_0^1 \chi(\eta)d\eta}{\tfrac{2}{3}\Delta\eta} = 2 \times \frac{\chi_0}{2} + \chi_1 + 2\chi_2 + \chi_3 + \ldots + 2\chi_{n-1} + \left(\tfrac{1}{2} + \frac{3a_n}{2\Delta\eta}\right)\chi_n, \qquad n \text{ odd} \qquad (164a)$$

$$= \frac{\chi_0}{2} + 2\chi_1 + \chi_2 + 2\chi_3 + \ldots 2\chi_{n-1} + \left(\tfrac{1}{2} + \frac{3a_n}{2\Delta\eta}\right)\chi_n, \qquad n \text{ even}. \qquad (164b)$$

Thus we see that the spanwise weighting factors consist of a succession of alternating 1's and 2's, beginning with 2 if n is odd and 1 if n is even, except for station n which has a weight $(\tfrac{1}{2} + 3a_n/2\Delta\eta)$ in all cases.

We now consider the various chordwise integrations involved. We start with $\chi(\eta) = \phi_{\mathrm{T.E.}}'$. For this case there is no integration, but due to the fact that in general the characteristic mesh does not fit exactly on the planform, it will be necessary to obtain $\phi_{\mathrm{T.E.}}'$ by interpolation or extrapolation. In the diagram shown above, for instance, at spanwise station 4 extrapolation would be necessary whereas at station 5 interpolation would be used.

37
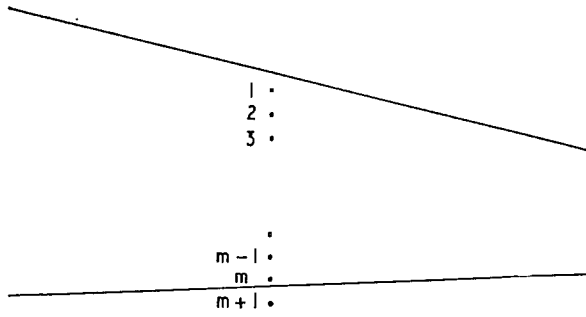
At any given spanwise station let the chordwise stations be numbered so that 1 is the first aft of the leading edge and let m be that station just on or forward of the trailing edge. These stations will be equally spaced, the interval between them being designated $\Delta\xi$. It is assumed initially that these stations are just the base-points of the system of rhombuses used in obtaining the potentials.

If there is no station at $m + 1$, then linear extrapolation is used to obtain $\phi_{\text{T.E.}}'$ and we obtain

$$\phi_{\text{T.E.}}' = \phi_m' + \frac{\phi_m' - \phi_{m-1}'}{\Delta\xi}(\xi_{\text{T.E.}} - \xi_m). \tag{165}$$

Similarly, if there is a station at $m + 1$, then linear interpolation is used and we obtain

$$\phi_{\text{T.E.}}' = \phi_m' + \frac{\phi_{m+1}' - \phi_m'}{\Delta\xi}(\xi_{\text{T.E.}} - \xi_m). \tag{166}$$

Thus for the extrapolation case the appropriate chordwise weighting factors are given by

$$O \times \phi_1' + O \times \phi_2' + \ldots + O \times \phi_{m-2}' - \frac{\xi_{\text{T.E.}} - \xi_m}{\Delta\xi}\phi_{m-1}' + \left(1 + \frac{\xi_{\text{T.E.}} - \xi_m}{\Delta\xi}\right)\phi_m'. \tag{167}$$

For the interpolation case the chordwise weighting factors are given by

$$O \times \phi_1' + O \times \phi_2' + \ldots + O \times \phi_{m-1}' + \left(1 - \frac{\xi_{\text{T.E.}} - \xi_m}{\Delta\xi}\right)\phi_m' + \frac{\xi_{\text{T.E.}} - \xi_m}{\Delta\xi}\phi_{m+1}'. \tag{168}$$

The case where m lies on the trailing edge can be regarded as a sub-case of (167).

Consider next $\chi(\eta) = \int_{\text{L.E.}}^{\text{T.E.}} \phi'd\xi$. This integral can be split up into three parts which we consider separately. Consider first $\int_{\xi_{\text{L.E.}}}^{\xi_1} \phi'd\xi$. The answer obtained for this depends on how ϕ' varies from zero at the leading edge to its value ϕ_1' at station 1. If the variation is linear, as is the case for supersonic leading edges or at the centre-line of a subsonic-leading-edge wing, the trapezium rule gives

$$\int_{\xi_{\text{L.E.}}}^{\xi_1} \phi'd\xi = \tfrac{1}{2}\phi_1'(\xi_1 - \xi_{\text{L.E.}}). \tag{169}$$

For stations other than the centre-line of wings with subsonic leading edges, ϕ' is assumed to vary like $\sqrt{(\xi - \xi_{\text{L.E.}})}$, and we obtain

$$\int_{\xi_{\text{L.E.}}}^{\xi_1} \phi'd\xi = \tfrac{2}{3}\phi_1'(\xi_1 - \xi_{\text{L.E.}}). \tag{170}$$

38

Over the region ξ_1 to ξ_m we obtain in all cases

$$\int_{\xi_1}^{\xi_m} \phi' d\xi = \Delta\xi[\tfrac{1}{2}\phi_1' + \phi_2' + \phi_3' + \ldots + \phi_{m-1}' + \tfrac{1}{2}\phi_m'].$$ (171)

Over the region ξ_m to $\xi_{\text{T.E.}}$ we obtain

$$\int_{\xi_m}^{\xi_{\text{T.E.}}} \phi' d\xi = \tfrac{1}{2}(\phi_m' + \phi_{\text{T.E.}}')(\xi_{\text{T.E.}} - \xi_m).$$ (172)

Combining these results for the case where extrapolation is used at the trailing edge, we obtain

$$\frac{1}{\Delta\xi}\int_0^1 \phi' d\xi = c_1\phi_1' + \phi_2' + \phi_3' + \ldots + \phi_{m-2}' +$$
$$+ \left[1 - \tfrac{1}{2}\left(\frac{\xi_{\text{T.E.}} - \xi_m}{\Delta\xi}\right)^2\right]\phi_{m-1}' + \left[\tfrac{1}{2} + \frac{\xi_{\text{T.E.}} - \xi_m}{\Delta\xi} + \tfrac{1}{2}\left(\frac{\xi_{\text{T.E.}} - \xi_m}{\Delta\xi}\right)^2\right]\phi_m'$$ (173)

and for the interpolation case

$$\frac{1}{\Delta\xi}\int_0^1 \phi' d\xi = c_1\phi_1' + \phi_2' + \phi_3' + \ldots + \phi_{m-1}' +$$
$$+ \left[\tfrac{1}{2} + \frac{\xi_{\text{T.E.}} - \xi_m}{\Delta\xi} - \tfrac{1}{2}\left(\frac{\xi_{\text{T.E.}} - \xi_m}{\Delta\xi}\right)^2\right]\phi_m' + \tfrac{1}{2}\left(\frac{\xi_{\text{T.E.}} - \xi_m}{\Delta\xi}\right)^2 \phi_{m+1}'$$ (174)

where

$$c_1 = \tfrac{1}{2} + \tfrac{1}{2}\frac{\xi_1 - \xi_{\text{L.E.}}}{\Delta\xi} \qquad \text{for supersonic leading edge or centre-line of subsonic-leading-edge wing.}$$ (175)

$$= \tfrac{1}{2} + \tfrac{2}{3}\frac{\xi_1 - \xi_{\text{L.E.}}}{\Delta\xi} \qquad \text{away from centre-line of subsonic-leading-edge wing.}$$ (176)

Consider next $\chi(\eta) = \int_{\text{L.E.}}^{\text{T.E.}} \phi' d\xi - \xi_{\text{T.E.}}\phi_{\text{T.E.}}'$. Using equation (165) we obtain for the extrapolation case

$$\frac{1}{\Delta\xi}\left[\int_{\text{L.E.}}^{\text{T.E.}} \phi' d\xi - \xi_{\text{T.E.}}\phi_{\text{T.E.}}'\right] = c_1\phi_1' + \phi_2' + \phi_3' + \ldots + \phi_{m-2}' +$$
$$+ \left[1 - \tfrac{1}{2}\left(\frac{\xi_{\text{T.E.}} - \xi_m}{\Delta\xi}\right)^2 + \frac{\xi_{\text{T.E.}}(\xi_{\text{T.E.}} - \xi_m)}{(\Delta\xi)^2}\right]\phi_{m-1}' +$$
$$+ \left[\tfrac{1}{2} + \frac{\xi_{\text{T.E.}} - \xi_m}{\Delta\xi} + \tfrac{1}{2}\left(\frac{\xi_{\text{T.E.}} - \xi_m}{\Delta\xi}\right)^2 - \frac{\xi_{\text{T.E.}}}{\Delta\xi}\left(1 + \frac{\xi_{\text{T.E.}} - \xi_m}{\Delta\xi}\right)\right]\phi_m'.$$ (177)

Using equation (166) we obtain for the interpolation case

$$\frac{1}{\Delta\xi}\left[\int_{\text{L.E.}}^{\text{T.E.}} \phi' d\xi - \xi_{\text{T.E.}}\phi_{\text{T.E.}}'\right] = c_1\phi_1' + \phi_2' + \phi_3' + \ldots + \phi_{m-1}' +$$
$$+ \left[\tfrac{1}{2} + \frac{\xi_{\text{T.E.}} - \xi_m}{\Delta\xi} - \tfrac{1}{2}\left(\frac{\xi_{\text{T.E.}} - \xi_m}{\Delta\xi}\right)^2 - \frac{\xi_{\text{T.E.}}}{\Delta\xi}\left(1 - \frac{\xi_{\text{T.E.}} - \xi_m}{\Delta\xi}\right)\right]\phi_m' +$$
$$+ \left[\tfrac{1}{2}\left(\frac{\xi_{\text{T.E.}} - \xi_m}{\Delta\xi}\right)^2 - \frac{\xi_{\text{T.E.}}}{\Delta\xi}\frac{\xi_{\text{T.E.}} - \xi_m}{\Delta\xi}\right]\phi_{m+1}'.$$ (178)

Finally we have to consider $\chi(\eta) = \int_{\text{L.E.}}^{\text{T.E.}} \xi\phi' d\xi$. The chordwise weights for this case can be obtained by multiplying the coefficients in equations (173), (174) by the corresponding $\xi_r's$.

39

To obtain the final system of weights we multiply the chordwise integration weights by the appropriate spanwise weighting factors. If we now multiply this system of weighting factors into the appropriate set of ϕ's we obtain a factored form of the integral required. The factored forms of the integrals obtained using (167) or (168); (173) or (174); (177) or (178) in combination with (163) or (164) are

$$\frac{1}{\frac{2}{3}\Delta\eta}\int_0^1 \phi_{\text{T.E.}}'d\eta\,,\quad \frac{1}{\frac{2}{3}\Delta\eta\Delta\xi}\int_0^1\left[\int_{\text{L.E.}}^{\text{T.E.}}\phi'd\xi\right]d\eta\,,\quad \frac{1}{\frac{2}{3}\Delta\eta\Delta\xi}\int_0^1\left[\int_{\text{L.E.}}^{\text{T.E.}}\phi'd\xi - \xi_{\text{T.E.}}\phi_{\text{T.E.}}'\right]d\eta\,,\quad (179)$$

respectively. Similarly applying (173) or (174) in combination with (163) or (164) to $\xi\phi$'s instead of ϕ's we obtain

$$\frac{1}{\frac{2}{3}\Delta\eta\Delta\xi}\int_0^1\left[\int_{\text{L.E.}}^{\text{T.E.}}\xi\phi'd\xi\right]d\eta\,. \quad (180)$$

The setting up of the coefficients to obtain the three integrals (179) is comparatively simple, because over the bulk of the planform the coefficients are simple integers. It is only round the boundaries of the planform that the coefficients become more complicated. Furthermore it will be noted that (177) and (178) only differ from (173) and (174) near the trailing edge.

It will be noted that the weighting coefficients described depend only on the planform geometry, the mesh size and the sweep of the characteristics, i.e. the Mach number. Thus, if the same mesh has been used to deal with several frequencies and several modes, the same sets of weighting coefficients apply unchanged.

In the exposition of the theory given above it was assumed that the nodal points for obtaining the factored integrals were the same as those used in computing the potentials. This need not necessarily be so and if the original mesh is particularly fine, some coarser sub-mesh can be selected for obtaining the factored integrals. We merely have to use the appropriate $\Delta\xi$ and $\Delta\eta$ i.e.

$$\Delta\xi = p\,\frac{2l\beta}{M}\frac{1}{c_0}\,,\qquad \Delta\eta = q\,\frac{2l}{M}\frac{1}{\sigma}\,, \quad (181)$$

where p and q are integers, not necessarily equal. On the rectangular wing for instance, it was sometimes convenient to use $q = 2$, $p = 1$.

Due to the presence of shocks, there may be discontinuities in slope in the potentials both spanwise and chordwise. In performing the spanwise integrations using Simpson's rule it is assumed that the spanwise discontinuities can be ignored without much loss of accuracy. If however the shocks are particularly strong, some alternative method of procedure is necessary. Since the trapezium rule is used for the chordwise integrations, discontinuities in slope are correctly allowed for unless these occur somewhere between nodal points of the integration mesh. This can normally be avoided by a judicious choice of mesh when initially obtaining the potentials.

8. *Formulae for Pitching and Plunging Derivatives.*

The pitch angle θ corresponds to a modal shape

$$g = -\theta x\,. \quad (182)$$

The corresponding derivatives are defined by the equations:

$$\mathscr{L} = \rho U^2 S\left[l_\theta + i\nu l_{\dot\theta}\right]\theta e^{i\omega t} \quad (183)$$

$$\mathscr{M} = \rho U^2 S\bar c\left[m_\theta + i\nu m_{\dot\theta}\right]\theta e^{i\omega t} \quad (184)$$

40

where $\mathscr{L}$ is the oscillatory lift, positive up and $\mathscr{M}$ is the oscillatory pitching-moment coefficient, positive nose up, about an axis through the wing vertex. If we compare these equations with those in terms of the lift and pitching-moment coefficients, i.e.

$$\mathscr{L} = \tfrac{1}{2} \rho U^2 S \left[C_{LR} + i C_{LI} \right]_{g=-x} \times \theta e^{i\omega t} \tag{185}$$

$$\mathscr{M} = \tfrac{1}{2} \rho U^2 S \bar{c} \left[C_{mR} + i C_{mI} \right]_{g=-x} \times \theta e^{i\omega t} \tag{186}$$

we obtain

$$l_\theta = \tfrac{1}{2} \left[C_{LR} \right]_{g=-x}, \qquad l_{\dot{\theta}} = \frac{1}{2\nu} \left[C_{LI} \right]_{g=-x} \tag{187}$$

$$m_\theta = \tfrac{1}{2} \left[C_{mR} \right]_{g=-x}, \qquad m_{\dot{\theta}} = \frac{1}{2\nu} \left[C_{mI} \right]_{g=-x}. \tag{188}$$

Plunging corresponds to a modal shape

$$g = z. \tag{189}$$

The corresponding derivatives are defined by the equations

$$\mathscr{L} = \rho U^2 S \left[l_z + i\nu l_{\dot{z}} \right] \frac{z}{c_0} e^{i\omega t} \tag{190}$$

$$\mathscr{M} = \rho U^2 S \bar{c} \left[m_z + i\nu m_{\dot{z}} \right] \frac{z}{c_0} e^{i\omega t} \tag{191}$$

If we compare these equations with those in terms of the lift and pitching-moment coefficients, we obtain

$$l_z = \tfrac{1}{2} \left[C_{LR} \right]_{g=c_0}, \qquad l_{\dot{z}} = \frac{1}{2\nu} \left[C_{LI} \right]_{g=c_0} \tag{192}$$

$$m_z = \tfrac{1}{2} \left[C_{mR} \right]_{g=c_0}, \qquad m_{\dot{z}} = \frac{1}{2\nu} \left[C_{mI} \right]_{g=c_0}. \tag{193}$$

9. *Results.*

As a check on the accuracy achieved in practice, velocity potentials were found by exact analytical methods for certain planforms and Mach numbers. Thus for a rectangular wing, solutions can be obtained over that portion of the planform not affected by interaction of the tip downwashes (Ref. 1). For a frequency parameter of $0 \cdot 6$ and $M = 1 \cdot 05$ the largest errors were 2% in ϕ_R' and 5% in ϕ_I' in a rigid pitching oscillation. On integrating the potentials to obtain the derivatives, smaller errors should result. As $M \to 1$ the rectangular wing potentials show more and more chordwise undulations, and from two-dimensional theory the wave-length should be $\pi\beta^2 U/\omega$. The results conform to this prediction.

Only quasi-steady results are available in analytic form for the delta wing, and agreement is good for small ν. Using the linear approximation for the edge rhombuses as suggested previously, some inaccuracies do arise which are accentuated by the highly swept planform. This gives rise to a kinked distribution of ϕ_I' in pitch or ϕ_R' in translation particularly at the lower frequencies. However, it is only for $M = 1 \cdot 01$ that the effect is very bad. Results for this case have been checked by performing the direct numerical integrations given by equations (80), (82), (83), (84) for the edge rhombus contributions. When this is done the potentials obtained vary smoothly and fit a mean line through the kinked values.

41

Checks on the tapered wing results were obtained from quasi-steady theory, and also using arbitrary-frequency-parameter theory valid for supersonic leading edges.

Figs. 2 to 9 give samples of the results together with comparison theories where possible. Tables 1, 2, 3 give values of derivatives for the three wings shown in Fig. 1. The Mach numbers and frequency parameters were chosen to fit in with an investigation being carried out at the National Physical Laboratory. The delta-wing results show an insensitivity to frequency parameter for M near $1 \cdot 0$.

10. *Conclusions.*

The method is capable of almost unlimited accuracy but the amount of extra labour required to reduce the last 5% error as $M \to 1$ is very great. For normal Mach numbers say greater than $1 \cdot 2$ for which linearized theory is usually applied, it is likely that the special treatment of edge rhombuses is not required. Then simple weights, say based on irregular rhombus area, might be sufficient. The process would then become very simple particularly for the linear interpolation weights case.

a, b, c		Coefficients used in the representation for $\phi'K$ or $\phi'L$ over an irregular rhombus. See equations (A.6), (A.16) to (A.18), (A.23) to (A.25), (A.31), (89), (B.1), (B.6) to (B.8), (B.13) to (B.15), (B.18), (B.22)
A, B		See (30a), (30b)
A, B, C, D		Symbols used to label rhombuses relative to point r, s. See figure preceding equation (22)
$C_{r+u,\,s+v}$		See equations (18), (19), (21)
C_1, C_2, C_3		Subsonic L.E.: equations (19), (21). Supersonic L.E.: equations (B.9) to (B.11)
$C_1' \; C_2'$		Subsonic L.E.: equations (26) to (29). Supersonic L.E.: equations (B.16) to (B.17)
C_1''		Supersonic L.E.: equations (B.19), (B.20)
$C_1{}^p(r, s)\,(p = 0, 1, 2)$		Coefficient in parabolic fitting to $C_1(r, s, g)$. See Section 5.5 (ii)
C_L	$=$	$C_{LR} + iC_{LI}$, complex lift coefficient. See equations (152), (156), (157)
C_m	$=$	$C_{mR} + iC_{mI}$, complex pitching-moment coefficient. See equations (158) to (160)
c_0		Wing root chord
$\bar{c}$		Wing mean chord
D_1, D_2, D_3		Subsonic L.E.: equations (35) to (37). Supersonic L.E.: equations (B.28) to (B.30)
D_1', D_2'		Subsonic L.E.: equations (38) to (41). Supersonic L.E.: equations (B.31), (B.32)
D_1''		Supersonic L.E.: equations (B.33), (B.34)
$E(r)$	$=$	$F_0(r) + F_1(r-1)$. See equations (56), (57), (67), (68)
$E^*(r)$	$=$	$F_0^*(r) + F_1^*(r-1)$. See equations (58) to (60), (71), (72)
E	$=$	$s + g - rK \geqslant 0$. See equation (A.11)
$f_u(\rho')$		Linear interpolation functions. See equation (51)
$F_u(r)$		See equations (55), (65), (66)
$F_u^*(r)$		See equations (61), (69), (70)
f_1, f_2, f_3, f_4		See equations (A.12) to (A.15) or (A.12a) to (A.15a) for transonic L.E. case

43

$f_1', f_2' \ldots f_{16}'$		See equations following equation (A.34)
$g(x, y)$		Modal shape of oscillation. See equation (3)
$g_i(\rho')$		Parabolic interpolation functions. See equation (17)
$G_i(r)$		See equations (20), (33), (34)
$G_i^*(r)$		See equations (26), (35), (36)
g		Side of an irregular rhombus expressed as a fraction of the side of a regular rhombus. See diagrams preceding equations (A.1), (A.23), (B.1), (B.13), (B.18)
g'	$=$	g/K
$H(v', r, s)$		See equation (64)
i, j		Suffixes which can take values $0, \frac{1}{2}, 1$ associated with parabolic interpolation weights. See equations (17) to (26)
$I(r)$		See equation (40)
I_1, I_2		See equations (A.42), (A.43)
j_1, j_2		See equations (B.26), (B.28)
K_1, K_2		See equations (12a), (12b)
k_1, k_2		See equations (29a), (29b)
K		See equation (A.4). Subsonic L.E. $1 \geqslant K > 0$, Transonic $K = 0$, Supersonic L.E. $0 > K \geqslant -1$
K_r		Coefficients associated with error propagation for a steady one-dimensional case. See equation (139)
$K_{rs}, \overline{K}_{rs}$		Coefficients associated with error propagation for oscillating 3-dimensional flow. See equations (140) to (142)
L		Reference length used in non-dimensionalising ϕ. See equation (8)
l		Length of side of basic rhombus in the characteristic mesh. See figure preceding equation (7a)
L_1, L_2		See equations (13a), (13b)
$l(x, y)$	$=$	$l_R + il_I$, complex lift per unit area
$\mathscr{L}$	$=$	$\mathscr{L}_R + i\mathscr{L}_I$, total complex lift
$l_\theta, l_{\dot{\theta}}, m_\theta, m_{\dot{\theta}}$		pitching derivatives defined by equations (183), (184)

$l_z, l_{\dot{z}}, m_z, m_{\dot{z}}$ plunging derivatives defined by equations (190), (191)

L, M, N Coefficients of a, b, c in contribution from an irregular rhombus. See equations (A.7) to (A.10); (B.1) to (B.4)

$\bar{L}, \bar{M}, \bar{N}$ Coefficients of a, b, c in contribution from an irregular rhombus. See equations (A.31) to (A.34); (A.32a) to (A.34a); (B.22) to (B.25)

M Free-stream Mach number

m $=$ $\tan \Lambda$, tangent of sweepback angle of L.E.

$\mathcal{M}$ $=$ $\mathcal{M}_R + \mathcal{M}_I$, complex leading-edge pitching moment

p Local pressure

p_∞ Free-stream pressure

P, Q, R See equations (105) to (107)

r, s Values of ρ, σ the characteristic co-ordinates based at the pivotal point. See equations (7a), (7b) and adjacent diagram

R See definition following equation (1)

$\mathcal{R}$ Real part of

s Semi-span of wing

S Planform area

t Time

T.E.   Trailing edge

u, v Local system of characteristic co-ordinates such that base point of current rhombus is $u = 0$, $v = 0$. See diagram adjacent to equation (15)

U Free-stream velocity

V Local fluid velocity vector

w $=$ $\dfrac{\partial \phi}{\partial z}$, Upwash

$W_{rs}, \bar{W}_{rs}$ Integration weights. See equations (23) to (25), (27); (42); (48); (62), (63); (86)

$W_{rs}{}^*, \bar{W}_{rs}{}^*$ Modified regular weights for use with parabolic interpolation on ϕ'. See equation (148)

W_{00}, $\overline{W}_{00}$		Pivotal weights. See equations (43), (44); (49), (50); (73), (74) for regular values. For irregular values, see equations (97), (98); (100) to (102), (111) to (113)
δW_{rs}		Part of weight stemming from $K_1 G_i G_j$ terms in equation (24). See equations (41); (47)
x, y, z		Rectangular co-ordinates. See definitions and diagram adjacent to equation (1)
x, y		Local co-ordinate system defined in diagram adjacent to equation (45)
$\alpha(x, y)$	$=$	$-\dfrac{\partial g(x, y)}{\partial x}$, in-phase incidence
α'		See equation (32)
β	$=$	$(M^2 - 1)^{1/2}$
$\tau_{uv}(r, s)$		Contributions to weights from irregular rhombuses. See equations (80); (A.19), (A.26); (B.9), (B.19)
$\bar{\tau}_{uv}(r, s)$		See equations (82); (A.21), (A.27); (B.11), (B.19)
$\delta_{uv}(r, s)$		See equations (83); (A.35), (A.38); (B.28), (B.33)
$\bar{\delta}_{uv}(r, s)$		See equations (84); (A.37), (A.39); (B.30), (B.33)
ϵ_{00}, ϵ_{10}, ϵ_{11}		See equations (90) to (93); (108), (111)
ϵ_{00}', ϵ_{10}'		See equations (94) to (96); (109), (112)
ϵ_{00}''		See equations (110), (113)
ξ, η		The ξ, η axes are coincident with the x, y axes shown in the diagram adjacent to equation (1)
ξ	$=$	$\dfrac{x}{c_0}$, non-dimensional form of x co-ordinate
η	$=$	$\dfrac{y}{\sigma}$, non-dimensional form of y co-ordinate

See equation (154)

Λ		Sweepback angle of given portion of L.E.
θ		Pitch angle. See equation (182)
ρ or ρ_∞		Free-stream density
ρ, σ		Characteristic co-ordinates based at pivotal point. See equations (7a), (7b) and adjacent diagram

ρ', σ' $\rho' = \rho - r,\ \sigma' = \sigma - s$

$\sigma_{\text{L.E.}}(\rho)$ Equation of starboard L.E. is $\sigma = \sigma_{\text{L.E.}}(\rho)$. See equation (A.3)

$\phi \ = \ \phi_R + i\phi_I$, complex potential

$\phi' \ = \ \dfrac{\phi}{UL}$, non-dimensional potential

ω Circular frequency of oscillation

$\bar{\omega} \ = \ \dfrac{\omega}{U\beta^2}$

$\nu \ = \ \dfrac{\omega c_0}{U}$, see equation (155). Frequency parameter based on root chord

$\nu' \ = \ \dfrac{l\omega}{\beta U}$, see equation (9)

$\lambda_{uv}(\rho', \sigma')$ Interpolation functions. See equations (16), (37), (46)

REFERENCES

No.	Author	Title, etc.
1	J. R. Richardson	A method of calculating the lifting forces on wings (unsteady subsonic and supersonic lifting-surface theory). A.R.C. R. & M. 3157. April, 1955.
2	W. P. Jones	Supersonic theory for oscillating wings of any plan form. A.R.C. R. & M. 2655. June, 1948.

TABLE 1

Rectangular Wing, $A = 2$

M	$\nu=0.03$		$\nu=0.1$		$\nu=0.3$		$\nu=0.6$	
$\dfrac{\sqrt{37}}{6}$ $=1.014$	$l_\theta= 1.54$	$l_z= 0.00150$	$l_\theta= 1.60$	$l_z= 0.0106$	$l_\theta= 1.80$	$l_z= 0.0117$	$l_\theta= 1.78$	$l_z=-0.0140$
	$l_{\dot\theta}= 2.80$	$l_{\dot z}=-1.53$	$l_{\dot\theta}= 2.49$	$l_{\dot z}=-1.59$	$l_{\dot\theta}= 1.40$	$l_{\dot z}=-1.71$	$l_{\dot\theta}= 1.01$	$l_{\dot z}=-1.61$
	$m_\theta=-0.0252$	$m_z=-0.00315$	$m_\theta=-0.119$	$m_z=-0.0258$	$m_\theta=-0.468$	$m_z=-0.102$	$m_\theta=-0.643$	$m_z=-0.161$
	$m_{\dot\theta}=-4.00$	$m_{\dot z}= 0.0194$	$m_{\dot\theta}=-3.38$	$m_{\dot z}= 0.116$	$m_{\dot\theta}=-1.88$	$m_{\dot z}= 0.433$	$m_{\dot\theta}=-1.08$	$m_{\dot z}= 0.567$
$\dfrac{\sqrt{17}}{4}$ $=1.031$			$l_\theta= 1.63$	$l_z= 0.0143$	$l_\theta= 1.79$	$l_z=-0.0004$		
			$l_{\dot\theta}= 2.86$	$l_{\dot z}=-1.61$	$l_{\dot\theta}= 1.24$	$l_{\dot z}=-1.70$		
			$m_\theta=-0.175$	$m_z=-0.0323$	$m_\theta=-0.486$	$m_z=-0.0917$		
			$m_{\dot\theta}=-4.03$	$m_{\dot z}= 0.167$	$m_{\dot\theta}=-1.75$	$m_{\dot z}= 0.446$		
1.05					$l_\theta= 1.85$	$l_z=-0.00451$	$l_\theta= 1.79$	$l_z=-0.0460$
					$l_{\dot\theta}= 1.16$	$l_{\dot z}=-1.77$	$l_{\dot\theta}= 0.888$	$l_{\dot z}=-1.61$
					$m_\theta=-0.595$	$m_z=-0.0841$	$m_\theta=-0.689$	$m_z=-0.134$
					$m_{\dot\theta}=-1.65$	$m_{\dot z}= 0.553$	$m_{\dot\theta}=-0.987$	$m_{\dot z}= 0.603$
1.075					$l_\theta= 1.69$	$l_z=-0.0258$		
					$l_{\dot\theta}= 0.890$	$l_{\dot z}=-1.60$		
					$m_\theta=-0.475$	$m_z=-0.0658$		
					$m_{\dot\theta}=-1.42$	$m_{\dot z}= 0.424$		

1·1						$l_\theta = 1·71$ $l_z = -0·0554$ $l_{\dot\theta} = 0·836$ $l_{\dot z} = -1·55$ $m_\theta = -0·675$ $m_z = -0·109$ $m_{\dot\theta} = -0·884$ $m_{\dot z} = 0·595$
$\dfrac{\sqrt{5}}{2} = 1·118$				$l_\theta = 1·70$ $l_z = -0·0919$ $l_{\dot\theta} = 0·0880$ $l_{\dot z} = -1·60$ $m_\theta = -0·521$ $m_z = 0·0120$ $m_{\dot\theta} = -0·529$ $m_{\dot z} = 0·452$		
$\dfrac{\sqrt{2}}{} = 1·414$						$l_\theta = 1·36$ $l_{\dot\theta} = 0·422$ $m_\theta = -0·578$ $m_{\dot\theta} = -0·330$

$$\mathscr{L} = \rho U^2 S \left[(l_\theta + i\nu l_{\dot\theta})\theta + (l_z + i\nu l_{\dot z})\frac{z}{c_0} \right] e^{i\omega t}$$

$$\mathscr{M} = \rho U^2 S \bar{c} \left[(m_\theta + i\nu m_{\dot\theta})\theta + (m_z + i\nu m_{\dot z})\frac{z}{c_0} \right] e^{i\omega t}$$

$\mathscr{L}$ = oscillatory lift, positive up

$\mathscr{M}$ = oscillatory pitching moment, positive nose up, about an axis through the wing vertex

c_0 = root chord

$\bar{c}$ = mean chord

$\nu = \dfrac{\omega c_0}{U}$

TABLE 2

Delta Wing, $\tan \Lambda = \dfrac{8}{3}$

M	$\nu=0.03$		$\nu=0.1$		$\nu=0.3$		$\nu=0.6$	
1·01	$l_\theta = 1\cdot15$ $l_{\dot\theta} = 0\cdot956$ $m_\theta = -1\cdot54$ $m_{\dot\theta} = -1\cdot44$		$l_\theta = 1\cdot15$ $l_{\dot\theta} = 1\cdot04$ $m_\theta = -1\cdot52$ $m_{\dot\theta} = -1\cdot58$		$l_\theta = 1\cdot13$ $l_{\dot\theta} = 1\cdot06$ $m_\theta = -1\cdot51$ $m_{\dot\theta} = -1\cdot64$	$l_z = -0\cdot00239$ $l_{\dot z} = -1\cdot11$ $m_z = -0\cdot00176$ $m_{\dot z} = 1\cdot48$	$l_\theta = 1\cdot14$ $l_{\dot\theta} = 1\cdot06$ $m_\theta = -1\cdot55$ $m_{\dot\theta} = -1\cdot62$	$l_z = 0\cdot00772$ $l_{\dot z} = -1\cdot09$ $m_z = -0\cdot0191$ $m_{\dot z} = 1\cdot47$
1·03					$l_\theta = 1\cdot14$ $l_{\dot\theta} = 1\cdot06$ $m_\theta = -1\cdot52$ $m_{\dot\theta} = -1\cdot60$	$l_z = -0\cdot00244$ $l_{\dot z} = -1\cdot12$ $m_z = 0\cdot00161$ $m_{\dot z} = 1\cdot49$	$l_\theta = 1\cdot13$ $l_{\dot\theta} = 1\cdot06$ $m_\theta = -1\cdot50$ $m_{\dot\theta} = -1\cdot60$	$l_z = 0\cdot0121$ $l_{\dot z} = -1\cdot08$ $m_z = -0\cdot0258$ $m_{\dot z} = 1\cdot44$
1·075					$l_\theta = 1\cdot14$ $l_{\dot\theta} = 1\cdot05$ $m_\theta = -1\cdot52$ $m_{\dot\theta} = -1\cdot59$	$l_z = -0\cdot00130$ $l_{\dot z} = -1\cdot12$ $m_z = 0\cdot000167$ $m_{\dot z} = 1\cdot49$	$l_\theta = 1\cdot14$ $l_{\dot\theta} = 1\cdot05$ $m_\theta = -1\cdot52$ $m_{\dot\theta} = -1\cdot59$	$l_z = 0\cdot0108$ $l_{\dot z} = -1\cdot10$ $m_z = -0\cdot0236$ $m_{\dot z} = 1\cdot46$
1·15					$l_\theta = 1\cdot11$ $l_{\dot\theta} = 1\cdot01$ $m_\theta = -1\cdot47$ $m_{\dot\theta} = -1\cdot53$	$l_z = 0\cdot000106$ $l_{\dot z} = -1\cdot10$ $m_z = -0\cdot00181$ $m_{\dot z} = 1\cdot45$		

TABLE 3

Symmetrical Tapered Wing,

$$c_0 = 10\,ft, \qquad s = 13\cdot7\,ft, \qquad \Lambda_{\text{L.E.}} = -\Lambda_{\text{T.E.}} = 15°$$

M	$\nu=0\cdot03$		$\nu=0\cdot1$		$\nu=0\cdot3$		$\nu=0\cdot6$	
1·01	$l_\theta=\ 3\cdot65$ $l_{\dot\theta}=-7\cdot41$ $m_\theta=-1\cdot62$ $m_{\dot\theta}=-2\cdot45$	$l_z=-0\cdot00858$ $l_{\dot z}=-3\cdot66$ $m_z=-0\cdot000618$ $m_{\dot z}=\ 1\cdot64$	$l_\theta=\ 3\cdot49$ $l_{\dot\theta}=-3\cdot20$ $m_\theta=-1\cdot90$ $m_{\dot\theta}=-2\cdot44$	$l_z=-0\cdot0547$ $l_{\dot z}=-3\cdot43$ $m_z=-0\cdot00631$ $m_{\dot z}=\ 1\cdot86$	$l_\theta=\ 2\cdot96$ $l_{\dot\theta}=-1\cdot37$ $m_\theta=-1\cdot88$ $m_{\dot\theta}=-0\cdot509$	$l_z=-0\cdot275$ $l_{\dot z}=-2\cdot73$ $m_z=\ 0\cdot0834$ $m_{\dot z}=\ 1\cdot72$		
1·0353	$l_\theta=\ 4\cdot02$ $l_{\dot\theta}=-9\cdot01$ $m_\theta=-2\cdot36$ $m_{\dot\theta}=\ 5\cdot62$	$l_z=-0\cdot00984$ $l_{\dot z}=-4\cdot02$ $m_z=\ 0\cdot00665$ $m_{\dot z}=\ 2\cdot36$	$l_\theta=\ 3\cdot60$ $l_{\dot\theta}=-6\cdot66$ $m_\theta=-2\cdot02$ $m_{\dot\theta}=\ 3\cdot34$	$l_z=-0\cdot0894$ $l_{\dot z}=-3\cdot55$ $m_z=\ 0\cdot0528$ $m_{\dot z}=\ 1\cdot98$	$l_\theta=\ 2\cdot91$ $l_{\dot\theta}=-1\cdot28$ $m_\theta=-1\cdot87$ $m_{\dot\theta}=-0\cdot534$	$l_z=-0\cdot266$ $l_{\dot z}=-2\cdot69$ $m_z=\ 0\cdot0787$ $m_{\dot z}=\ 1\cdot70$	$l_\theta=\ 2\cdot59$ $l_{\dot\theta}=-0\cdot111$ $m_\theta=-1\cdot79$ $m_{\dot\theta}=-0\cdot561$	$l_z=-0\cdot497$ $l_{\dot z}=-2\cdot16$ $m_z=\ 0\cdot208$ $m_{\dot z}=\ 1\cdot47$
1·102					$l_\theta=\ 2\cdot89$ $l_{\dot\theta}=-1\cdot93$ $m_\theta=-1\cdot87$ $m_{\dot\theta}=\ 1\cdot35$	$l_z=-0\cdot318$ $l_{\dot z}=-2\cdot74$ $m_z=\ 0\cdot248$ $m_{\dot z}=\ 1\cdot73$		
1·0645					$l_\theta=\ 2\cdot79$ $l_{\dot\theta}=-2\cdot01$ $m_\theta=-1\cdot64$ $m_{\dot\theta}=\ 0\cdot654$	$l_z=-0\cdot329$ $l_{\dot z}=-2\cdot60$ $m_z=\ 0\cdot184$ $m_{\dot z}=\ 1\cdot46$		

APPENDIX A

1. *The Derivation of* $\tau_{uv}(r, s)$ *and* $\bar{\tau}_{uv}(r, s)$ *for an Irregular Rhombus Adjacent to a Subsonic Leading Edge.*
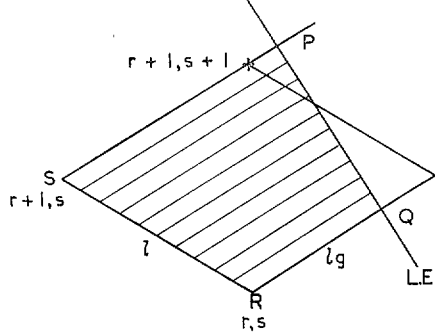
Let l be the side of a characteristic rhombus, then we have SR = l. We define RQ to be lg. If the pivotal point is x, y, the current co-ordinates ξ, η are related to ρ and σ by equations (7a) and (7b). Thus, since Q has co-ordinates $\rho = r$, $\sigma = s + g$, we have

$$\xi_Q = x - \frac{l\beta}{M}(r+s+g), \qquad \eta_Q = y + \frac{l}{M}(s-r+g). \tag{A.1}$$

If the sweepback angle of the leading edge is Λ and $\tan \Lambda = m$ then the equation of the leading edge is

$$\frac{\xi - \xi_Q}{\eta - \eta_Q} = m. \tag{A.2}$$

On substituting equations (7a), (7b) and (A.1) into equation (A.2), we obtain the equation of the leading edge as

$$\sigma_{\mathrm{L.E.}}(\rho) = (\rho - r)K + s + g, \tag{A.3}$$

where

$$K = \frac{1 - k}{1 + k} \tag{A.4}$$

and

$$k = \frac{\beta}{m}. \tag{A.5}$$

It will be noted that for a subsonic leading edge $k < 1$ and hence $K > 0$.

An examination of the equations (80) and (82) for τ and $\bar{\tau}$ quickly shows that due to the complexity of the functions K_1 and K_2, it will be impossible to perform the integrations analytically. We proceed therefore in a slightly different manner. Returning to equation (77) we take as the representation for $\phi_R' K_1$,

$$\phi_R'(\rho, \sigma)K_1(\rho, \sigma) = (a\sigma + b\rho + c)(\sigma_{\mathrm{L.E.}} - \sigma)^{1/2}. \tag{A.6}$$

This representation gives the right variation at a subsonic leading edge and allows the fitting of $\phi_R' K_1$ at up to 3 vertices inside the planform edge.

52

Thus the contribution from (77) will be

$$\int_r^{r+1} \int_s^{\sigma_{\text{L.E.}}(\rho)} \frac{(a\sigma + b\rho + c)\sqrt{(\sigma_{\text{L.E.}} - \sigma)}}{4(\rho\sigma)^{3/2}} \, d\rho \, d\sigma$$

$$= aL(r, s, g, K) + bM(r, s, g, k) + cN(r, s, g, K), \tag{A.7}$$

where

$$L(r, s, g, K) = -\frac{E\pi}{4}\left\{\frac{1}{(r+1)^{1/2}} - \frac{1}{r^{1/2}}\right\} + \frac{\pi K}{4}\{(r+1)^{1/2} - r^{1/2}\} - \tfrac{1}{2}s^{1/2}f_1(r, g, K) -$$

$$- \frac{E}{4}f_2(r, s, g, K) - \frac{K}{4}f_3(r, s, g, K) \tag{A.8}$$

$$M(r, s, g, K) = -\frac{\pi}{2}\{(r+1)^{1/2} - r^{1/2}\} + \frac{1}{2s^{1/2}}f_4(r, g, K) + \tfrac{1}{2}f_3(r, s, g, K) \tag{A.9}$$

$$N(r, s, g, K) = \frac{\pi}{2}\left\{\frac{1}{(r+1)^{1/2}} - \frac{1}{r^{1/2}}\right\} + \frac{1}{s^{1/2}}f_1(r, g, K) + \tfrac{1}{2}f_2(r, s, g, K) \tag{A.10}$$

and

$$E = s + g - rK \geqslant 0 \tag{A.11}$$

$$f_1(r, g, K) = -\left(\frac{g+K}{r+1}\right)^{1/2} + \left(\frac{g}{r}\right)^{1/2} + K^{1/2}\log_e\left[\frac{\{(r+1)K\}^{1/2} + (g+K)^{1/2}}{(rK)^{1/2} + g^{1/2}}\right] \tag{A.12}$$

$$f_2(r, s, g, K) = -\frac{2}{(r+1)^{1/2}}\sin^{-1}\left(\frac{s}{s+g+K}\right)^{1/2} + \frac{2}{r^{1/2}}\sin^{-1}\left(\frac{s}{s+g}\right) -$$

$$- \left(\frac{K}{E}\right)^{1/2}\log_e\left[\frac{\{(r+1)sK\}^{1/2} + \{E(g+K)\}^{1/2}}{\{(r+1)sK\}^{1/2} - \{E(g+K)\}^{1/2}} \cdot \frac{(rsK)^{1/2} - (Eg)^{1/2}}{(rsK)^{1/2} + (Eg)^{1/2}}\right] \tag{A.13}$$

$$f_3(r, s, g, K) = 2(r+1)^{1/2}\sin^{-1}\left(\frac{s}{s+g+K}\right)^{1/2} - 2r^{1/2}\sin^{-1}\left(\frac{s}{s+g}\right)^{1/2} +$$

$$+ 2\left(\frac{s}{K}\right)^{1/2}\log_e\left[\frac{\{(r+1)K\}^{1/2} + (g+K)^{1/2}}{(rK)^{1/2} + g^{1/2}}\right] -$$

$$- \left(\frac{E}{K}\right)^{1/2}\log_e\left[\frac{\{(r+1)sK\}^{1/2} + \{E(g+K)\}^{1/2}}{\{(r+1)sK\}^{1/2} - \{E(g+K)\}^{1/2}} \cdot \frac{(rsK)^{1/2} - (Eg)^{1/2}}{(rsK)^{1/2} + (Eg)^{1/2}}\right] \tag{A.14}$$

$$f_4(r, g, K) = \frac{g - Kr}{K^{1/2}}\log_e\left[\frac{\{(r+1)K\}^{1/2} + (g+K)^{1/2}}{(rK)^{1/2} + g^{1/2}}\right] + \{(r+1)(g+K)\}^{1/2} - (rg)^{1/2}. \tag{A.15}$$

To deduce $\tau_{uv}(r, s)$ we must make use of equation (79), which means that we must first express a, b, c in terms of $\phi_{R\,r,s}{}', \phi_{R\,r+1,s}{}', \phi_{R\,r+1,s+1}{}'$. Substituting the three pairs of co-ordinates into equation (A.6), we obtain three equations which, on solving a, b, c, give

$$a = -\frac{[\phi_R'K_1]_{r+1,s}}{(g+K)^{1/2}} + \frac{[\phi_R'K_1]_{r+1,s+1}}{(g+K-1)^{1/2}} \tag{A.16}$$

$$b = -\frac{[\phi_R'K_1]_{r,s}}{g^{1/2}} + \frac{[\phi_R'K_1]_{r+1,s}}{(g+K)^{1/2}} \tag{A.17}$$

$$c = (s-r)\frac{[\phi_R'K_1]_{r+1,s}}{(g+K)^{1/2}} - s\frac{[\phi_R'K_1]_{r+1,s+1}}{(g+K-1)^{1/2}} + (r+1)\frac{[\phi_R'K_1]_{r,s}}{g^{1/2}}. \tag{A.18}$$

E 2

Returning to equation (A.7) and picking out the coefficients of $\phi_R{}'(r, s)$, $\phi_R{}'(r+1, s)$, $\phi_R{}'(r+1, s+1)$ in turn, we obtain

$$
\left.
\begin{aligned}
\tau_{00}(r, s) &= K_1(r, s)C_1(r, s) \\
\tau_{10}(r, s) &= K_1(r+1, s)C_2(r, s) \\
\tau_{11}(r, s) &= K_1(r+1, s+1)C_3(r, s)
\end{aligned}
\right\}
\tag{A.19}
$$

where

$$
\left.
\begin{aligned}
C_1(r, s) &= \frac{1}{g^{1/2}} \left[- M(r, s, g, K) + (r+1)N(r, s, g, K) \right] \\
C_2(r, s) &= \frac{1}{(g+K)^{1/2}} \left[- L(r, s, g, K) + M(r, s, g, K) + (s-r)N(r, s, g, K) \right] \\
C_3(r, s) &= \frac{1}{(g+K-1)^{1/2}} \left[L(r, s, g, K) - sN(r, s, g, K) \right].
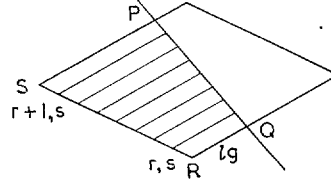\end{aligned}
\right\}
\tag{A.20}
$$

In a similar manner

$$
\left.
\begin{aligned}
\bar{\tau}_{00}(r, s) &= K_2(r, s)C_1(r, s) \\
\bar{\tau}_{10}(r, s) &= K_2(r+1, s)C_2(r, s) \\
\bar{\tau}_{11}(r, s) &= K_2(r+1, s+1)C_3(r, s).
\end{aligned}
\right\}
\tag{A.21}
$$

It is easily verified that for the three vertex case the length $SP = (g+K)l$ must be greater than l. Hence the inequality

$$
g > 1 - K \tag{A.22}
$$

must be satisfied.

In a similar manner, we find for the two vertex case,

$$
a = 0 \tag{A.23}
$$

$$
b = \frac{[\phi_R{}'K_1]_{r+1, s}}{(g+K)^{1/2}} - \frac{[\phi_R{}'K_1]_{r, s}}{g^{1/2}} \tag{A.24}
$$

$$
c = - r \frac{[\phi_R{}'K_1]_{r+1, s}}{(g+K)^{1/2}} + (r+1) \frac{[\phi_R{}'K_1]_{r, s}}{g^{1/2}}, \tag{A.25}
$$

and hence

$$
\left.
\begin{aligned}
\tau_{00}(r, s) &= K_1(r, s)C_1{}'(r, s) \\
\tau_{10}(r, s) &= K_1(r+1, s)C_2{}'(r, s)
\end{aligned}
\right\}
\tag{A.26}
$$

$$
\left.
\begin{aligned}
\bar{\tau}_{00}(r, s) &= K_2(r, s)C_1{}'(r, s) \\
\bar{\tau}_{10}(r, s) &= K_2(r+1, s)C_2{}'(r, s)
\end{aligned}
\right\}
\tag{A.27}
$$

where

$$
C_1{}'(r, s) = \frac{1}{g^{1/2}} \left[- M(r, s, g, K) + (r+1)N(r, s, g, K) \right] = C_1(r, s) \tag{A.28}
$$

$$
C_2{}'(r, s) = \frac{1}{(g+K)^{1/2}} \left[M(r, s, g, K) - rN(r, s, g, K) \right] = C_2 + C_3 \left(\frac{g + K - 1}{g + K} \right)^{1/2}. \tag{A.29}
$$

54

Clearly we must have

$$g > 0,\qquad\text{(A.30)}$$

for the 2 vertex case.

For either the two vertex or three vertex cases, for given r, s and K we must always have

$$g > rK - s.\qquad\text{(A.11a)}$$

If this inequality is violated, it implies that the pivotal point would lie outside the leading edge for the given value of g.

2. The Derivation of $\delta_{uv}(r, s)$ and $\bar{\delta}_{uv}(r, s)$ for an Irregular Rhombus Adjacent to a Subsonic Leading Edge.

The method of procedure is the same as before with L_1 replacing K_1, L_2 replacing K_2 and $1/(\rho\sigma)^{1/2}$ replacing $1/4(\rho\sigma)^{3/2}$. The counterpart of equation (A.7) becomes

$$\int_r^{r+1}\int_s^{\sigma_{\mathrm{L.E.}}(\rho)} \frac{(a\sigma+b\rho+c)(\sigma_{\mathrm{L.E.}}-\sigma)^{1/2}}{(\rho\sigma)^{1/2}}\,d\rho\,d\sigma \qquad\text{(A.31)}$$

$$= a\bar{L}(r, s, g, K) + b\bar{M}(r, s, g, K) + c\bar{N}(r, s, g, K),$$

where

$$
\begin{aligned}
\bar{L}(r, s, g, K) &= \frac{\pi K^2}{20}f_1'(r) + \frac{\pi}{6}EKf_2'(r) + \frac{\pi}{4}E^2 f_3'(r) + \frac{1}{16}\left(\frac{s}{K}\right)^{1/2}f_4'(r, g, K) + \\
&\quad + \frac{1}{4}s^{1/2}(E-2s)f_5'(r, g, K) - \frac{K^2}{10}f_6'(r, s, g, K) - \frac{KE}{3}f_7'(r, s, g, K) - \\
&\quad - \frac{E^2}{2}f_8'(r, s, g, K) - \\
&\quad - \frac{1}{2}\left(\frac{s}{K}\right)^{1/2}\left[\left\{\frac{3K^2}{20}f_9'(r, g') + \frac{E^2}{2} - \frac{KE}{2}f_{10}'\left(r, g', \frac{E}{K}\right) + \frac{E^2}{10} + \right.\right. \\
&\quad \left.+ \frac{K}{20}f_{11}'(r, g', E)\right\}f_{12}'(r, g') + \\
&\quad \left.+ \frac{K^2}{20}f_{13}'(r, g') + \left\{\frac{KE}{3} - \frac{K^2}{10}f_{14}'\left(r, g', \frac{E}{K}\right)\right\}f_{15}'(r, g')\right] + \frac{4}{15}\frac{E^3}{K}f_{16}'
\end{aligned}
\qquad\text{(A.32)}
$$

$$
\begin{aligned}
\bar{M}(r, s, g, K) &= \frac{\pi}{5}Kf_1'(r) + \frac{\pi}{3}Ef_2'(r) - \frac{s^{1/2}}{4K^{3/2}}f_4'(r, g, K) - \frac{2K}{5}f_6'(r, s, g, K) - \\
&\quad - \frac{2E}{3}f_7'(r, s, g, K) - \frac{4}{15}\frac{E^3}{K^2}f_{16}' - \\
&\quad - \frac{1}{2}\left(\frac{s}{K}\right)^{1/2}\left[\left\{\frac{3}{5}Kf_9'(r, g') - Ef_{10}'(r, g', KE) + \frac{2E^2}{5K} + \right.\right. \\
&\quad \left.+ \frac{1}{5}f_{11}'(r, g', E)\right\}f_{12}'(r, g) + \\
&\quad \left.+ \frac{1}{5}Kf_{13}'(r, g') + \left\{\frac{2}{3}E - \frac{2K}{5}f_{14}'(r, g', KE)\right\}f_{15}'(r, g')\right] - \frac{4}{15}\frac{E^3}{K^2}f_{16}'.
\end{aligned}
\qquad\text{(A.33)}
$$

$$\bar{N}(r, s, g, K) = \frac{1}{3}\pi K f_2'(r) + \pi E f_3'(r) - s^{1/2} f_5'(r, g, K) - \frac{2}{3} K f_7'(r, s, g, K) -$$
$$- 2E f_8'(r, s, g, K) + \frac{4}{3}\frac{E^2}{K} f_{16}' -$$
$$- \frac{1}{2}\left(\frac{s}{K}\right)^{1/2}\left[\{2E - K f_{10}'(r, g', KE)\} f_{12}'(r, g') + \frac{2}{3} K f_{15}'(r, g')\right] \qquad (A.34)$$

and

$$f_1'(r) = (r+1)^{5.2} - r^{5/2}, \quad f_2'(r) = (r+1)^{3/2} - r^{3/2}, \quad f_3'(r) = (r+1)^{1/2} - r^{1/2}$$

$$f_4'(r, g, K) = \{(r+1)K(g+K)\}^{1/2}[(r+2)K+g] - (rKg)^{1/2}[rK+g] -$$
$$- (g - Kr)^2 \log_e\left[\frac{\{(r+1)K\}^{1/2} + (g+K)^{1/2}}{(rK)^{1/2} + g^{1/2}}\right]$$

$$f_5'(r, g, K) = \frac{g - rK}{K^{1/2}} \log_e\left[\frac{\{(r+1)K\}^{1/2} + (g+K)^{1/2}}{(rK)^{1/2} + g^{1/2}}\right] + \{(r+1)(g+K)\}^{1/2} - (rg)^{1/2}$$

$$f_6'(r, s, g, K) = (r+1)^{5/2} \sin^{-1}\left(\frac{s}{s+g+K}\right)^{1/2} - r^{5/2} \sin^{-1}\left(\frac{s}{s+g}\right)^{1/2}$$

$$f_7'(r, s, g, K) = (r+1)^{3/2} \sin^{-1}\left(\frac{s}{s+g+K}\right)^{1/2} - r^{3/2} \sin^{-1}\left(\frac{s}{s+g}\right)^{1/2}$$

$$f_8'(r, s, g, K) = (r+1)^{1/2} \sin^{-1}\left(\frac{s}{s+g+K}\right)^{1/2} - r^{1/2} \sin^{-1}\left(\frac{s}{s+g}\right)^{1/2}$$

$$f_9'(r, g') = \frac{1}{4}(g' - r)^2, \qquad g' = \frac{g}{K}$$

$$f_{10}'\left(r, g', \frac{E}{K}\right) = \frac{1}{3}\left(g' - r + 2\frac{E}{K}\right), \qquad f_{11}'(r, g', E) = E(g' - r)$$

$$f_{12}'(r, g') = \log_e\left[\frac{\frac{1}{2}(2+g'+r) + \{(r+1)(1+g')\}^{1/2}}{\frac{1}{2}(2+g'+r) - 1 + (rg')^{1/2}}\right]$$

$$f_{13}'(r, g') = \frac{1}{2}(2+g'+r)\{(r+1)(1+g')\}^{1/2} - \frac{1}{2}(g'+r)(rg')$$

$$f_{14}'\left(r, g', \frac{E}{K}\right) = \frac{E}{K} + g' - r, \qquad f_{15}' = \{(r+1)(1+g')\}^{1/2} - (rg')^{1/2}$$

$$f_{16}'(r, s, g, K, E) = \frac{1}{2}\left(\frac{K}{E}\right)^{1/2} \log_e\left[\frac{\{(r+1)sK\}^{1/2} + \{E(g+K)\}^{1/2}}{\{(r+1)sK\}^{1/2} - \{E(g+K)\}^{1/2}} \frac{(rsK)^{1/2} - (Eg)^{1/2}}{(rsK)^{1/2} + (Eg)^{1/2}}\right].$$

Using equations similar to (A.16), (A.17), (A.18), we obtain from (A.31) for the three vertex case

$$\delta_{00}(r, s) = L_1(r, s)D_1(r, s), \qquad \delta_{10}(r, s) = L_1(r+1, s)D_2(r, s),$$
$$\delta_{11}(r, s) = L_1(r+1, s+1)D_3(r, s) \qquad (A.35)$$

where

$$D_1(r, s) = \frac{1}{g^{1/2}}\left[-\bar{M} + (r+1)\bar{N}\right]$$
$$D_2(r, s) = \frac{1}{(g+K)^{1/2}}\left[-\bar{L} + \bar{M} + (s-r)\bar{N}\right] \qquad (A.36)$$
$$D_3(r, s) = \frac{1}{(g+K-1)^{1/2}}\left[\bar{L} - s\bar{N}\right].$$

Similarly

$$\bar{\delta}_{00}(r, s) = L_2(r, s)D_1(r, s), \qquad \bar{\delta}_{10}(r, s) = L_2(r+1, s)D_2(r, s),$$

$$\bar{\delta}_{11}(r, s) = L_2(r+1, s+1)D_3(r, s). \tag{A.37}$$

For the two vertex case, we have

$$\delta_{00}(r, s) = L_1(r, s)D_1'(r, s), \qquad \delta_{10}(r, s) = L_1(r+1, s)D_2'(r, s) \tag{A.38}$$

$$\bar{\delta}_{00}(r, s) = L_2(r, s)D_1'(r, s), \qquad \bar{\delta}_{10}(r, s) = L_2(r+1, s)D_2'(r, s) \tag{A.39}$$

where

$$D_1'(r, s) = \frac{1}{(g)^{1/2}} [-\bar{M} + (r+1)\bar{N}] = D_1(r, s) \tag{A.40}$$

$$D_2'(r, s) = \frac{1}{(g+K)^{1/2}} [\bar{M} - r\bar{N}] = D_2 + D_3 \left(\frac{g + K - 1}{g + K}\right)^{1/2}. \tag{A.41}$$

3. *Derivation of* τ_{uv}, $\bar{\tau}_{uv}$, δ_{uv}, $\bar{\delta}_{uv}$ *for an Irregular Rhombus Adjacent to a Transonic Leading Edge.*

The equations given earlier for the subsonic-leading-edge case remain valid, except that we have to take the limit as K tends to zero. Thus in equations (A.8), (A.9), (A.10) we take $K = 0$; with

$$f_1 = g^{1/2} \left[\frac{1}{r^{1/2}} - \frac{1}{(r+1)^{1/2}}\right] \tag{A.12a}$$

$$f_2 = 2 \sin^{-1} \left(\frac{s}{s+g}\right)^{1/2} \left[\frac{1}{r^{1/2}} - \frac{1}{(r+1)^{1/2}}\right] \tag{A.13a}$$

$$f_3 = 2 \sin^{-1} \left(\frac{s}{s+g}\right)^{1/2} [(r+1)^{1/2} - r^{1/2}] \tag{A.14a}$$

$$f_4 = 2g^{1/2}[(r+1)^{1/2} - r^{1/2}]. \tag{A.15a}$$

To obtain the equations analogous to (A.32), (A.33), (A.34), it is simpler to perform the integrations again from first principles, using the fact that the equation of the leading edge is now

$$\sigma_{\text{L.E.}} = s + g \quad \text{independent of} \quad \rho.$$

We obtain

$$\bar{L} = 2 [(r+1)^{1/2} - r^{1/2}] I_2 \tag{A.32a}$$

$$\bar{M} = \tfrac{2}{3} [(r+1)^{3/2} - r^{3/2}] I_1 \tag{A.33a}$$
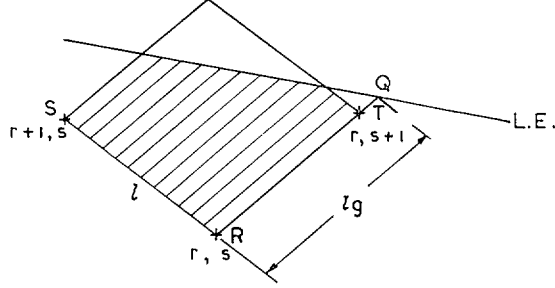
$$\bar{N} = 2 [(r+1)^{1/2} - r^{1/2}] I_1 \tag{A.34a}$$

where

$$I_1 = (s+g) \left[\frac{\pi}{2} - \sin^{-1} \left(\frac{s}{s+g}\right)^{1/2}\right] - (sg)^{1/2} \tag{A.42}$$

$$I_2 = \frac{1}{4} (s+g)^2 \left[\frac{\pi}{2} - \sin^{-1} \left(\frac{s}{s+g}\right)^{1/2}\right] - \frac{1}{4} (s-g) (sg)^{1/2}. \tag{A.43}$$

57

1. *The Derivation of $\tau_{uv}(r, s)$ and $\bar{\tau}_{uv}(r, s)$ for an Irregular Rhombus Adjacent to a Supersonic Leading Edge.*

The procedure is much the same as for the subsonic-leading-edge case, except that now the parameter K is negative and $(\sigma_{\text{L.E.}} - \sigma)^{1/2}$ is now replaced by $\sigma_{\text{L.E.}} - \sigma$ throughout. Equation (A.7) now becomes:

$$\int_r^{r+1} \int_s^{\sigma_{\text{L.E.}}(\rho)} \frac{(a\sigma + b\rho + c)(\sigma_{\text{L.E.}} - \sigma)}{4(\rho\sigma)^{3/2}} \, d\rho \, d\sigma$$

$$= aL(r, s, g, K) + bM(r, s, g, K) + cN(r, s, g, K), \tag{B.1}$$

where

$$L(r, s, g, K) = -\frac{1}{3}\left[2E\left(\frac{E + K\rho}{\rho}\right)^{1/2} - 3E(-K)^{1/2}\sin^{-1}\left(-\frac{E + K\rho}{E}\right)^{1/2} + \{K^2\rho(E + K\rho)\}^{1/2}\right]_r^{r+1} +$$

$$+ \left[Es^{1/2} - \frac{1}{3}s^{3/2}\right]\left[\frac{1}{(r+1)^{1/2}} - \frac{1}{r^{1/2}}\right] - Ks^{1/2}[(r+1)^{1/2} - r^{1/2}] \tag{B.2}$$

$$M(r, s, g, K) = -\left[\frac{E}{(-K)^{1/2}}\sin^{-1}\left(\frac{-K\rho}{E}\right)^{1/2} + \{\rho(E + K\rho)\}^{1/2}\right]_r^{r+1} +$$

$$+ \left[\frac{E}{s^{1/2}} + s^{1/2}\right][(r+1)^{1/2} - r^{1/2}] + \frac{\frac{1}{3}K}{s^{1/2}}[(r+1)^{3/2} - r^{3/2}] \tag{B.3}$$

$$N(r, s, g, K) = 2\left[(-K)^{1/2}\sin^{-1}\left(\frac{-K\rho}{E}\right) + \left(\frac{E + K\rho}{\rho}\right)^{1/2}\right]_r^{r+1} -$$

$$- \left[s^{1/2} + \frac{E}{s^{1/2}}\right]\left[\frac{1}{(r+1)^{1/2}} - \frac{1}{r^{1/2}}\right] + \frac{K}{s^{1/2}}[(r+1)^{1/2} - r^{1/2}]. \tag{B.4}$$

As before E is given by equation (A.11).

To deduce $\tau_{uv}(r, s)$ we must make use of equation (79), so that we must first express a, b, c in terms of $\phi_R{'}_{r, s}$, $\phi_R{'}_{r+1, s}$, $\phi_R{'}_{r, s+1}$. Substituting the three pairs of co-ordinates into

$$\phi_R'(\rho, \sigma)K_1(\rho, \sigma) = (a\sigma + b\rho + c)(\sigma_{\text{L.E.}} - \sigma) \tag{B.5}$$

we obtain three equations which, on solving for a, b, c, give

$$a = \frac{[\phi_R'K_1]_{r, s+1}}{g - 1} - \frac{[\phi_R'K_1]_{r, s}}{g} \tag{B.6}$$

$$b = \frac{[\phi_R'K_1]_{r+1, s}}{g + K} - \frac{[\phi_R'K_1]_{r, s}}{g} \tag{B.7}$$

$$c = \frac{[\phi_R'K_1]_{r, s}}{g}(r + s + 1) - r\frac{[\phi_R'K_1]_{r+1, s}}{g + K} - s\frac{[\phi_R'K_1]_{r, s+1}}{g - 1}. \tag{B.8}$$

Returning to equation (B.1) and picking out the coefficients of $\phi_R'(r, s)$, $\phi_R'(r+1, s)$, $\phi_R'(r, s+1)$ in turn, we obtain

$$\left.\begin{aligned}
\tau_{00}(r, s) &= K_1(r, s)C_1(r, s) \\
\tau_{10}(r, s) &= K_1(r+1, s)C_2(r, s) \\
\tau_{01}(r, s) &= K_1(r, s+1)C_3(r, s)
\end{aligned}\right\} \tag{B.9}$$

where

$$\left.\begin{aligned}
C_1(r, s) &= \frac{1}{g}\left[-L - M + (r+s+1)N\right] \\
C_2(r, s) &= \frac{1}{g+K}\left[M - rN\right] \\
C_3(r, s) &= \frac{1}{g-1}\left[L - sN\right].
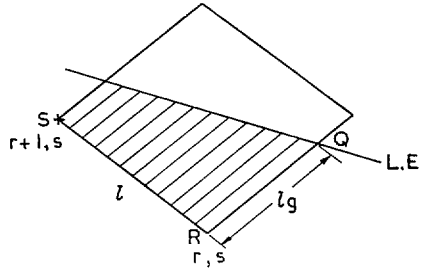\end{aligned}\right\} \tag{B.10}$$

Similarly

$$\left.\begin{aligned}
\tau_{00}(r, s) &= K_2(r, s)C_1(r, s) \\
\tau_{10}(r, s) &= K_2(r+1, s)C_2(r, s) \\
\tau_{01}(r, s) &= K_2(r, s+1)C_3(r, s).
\end{aligned}\right\} \tag{B.11}$$

For the three vertex case it will be clear that the point Q must lie outboard of T and hence

$$g > 1, \tag{B.12}$$

must be satisfied.

In a similar manner we find for the 2 vertex case

$$a = 0 \tag{B.13}$$

$$b = \frac{[\phi_R'K_1]_{r+1,s}}{g+K} - \frac{[\phi_R'K_1]_{r,s}}{g} \tag{B.14}$$

$$c = (r+1)\frac{[\phi_R'K_1]_{r,s}}{g} - r\frac{[\phi_R'K_1]_{r+1,s}}{g+K}. \tag{B.15}$$
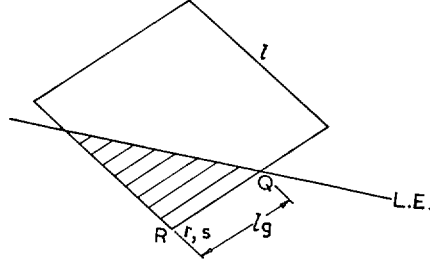
Equations (A.26), (A.27) now hold good as before, where

$$C_1'(r, s) = \frac{1}{g}\left[-M + (r+1)N\right] = C_1 + \frac{g-1}{g}C_3 \tag{B.16}$$

$$C_2'(r, s) = \frac{1}{g+K}\left[M - rN\right] = C_2. \tag{B.17}$$

59

Clearly for the two vertex case, we must have

$$-K < g \leqslant 1. \tag{B.17a}$$

For the one vertex case we get

$$a = 0, \qquad b = 0, \qquad c = \frac{[\phi_R{}' K_1]_{r,s}}{g}. \tag{B.18}$$

Hence

$$\tau_{00}(r, s) = K_1(r, s) C_1''(r, s), \qquad \bar\tau_{00}(r, s) = K_2(r, s) C_1''(r, s), \tag{B.19}$$

where

$$C_1''(r, s) = \frac{N}{g}. \tag{B.20}$$

For the one vertex case

$$0 < g \leqslant -K. \tag{B.21}$$

2. *The Derivation of $\delta_{uv}(r, s)$ and $\bar\delta_{uv}(r, s)$ for an Irregular Rhombus Adjacent to a Supersonic Leading Edge.*

The method of procedure is the same as above with L_1 replacing K_1, L_2 replacing K_2 and $1/(\rho\sigma)^{1/2}$ replacing $1/4(\rho\sigma)^{3/2}$.

The counterpart of equation (B.1) becomes

$$\int_r^{r+1} \int_s^{\sigma_{\text{L.E.}}(\rho)} \frac{(a\sigma + b\rho + c)(\sigma_{\text{L.E.}} - \sigma)}{(\rho\sigma)^{1/2}} \, d\rho \, d\sigma$$
$$= a\bar L(r, s, g, K) + b\bar M(r, s, g, K) + c\bar N(r, s, g, K) \tag{B.22}$$

where

$$\bar L(r, s, g, K) = \left[\frac{8}{15} \rho^{1/2}(E + K\rho)^{5/2} \right]_r^{r+1} - \frac{4}{3} j_1(r, E, K) +$$
$$+ \left[\frac{4}{5} s^{5/2} - \frac{4}{3} E s^{3/2} \right] [(r+1)^{1/2} - r^{1/2}] - \frac{4}{9} K s^{3/2} [(r+1)^{3/2} - r^{3/2}] \tag{B.23}$$

$$\bar M(r, s, g, K) = \frac{4}{3} j_1(r, E, K) + \left[\frac{4}{9} s^{3/2} - \frac{4}{3} E s^{1/2} \right] [(r+1)^{3/2} - r^{3/2}] - \frac{4}{5} s^{1/2} K [(r+1)^{5/2} - r^{5/2}] \tag{B.24}$$

$$\bar N(r, s, g, K) = \frac{4}{3} j_2(r, E, K) + \left[\frac{4}{3} s^{3/2} - 4 E s^{1/2} \right] [(r+1)^{1/2} - r^{1/2}] - \frac{4}{3} s^{1/2} K [(r+1)^{3/2} - r^{3/2}] \tag{B.25}$$

and

$$j_1(r, E, K) = \left[-\frac{E^3}{16(-K)^{3/2}} \left\{ \frac{\pi}{2} - 2\sin^{-1}\left(\frac{-K\rho}{E} \right)^{1/2} \right\} + \frac{E}{8K}(E + 2K\rho) \{\rho(E + K\rho)\}^{1/2} + \right.$$
$$\left. + \frac{1}{3} \rho(E + K\rho) \{\rho(E + K\rho)\}^{1/2} \right]_r^{r+1} \tag{B.26}$$

$$j_2(r, E, K) = \left[\frac{3E^2}{4(-K)^{1/2}} \sin^{-1}\left(\frac{-K\rho}{E} \right)^{1/2} + \frac{1}{4}(5E + 2K\rho) \{\rho(E + K\rho)\}^{1/2} \right]_r^{r+1}. \tag{B.27}$$

Using equations similar to (B.6), (B.7), (B.8) for the three vertex case, we obtain from (B.22)

$$\delta_{00}(r, s) = L_1(r, s)D_1(r, s), \qquad \delta_{10}(r, s) = L_1(r+1, s)D_2(r, s),$$

$$\delta_{01}(r, s) = L_1(r, s+1)D_3(r, s) \tag{B.28}$$

where

$$D_1(r, s) = \frac{1}{g}\left[-\bar{L} - \bar{M} + (r+s+1)\bar{N}\right]$$

$$D_2(r, s) = \frac{1}{g + K}[\bar{M} - r\bar{N}], \qquad D_3(r, s) = \frac{1}{g - 1}[\bar{L} - s\bar{N}]. \tag{B.29}$$

Similarly

$$\bar{\delta}_{00}(r, s) = L_2(r, s)D_1(r, s), \qquad \bar{\delta}_{10}(r, s) = L_2(r+1, s)D_2(r, s)$$

$$\bar{\delta}_{01}(r, s) = L_2(r, s+1)D_3(r, s) \tag{B.30}$$

For the two vertex case, we have equations (A.38), (A.39), where

$$D_1{}'(r, s) = \frac{1}{g}\left[-\bar{M} + (r+1)\bar{N}\right] = D_1 + \frac{g - 1}{g}D_3 \tag{B.31}$$

$$D_2{}'(r, s) = \frac{1}{g + K}[\bar{M} - r\bar{N}] = D_2. \tag{B.32}$$

For the one vertex case, we have

$$\delta_{00}(r, s) = L_1(r, s)D_1{}''(r, s), \qquad \bar{\delta}_{00}(r, s) = L_2(r, s)D_1{}''(r, s) \tag{B.33}$$

where

$$D_1{}''(r, s) = \frac{\bar{N}}{g}. \tag{B.34}$$

Rectangular wing.   A/$_R$ = 2
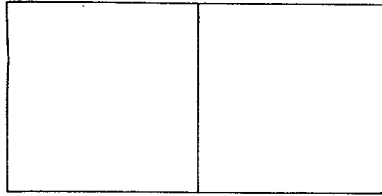
s = 10
c = 10

Delta wing·   A/$_R$ = 1·5
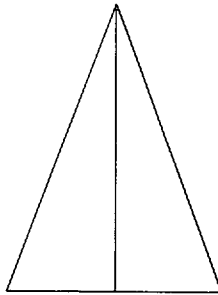
s = 3·75
c = 10
Tan $\Lambda_{L.E.}$ = $8/_3$

Tapered wing.   A/$_R$ = 4·33
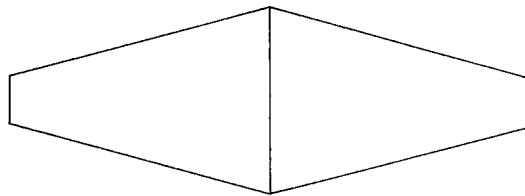
s = 13·7
c = 10
$\Lambda_{L.E.}$ = 15°

Fɪɢ. 1.   Planforms for which derivatives were evaluated.
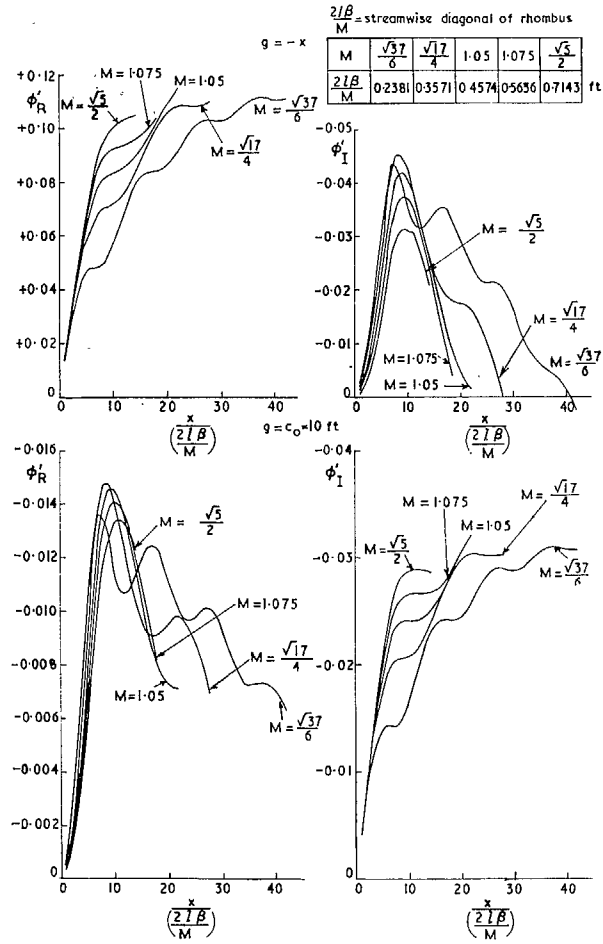
FIG. 2. Rectangular wing $A = 2$, $\nu = 0 \cdot 3$, $c_0 = 10$ ft, $\phi' = \phi/UL$, $L = 100$ ft. Centre-line ϕ's plotted against chord for various Mach numbers.

FIG. 3. Rectangular wing $A = 2$, $M = \sqrt{(37)}/6$, $c_0 = 10$ ft. Centre-line ϕ's plotted against chord for various ν.

Fig. 4 left panel labels:

$M = 1.15$ $\nu = \dfrac{\omega c_0}{U} = 0.3$

$-2\,\phi'_{\underline{I}} \times 10$

$\tfrac{1}{2}\,\phi'_{\underline{R}} \times 10$

$-2\,\phi'_{\underline{R}} \times 100$

$2\,\phi'_{\underline{I}} \times 10$

x/c_0

Fig. 4 right panel labels:

$M = 1.075$ $\nu = \dfrac{\omega c_0}{U} = 0.6$

$-\phi'_{\underline{I}} \times 10$

$\tfrac{1}{2}\,\phi'_{\underline{R}} \times 10$

$-\phi'_{\underline{R}} \times 40$

$\phi'_{\underline{I}} \times 10$

x/c_0

Fig. 4 lower-left panel labels:

$M = 1.075$ $\nu = 0.3$

$-\tfrac{5}{2}\,\phi'_{\underline{I}} \times 10$

$\tfrac{1}{2}\,\phi'_{\underline{R}} \times 10$

$\tfrac{5}{2}\,\phi'_{\underline{I}} \times 10$

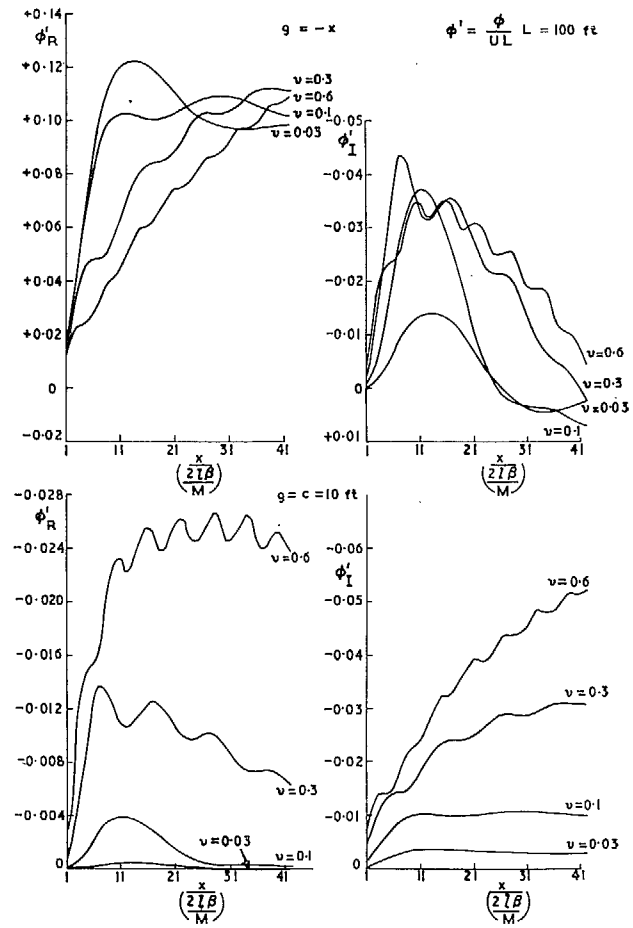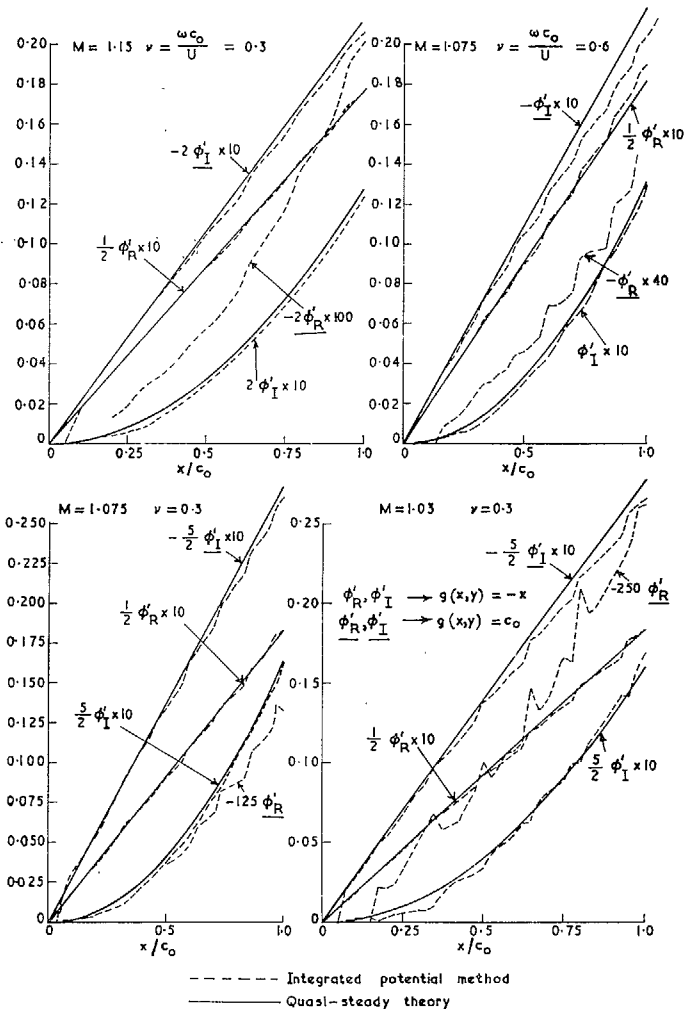$-125\,\phi'_{\underline{R}}$

x/c_0

Fig. 4 lower-right panel labels:

$M = 1.03$ $\nu = 0.3$

$\phi'_{\underline{R}},\ \phi'_{\underline{I}} \longrightarrow g(x,y) = -x$

$\underline{\phi'_{\underline{R}}},\ \underline{\phi'_{\underline{I}}} \longrightarrow g(x,y) = c_0$

$-\tfrac{5}{2}\,\phi'_{\underline{I}} \times 10$

$-250\,\phi'_{\underline{R}}$

$\tfrac{1}{2}\,\phi'_{\underline{R}} \times 10$

$\tfrac{5}{2}\,\phi'_{\underline{I}} \times 10$

x/c_0

– – – – – Integrated potential method

——— Quasi-steady theory

FIG. 4. Delta wing, $\tan \Lambda = 8/3$, $c_0 = 10$ ft,
$\phi' = \phi/UL$, $L = 100$ ft.

Fig. 5 upper panel labels:

$M = 1.03$ $\nu = 0.6$

$\phi'_{\underline{R}},\ \phi'_{\underline{I}} \longrightarrow g(x,y) = -x$

$\underline{\phi'_{\underline{R}}},\ \underline{\phi'_{\underline{I}}} \longrightarrow g(x,y) = c_0$

$-\tfrac{5}{4}\,\phi'_{\underline{I}} \times 10$

$\tfrac{1}{2}\,\phi'_{\underline{R}} \times 10$

$-\tfrac{5}{4}\,\phi'_{\underline{I}} \times 10$

$-\tfrac{5}{2}\,\phi'_{\underline{R}} \times 10$

x/c_0

Fig. 5 lower panel labels:

$M = 1.01$ $\nu = 0.3$

$g(x,y) = -x$

$10\,\phi'_{\underline{R}}$

$\dfrac{y}{s} = 0.564$

$\dfrac{y}{s} = 0.752$

$\dfrac{y}{s} = 0.188$

$\dfrac{y}{s} = 0.376$

$\tfrac{1}{2}\,\phi'_{\underline{R}}$ for $\dfrac{y}{s} = 0$

$\dfrac{y}{s} = 0.940$

x/c_0

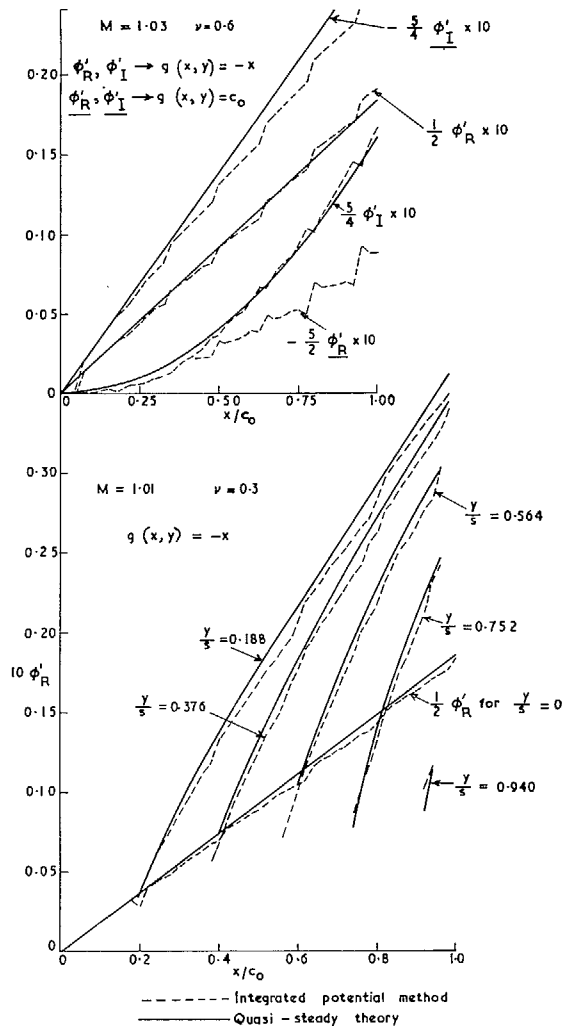– – – – – Integrated potential method

——— Quasi-steady theory

FIG. 5. Delta wing, $\tan \Lambda = 8/3$, $c_0 = 10$ ft,
$\phi' = \phi/UL$, $L = 100$ ft.

FIG. 6. Symmetrical tapered wing, $M = 1\cdot0645$, $\nu = 0\cdot3 = \omega c_0/U$, $c_0 =$ root chord $= 10$ ft, $s =$ semi-span $= 13\cdot7$ ft, $\Lambda_{\text{L.E.}} = -\Lambda_{\text{T.E.}} = 15°$.
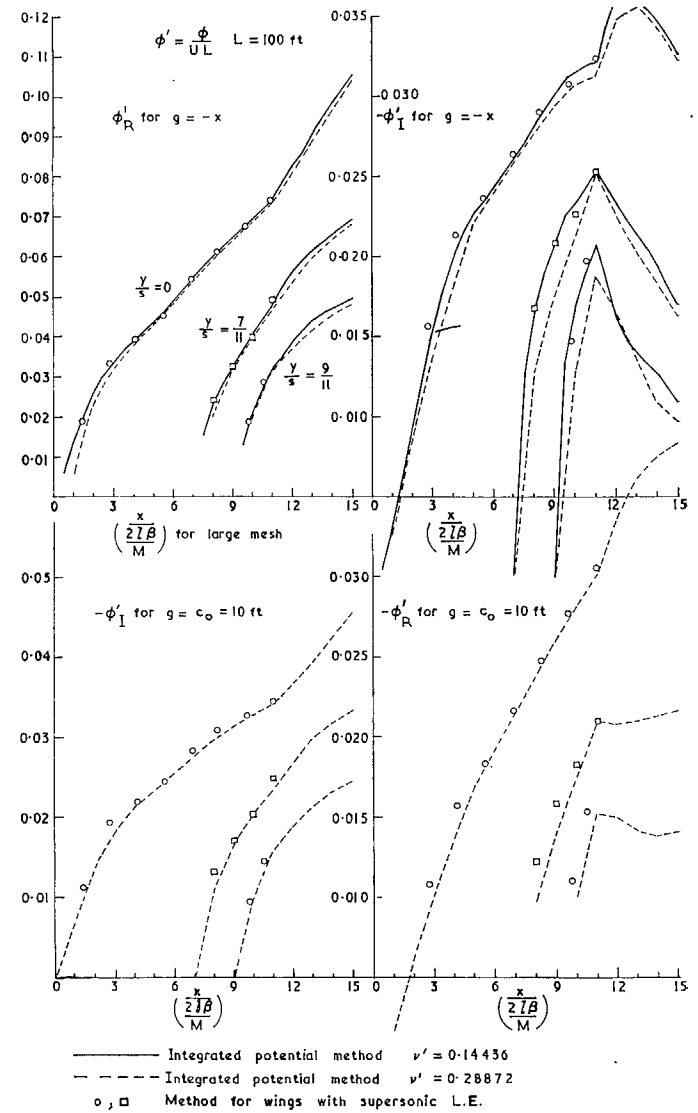
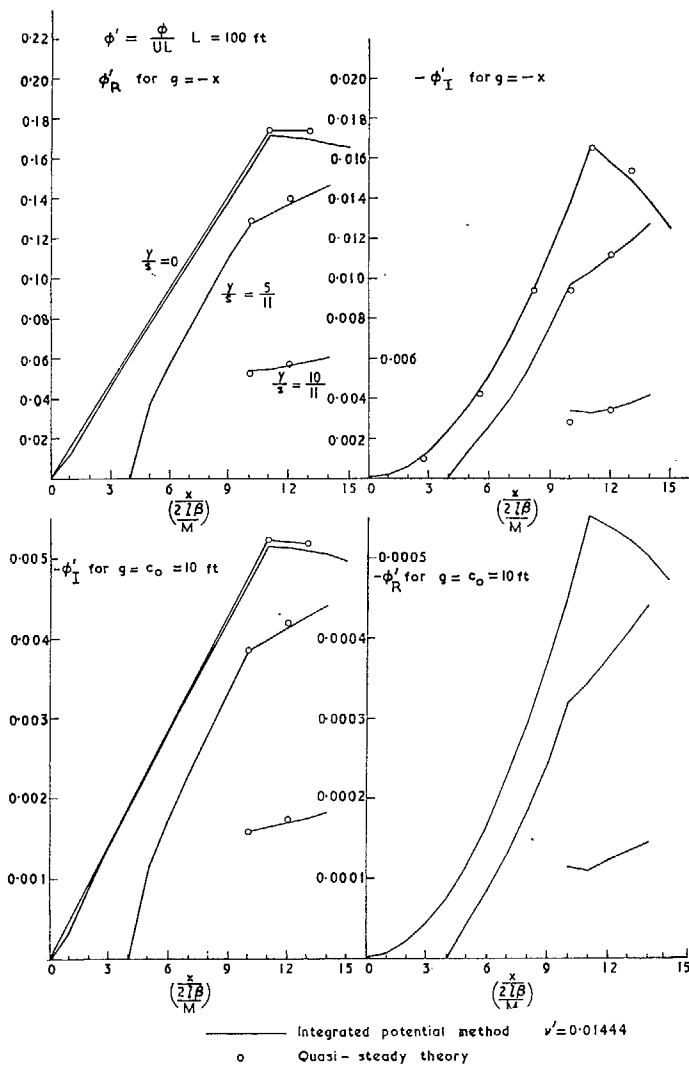FIG. 7. Symmetrical tapered wing, $M = 1\cdot0353$, transonic L.E. $\nu = 0\cdot6 = \omega c_0/U$.

$\phi' = \dfrac{\phi}{UL}$ L = 100 ft

ϕ'_R for g = -x

$-\phi'_I$ for g = -x

0·22
0·20
0·18
0·16
0·14
0·12
0·10
0·08
0·06
0·04
0·02

$\frac{y}{s} = 0$

$\frac{y}{s} = \frac{5}{11}$

$\frac{y}{s} = \frac{10}{11}$

0·020
0·018
0·016
0·014
0·012
0·010
0·008
0·006
0·004
0·002

0 3 6 9 12 15
$\left(\dfrac{x}{\frac{2\bar{l}\beta}{M}}\right)$

$-\phi'_I$ for $g = c_o = 10$ ft

$-\phi'_R$ for $g = c_o = 10$ ft

0·005
0·004
0·003
0·002
0·001

0·0005
0·0004
0·0003
0·0002
0·0001

——— Integrated potential method $\nu' = 0.01444$

o   Quasi – steady theory

FIG. 8. Symmetrical tapered wing, $M = 1.0353$,
transonic L.E. $\nu = 0.03 = \omega c_0/U$.

$\phi' = \dfrac{\phi}{UL}$ L = 100 ft

ϕ'_R for g = -x

$-\phi'_I$ for g = -x

0·16
0·14
0·12
0·10
0·08
0·06
0·04
0·02

$\frac{y}{s} = 0$

$\frac{y}{s} = 0.412$

$\frac{y}{s} = 0.721$

0·05
0·04
0·03
0·02
0·01

5 10 15 20 25
$\left(\dfrac{x}{\frac{2\bar{l}\beta}{M}}\right)$

$-\phi'_I$ for $g = c_0 = 10$ ft

$-\phi'_R$ for $g = c_0 = 10$ ft

0·016
0·014
0·012
0·010
0·008
0·006
0·004
0·002

0·005
0·004
0·003
0·002
0·001

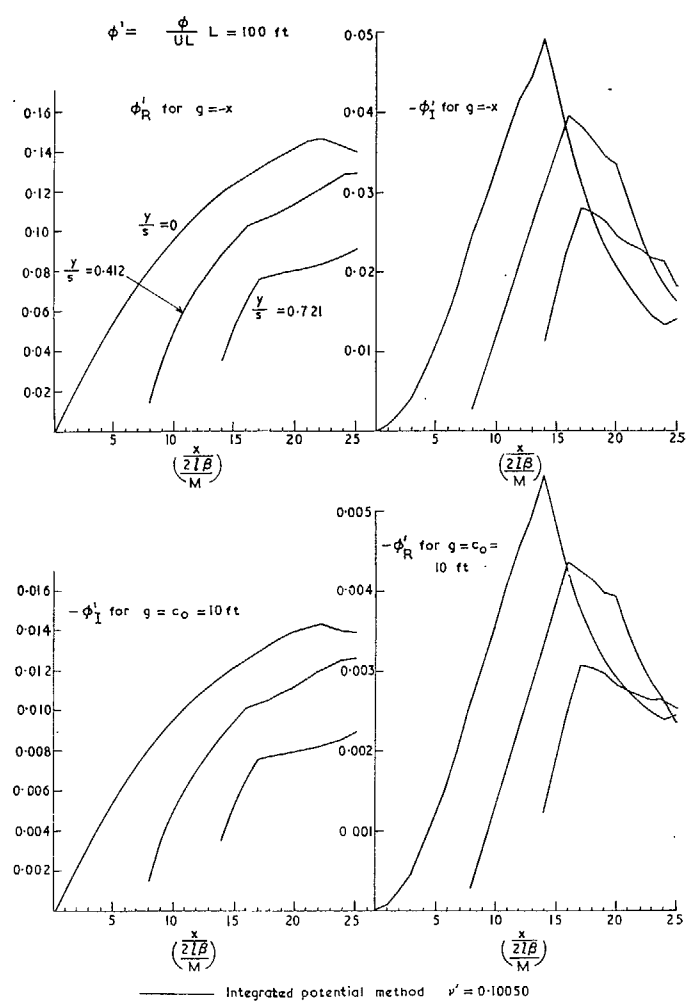——— Integrated potential method $\nu' = 0.10050$

FIG. 9. Symmetrical tapered wing, $M = 1.01$,
subsonic L.E. $\nu = 0.1 = \omega c_0/U$.

Publications of the Aeronautical Research Council

ANNUAL TECHNICAL REPORTS OF THE AERONAUTICAL RESEARCH COUNCIL (BOUND VOLUMES)

1945 Vol. I. Aero and Hydrodynamics, Aerofoils. £6 10s. (£6 14s.)
Vol. II. Aircraft, Airscrews, Controls. £6 10s. (£6 14s.)
Vol. III. Flutter and Vibration, Instruments, Miscellaneous, Parachutes, Plates and Panels, Propulsion.
£6 10s. (£6 14s.)
Vol. IV. Stability, Structures, Wind Tunnels, Wind Tunnel Technique. £6 10s. (£6 14s.)

1946 Vol. I. Accidents, Aerodynamics, Aerofoils and Hydrofoils. £8 8s. (£8 12s. 6d.)
Vol. II. Airscrews, Cabin Cooling, Chemical Hazards, Controls, Flames, Flutter, Helicopters, Instruments and Instrumentation, Interference, Jets, Miscellaneous, Parachutes. £8 8s. (£8 12s.)
Vol. III. Performance, Propulsion, Seaplanes, Stability, Structures, Wind Tunnels. £8 8s. (£8 12s.)

1947 Vol. I. Aerodynamics, Aerofoils, Aircraft. £8 8s. (£8 12s. 6d.)
Vol. II. Airscrews and Rotors, Controls, Flutter, Materials, Miscellaneous, Parachutes, Propulsion, Seaplanes, Stability, Structures, Take-off and Landing. £8 8s. (£8 12s. 6d.)

1948 Vol. I. Aerodynamics, Aerofoils, Aircraft, Airscrews, Controls, Flutter and Vibration, Helicopters, Instruments, Propulsion, Seaplane, Stability, Structures, Wind Tunnels. £6 10s. (£6 14s.)
Vol. II. Aerodynamics, Aerofoils, Aircraft, Airscrews, Controls, Flutter and Vibration, Helicopters, Instruments, Propulsion, Seaplane, Stability, Structures, Wind Tunnels. £5 10s. (£5 14s.)

1949 Vol. I. Aerodynamics, Aerofoils. £5 10s. (£5 14s.)
Vol. II. Aircraft, Controls, Flutter and Vibration, Helicopters, Instruments, Materials, Seaplanes, Structures, Wind Tunnels. £5 10s. (£5 13s. 6d.)

1950 Vol. I. Aerodynamics, Aerofoils, Aircraft. £5 12s. 6d. (£5 16s. 6d.)
Vol. II. Apparatus, Flutter and Vibration, Meteorology, Panels, Performance, Rotorcraft, Seaplanes.
£4 (£4 3s. 6d.)
Vol. III. Stability and Control, Structures, Thermodynamics, Visual Aids, Wind Tunnels. £4 (£4 3s. 6d.)

1951 Vol. I. Aerodynamics, Aerofoils. £6 10s. (£6 14s.)
Vol. II. Compressors and Turbines, Flutter, Instruments, Mathematics, Ropes, Rotorcraft, Stability and Control, Structures, Wind Tunnels. £5 10s. (£5 14s.)

1952 Vol. I. Aerodynamics, Aerofoils. £8 8s. (£8 12s.)
Vol. II. Aircraft, Bodies, Compressors, Controls, Equipment, Flutter and Oscillation, Rotorcraft, Seaplanes, Structures. £5 10s. (£5 13s. 6d.)

1953 Vol. I. Aerodynamics, Aerofoils and Wings, Aircraft, Compressors and Turbines, Controls. £6 (£6 4s.)
Vol. II. Flutter and Oscillation, Gusts, Helicopters, Performance, Seaplanes, Stability, Structures, Thermodynamics, Turbulence. £5 5s. (£5 9s.)

1954 Aero and Hydrodynamics, Aerofoils, Arrester gear, Compressors and Turbines, Flutter, Materials, Performance, Rotorcraft, Stability and Control, Structures. £7 7s. (£7 11s.)

Special Volumes

Vol. I. Aero and Hydrodynamics, Aerofoils, Controls, Flutter, Kites, Parachutes, Performance, Propulsion, Stability. £6 6s. (£6 9s. 6d.)
Vol. II. Aero and Hydrodynamics, Aerofoils, Airscrews, Controls, Flutter, Materials, Miscellaneous, Parachutes, Propulsion, Stability, Structures. £7 7s. (£7 10s. 6d.)
Vol. III. Aero and Hydrodynamics, Aerofoils, Airscrews, Controls, Flutter, Kites, Miscellaneous, Parachutes, Propulsion, Seaplanes, Stability, Structures, Test Equipment. £9 9s. (£9 13s. 6d.)

Reviews of the Aeronautical Research Council
1949-54 5s. (5s. 6d.)

Index to all Reports and Memoranda published in the Annual Technical Reports
1909-1947   R. & M. 2600 (out of print)

Indexes to the Reports and Memoranda of the Aeronautical Research Council
Between Nos. 2451-2549: R. & M. No. 2550 2s. 6d. (2s. 9d.); Between Nos. 2651-2749: R. & M. No. 2750 2s. 6d. (2s. 9d.); Between Nos. 2751-2849: R. & M. No. 2850 2s. 6d. (2s. 9d.); Between Nos. 2851-2949: R. & M. No. 2950 3s. (3s. 3d.); Between Nos. 2951-3049: R. & M. No. 3050 3s. 6d. (3s. 9d.); Between Nos. 3051-3149: R. & M. No. 3150 3s. 6d. (3s. 9d.); Between Nos. 3151-3249: R. & M. No. 3250 3s. 6d. (3s. 9d.); Between Nos. 3251-3349: R. & M. No. 3350 3s. 6d. (3s. 11d.)

Prices in brackets include postage

Government publications can be purchased over the counter or by post from the Government Bookshops in London, Edinburgh, Cardiff, Belfast, Manchester, Birmingham and Bristol, or through any bookseller